European Journal of Medicinal Chemistry 224 (2021) 113672

Contents lists available at ScienceDirect

European Journal of Medicinal Chemistry

journal homepage: http://www.elsevier.com/locate/ejmech

Discovery of 2,4-pyrimidinediamine derivatives as potent dual inhibitors of ALK and HDAC

Tao Pan [a, 1], Yanrong Dan [a, 1], Dafeng Guo [a, 1], Junhao Jiang [a, b], Dongzhi Ran [a, b], Lin Zhang [a], Binghua Tian [a], Jianyong Yuan [a, b], Yu Yu [a, b, *], Zongjie Gan [a, b, **]

[a] Department of Medicinal Chemistry, College of Pharmacy, Chongqing Medical University, Chongqing 400016, PR China
[b] Chongqing Research Center for Pharmaceutical Engineering, Chongqing Medical University, Chongqing 400016, PR China

ARTICLE INFO

Article history:
Received 28 May 2021
Received in revised form
22 June 2021
Accepted 24 June 2021
Available online 29 June 2021

Keywords:
ALK/HDAC dual Inhibitors
Pharmacophore merged strategy
2,4-Pyrimidinediamine
NSCLC

ABSTRACT

Combination of anaplastic lymphoma kinase (ALK) inhibitor with histone deacetylases (HDAC) inhibitor could exert synergistically anti-proliferative effects on ALK positive non-small cell lung cancer (NSCLC) naïve or resistant cells. In this work, we designed and synthesized a series of 2,4-pyrimidinediamine derivatives as dual ALK and HDAC inhibitors based on pharmacophore merged strategy. Among which, compound **10f** displayed the most potent and balanced inhibitory activity against ALK (IC_{50} = 2.1 nM) and HDAC1 (IC_{50} = 7.9 nM), respectively. In particular, **10f** was also potent against the frequently observed Crizotinib-resistant ALK^{L1196M} (IC_{50} = 1.7 nM) as well as the Ceritinib-resistant ALK^{G1202R} (IC_{50} = 0.4 nM) mutants. In antiproliferative activity assay, **10f** exhibited impressive activity on ALK-addicted cancer cell lines at low micromole concentrations, which was comparable to that of Crizotinib and Ceritinib. Further flow cytometric analysis indicated that **10f** could effectively induce cell death via cell apoptosis and cell cycle arrest. Taken together, these results suggested **10f** would be a promising lead compound for the ALK-positive NSCLC treatment, especially the Ceritinib- or Crizotinib-resistant NSCLC.

© 2021 Elsevier Masson SAS. All rights reserved.

1. Introduction

Chromosomal rearrangement of the anaplastic lymphoma kinase (ALK) gene has been identified as one of the most frequent oncogenic drivers that are associated with many malignancies [1], which include diffuse large B-cell lymphoma (DLBCL) [2], inflammatory myofibroblastic tumors (IMTs) [3], and non-small cell lung cancer (NSCLC) [4]. For instance, echinoderm microtubule-associated protein-like 4 (EML4)-ALK gene fusion, the predominant ALK rearrangement that is associated with NSCLC, can promote dimerization and constitutive phosphorylation of ALK proteins, thereby leading to aberrant proliferation and survival of cancer cells via continuous activation of ALK and its downstream signaling pathways [5]. Hence, ALK was proven to be a critical player in NSCLC development, and the development of inhibitors for blocking ALK signaling pathways represents an effective therapeutic strategy for the treatment of *ALK*-driven NSCLC [6–8].

Crizotinib (Fig. 1), which became the first small molecular ALK inhibitor to be approved by the FDA in 2011, initially demonstrated potent efficacy against *ALK*-rearranged NSCLC [9]. Unfortunately, patients who are treated with Crizotinib eventually relapse within 1–2 years due to acquired drug resistance [10,11]. To overcome the acquired resistance to Crizotinib, second-generation and third-generation ALK inhibitors with improved potency and selectivity, such as Ceritinib [12], Alectinib [13], Brigatinib [14] and Lorlatinib [15] (Fig. 1), are subsequently administered. These newly approved inhibitors exhibit remarkable antitumor activity in Crizotinib-sensitive and Crizotinib-resistant NSCLC models and provide clinical benefit to patients who have progressed following Crizotinib treatment. However, similar to Crizotinib, drug resistance to next-generation ALK-TKIs inevitably arises due to multiple resistance mechanisms, which include the emergence of new secondary mutations in the kinase domain, bypass pathway activation, and epithelial-to-mesenchymal transition (EMT), among others [16–19].

* Corresponding author. Department of Medicinal Chemistry, College of Pharmacy, Chongqing Medical University, Chongqing 400016, PR China.
** Corresponding author. Chongqing Research Center for Pharmaceutical Engineering, Chongqing Medical University, Chongqing 400016, PR China.
E-mail addresses: yuyu3519@163.com (Y. Yu), gzj@cqmu.edu.cn (Z. Gan).
[1] These authors contributed equally to this work.

https://doi.org/10.1016/j.ejmech.2021.113672
0223-5234/© 2021 Elsevier Masson SAS. All rights reserved.

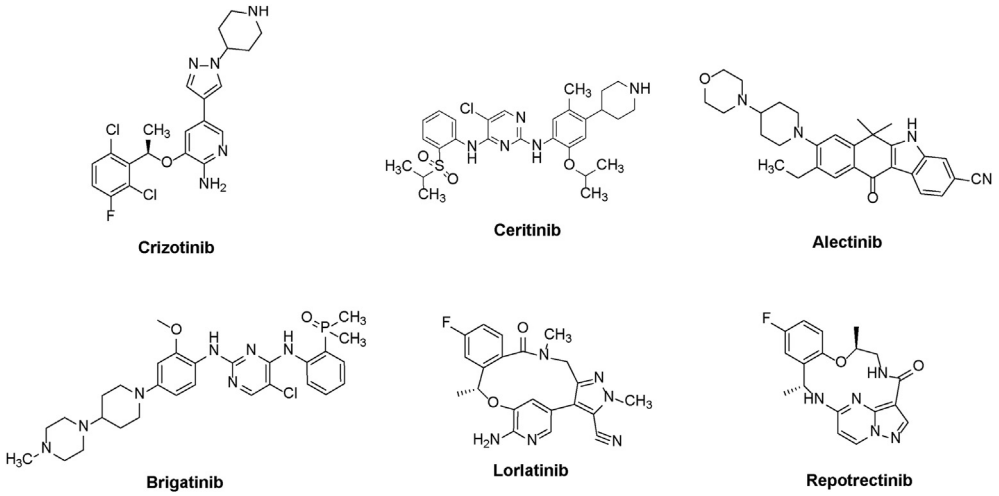

Fig. 1. Chemical structures of ALK inhibitors.

Amino residue mutations have been identified as the most common reason for drug resistance [20]. For example, in contrast with the gatekeeper mutation L1196 M, which predominantly confers resistance to Crizotinib [21], the solvent front G1202R mutation, has been regarded as one of the most frequent causes of resistance to second-generation inhibitors [16,22,23]. Therefore, the discovery and development of effective ALK inhibitors that could counteract G1202R-induced resistance have attracted substantial attention [24,25]. Recently, it was found that an unfavorable steric obstruction caused by the bulky group in ALK inhibitors with 1202R residue is likely responsible for their loss of potency against the G1202R mutant [23]. Replacing the piperidine group in Ceritinib with aliphatic amines or glycine, could attenuate and diminish the steric hindrance, thereby resulting in novel compounds with enhanced activities against this mutant [26,27]. Consequently, these findings would be beneficial for the development of novel and potent ALK inhibitors that can overcome the resistance that is caused by the G1202R mutation.

Histone deacetylases (HDACs) are a class of enzymes that remove acetyl groups from lysine residues in histones and play important roles in the proliferation, differentiation and apoptosis of tumor cells [28]. In addition to the G1202R mutation that is identified as a common resistance mechanism for Ceritinib, accumulating evidence has shown that EMT mediated by HDACs is also associated with the sensitivity to the second-generation ALK inhibitors [16], while combination with HDAC inhibitors could improve the efficacy of ALK inhibitors in combating drug resistance [29]. For example, Cho and coworkers demonstrated that combining Ceritinib with an HDAC inhibitor, namely, Panobinostat, could have synergistic antiproliferative effects on NSCLC naïve or resistant cells and xenografts [30]. Another study similarly showed that co-treatment with HDAC inhibitor quisinostat could restore the sensitivity of lung adenocarcinoma cells to Critzotinib [31]. Therefore, the success of the synergy between ALK inhibitors and HDAC inhibitors in increasing anti-ALK activity to circumvent drug resistance provided a rational combinational approach in NSCLC therapeutics.

Based on these studies, we hypothesized that developing a single molecule that can concurrently inhibit both ALK and HDACs would be a potential strategy to overcome resistance. To design dual inhibitors, a pharmacophore merging approach was utilized. As illustrated in Fig. 2, almost all approved HDAC inhibitors share a common pharmacophore: a surface recognition “CAP” group, a hydrophobic linker and a zinc-binding group (ZBG) [32]. The cap group is critical for HDAC selectivity and can accommodate variable structures. Hence, the *N*4-(2-(isopropylsulfonyl)phenyl)-*N*2-phenylpyrimidine motif in Ceritinib, which shows satisfactory binding affinity with ALK^{wt} according to the cocrystal structure (PDB: 4MKC), was selected as the cap group [12]. Additionally, a flexible long-chain aliphatic group was chosen as the linker to replace the piperidine in Ceritinib to avoid steric hindrance. Meanwhile, a zinc-binding group (ZBG), such as hydroxamic acid, was incorporated into the tail of the sidechain to chelate the catalytic zinc ion in HDACs, with the objective of dual inhibition. Finally, a series of diarylaminopyrimidine derivatives with potent and balanced inhibitory activities against ALK, including ALK^{G1202R}, and HDACs were designed and synthesized in this study (Fig. 2).

2. Results and discussion

2.1. Chemistry

The synthetic route to target compounds **6a-t** is illustrated in Scheme 1. The key intermediate, namely, 2,5-dichloro-*N*-(2-(isopropylsulfonyl)phenyl)pyrimidin-4-amine (**1**), was prepared according to procedures from the literature [33]. Briefly, compound **1** readily reacted with substituted methyl 4-aminobenzoate or 3-aminobenzoate **2a-h** to produce compounds **3a-h**. Hydrolysis of compounds **3a-h** under basic conditions provided corresponding carboxylic intermediates **4a-h**, which subsequently condensed with methyl aminoalkanoates in CH_2Cl_2 in the presence of 1-ethyl-3-(3-dimethyllaminopropyl)carbodiimide hydrochloride (EDCI) and 1-hydroxybenzotriazole (HOBT) to produce important ester intermediates **5b-t**. Finally, the transformation of compounds **5b-t** into the target hydroxamic acid compounds **6a-t** was realized with a freshly prepared NH_2OH/KOH methanol solution at 0 °C with moderate yields.

Another series of target compounds **10a-j** and **16a-m** were prepared via a similar synthetic procedure, as illustrated in Scheme 2 and Scheme 3, respectively. In Scheme 2, intermediates **8a-c** were obtained with moderate to satisfactory yields by treating **1** with commercially available starting materials *m*-phenylenediamine **7a**, *p*-phenylenediamine **7b** and 2-methyl-*m*-phenylenediamine **7c** under hydrochloride-promoted conditions. The coupling of resultants **8a-c** with monomethyl dicarboxylates of various chain lengths generated corresponding compounds **9a-j**, which were

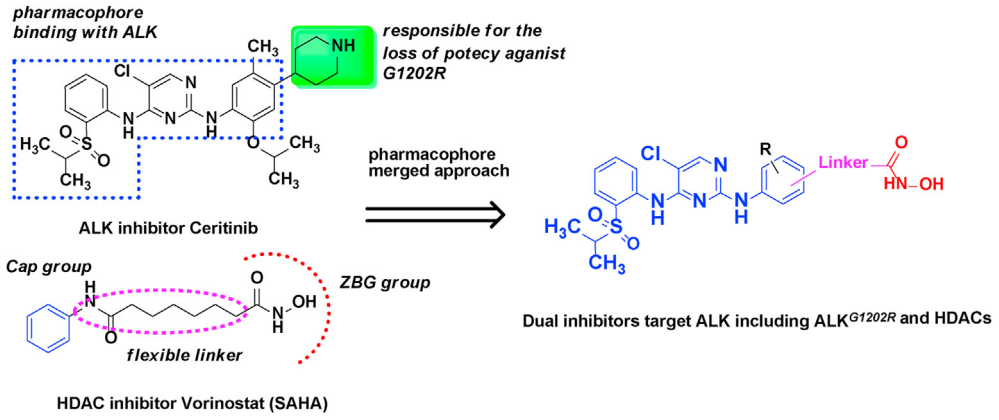

Fig. 2. Design strategy for a dual inhibitor that targets ALK, including ALK^{G1202R}, and HDACs.

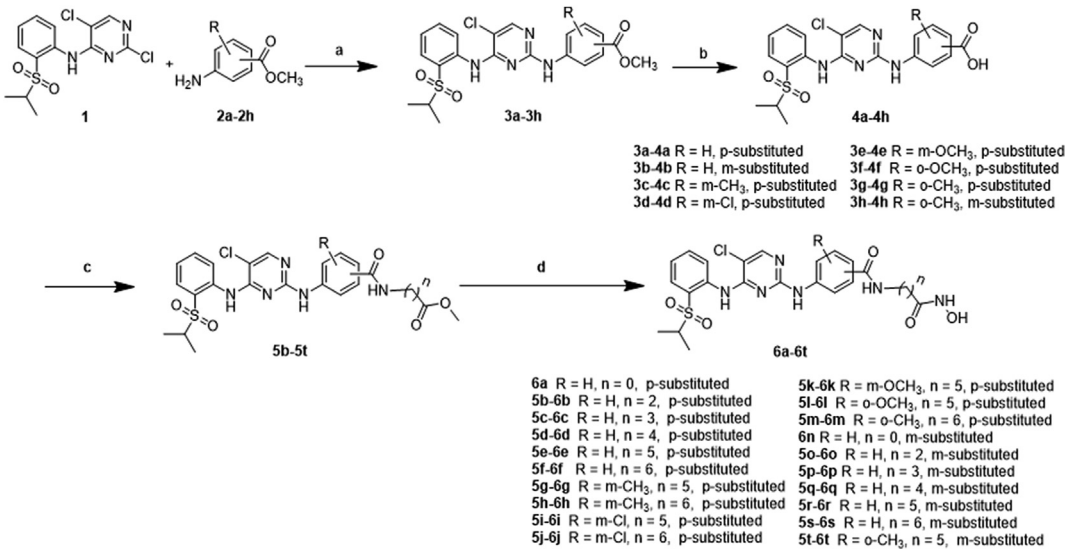

Scheme 1. *Reagents and conditions*: (a) HCl, *i*-PrOH, 90 °C, 6 h, 57.1%–72.4%; (b) 35% NaOH aqueous solution, 50 °C, 3 h, 62.5%–97.7%; (c) corresponding methyl aminoalkanoates, EDCI, HOBT, DIPEA, CH_2Cl_2, r.t., 12 h, 37.9%–71.2%; and (d) NH_2OH, KOH, CH_3OH, 0 °C, 2 h, 20.6%–66.6%.

directly converted into hydroxamic acid target compounds **10a-j** by NH_2OH/KOH in dry methanol. In Scheme 3, intermediates **13a-m** were afforded in a similar way employing aromatic amines **11a-j** and substituted-2,4-dichloropyrimidines **12a-e** as starting materials. Next, condensation of **13a-m** with monomethyl suberate catalyzed by EDCI/HOBT produced compounds **14a-m**, which were finally transferred into hydroxamic acid target compounds **16a-m** under the same reaction conditions.

The synthetic route to desired compound **20** is illustrated in Scheme 4. Reaction of compound **1** with 4-bromoaniline in the catalysis of hydrochloride in isopropanol produced intermediate **18** which subsequently underwent a standard Heck coupling reaction with methyl acrylate in the presence of $Pd(OAC)_2$ to yield intermediate **19.** Finally, treatment of compound **19** with NH_2OH/KOH in methanol yielded target compound **20**.

2.2. Biological evaluation

2.2.1. In vitro ALK and HDAC kinase inhibition assays of target compounds

All synthetic compounds were subjected to ALK^{wt} and HDAC1 enzymatic inhibition assays in which SAHA and Crizotinib were employed as positive controls to validate our hypothesis. Fortunately, as presented in Table 1, all designed compounds retained significant potency toward ALK^{wt} at the 10 nM concentration and remained as potent as Crizotinib, thereby demonstrating that modifications to the piperidine part would be permissible. More interestingly, a subset of these analogs demonstrated promising potency against HDAC1 kinase simultaneously, especially compound **6f,** displayed HDAC inhibitory activity that was comparable to that of SAHA, with an IC_{50} value of 12 nM. This encouraging outcome demonstrated the rationality of our design strategy and prompted us to further investigate preliminary SAR. Unsurprisingly, it was found that shortening the linker length (compounds **6a-d**) dramatical decreased the HDAC1 inhibitory activities, which was likely due to the attenuated chelating interaction between the hydroxamic acid group and the zinc cation [34]. For example, compound **6a** (IC_{50} = 495 nM) was over 10-fold less potent than compound **6f**. A similar trend was also observed for aniline derivatives **10a-f**, among which compound **10f,** which has an optimal length of six carbons, elicited the most potent inhibitory activity, with an IC_{50} value of 7.9 nM as well. However, in contrast to the linker length, which plays a key role in HDAC inhibition, the carbon number had no readily observable influence on ALK inhibition

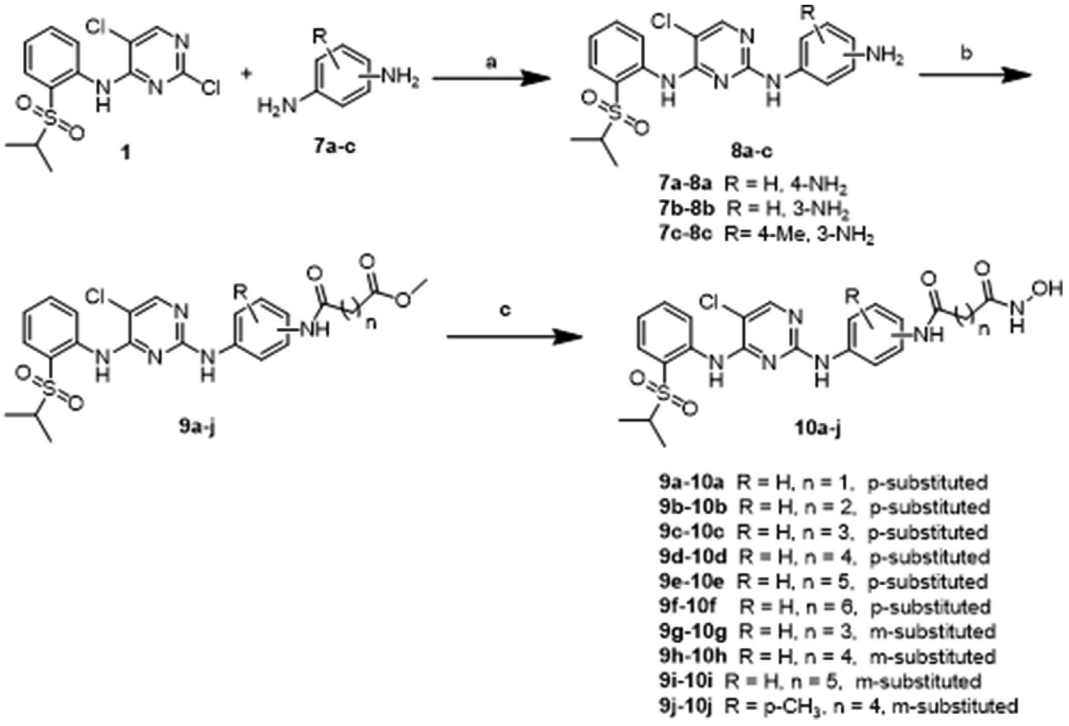

Scheme 2. *Reagents and conditions*: (a) HCl, *i*-PrOH, 90 °C, 6 h, 42.6%–59.9%; (b) corresponding mono-methyl dicarboxylates, EDCI, HOBT, DIPEA, CH_2Cl_2, r.t., 12 h, 31.5%–65.4%; and (c) NH_2OH, KOH, CH_3OH, 0 °C, 2 h, 40.0%–81.2%.

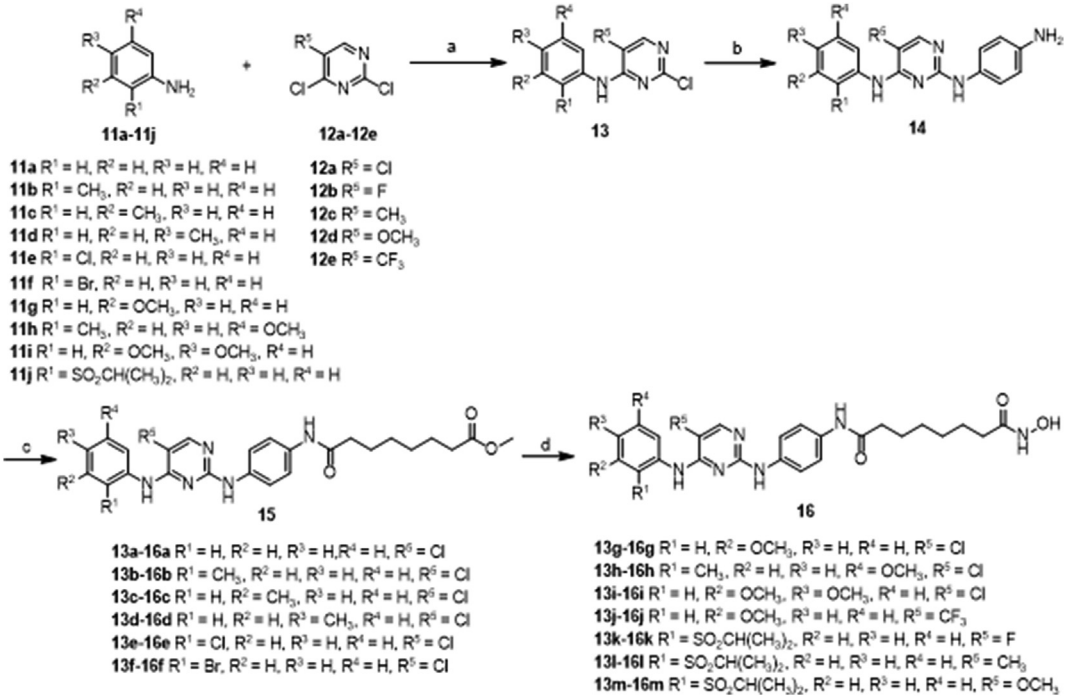

Scheme 3. *Reagents and conditions*: (a) DIPEA, *i*-PrOH, 85 °C, 6 h or NaH, DMF, 0 °C, 2 h, 30.2%–85.7%; (b) TsOH, *i*-PrOH, 90 °C, 6 h, 55.4%–76.6%; (c) monomethyl suberate, EDCI, HOBT, DIPEA, DMF, r.t., 12 h, 30.5%–77.2%; and (d) NH_2OH, KOH, CH_3OH, 0 °C, 2 h, 68.5%–89.3%.

based on the results for compounds **6a-f** and **10a-i**.

To explore the substituent effects on the binding efficiency, CH_3, Cl and OCH_3 groups were introduced at the C2-position or C3-position of the *N*2-phenyl ring. Target compounds that containing CH_3 groups were slightly more active against HDAC1 compared with the corresponding Cl- and OCH_3-substituted compounds (**6h** vs **6j** and **6k**, and **6m** vs **6l**), hence, a small electron-donating group in the *N*2-phenyl ring may be favorable for HDAC1 inhibition. In addition, shifting the linker from the para-to meta-position resulted in compounds **6n-t**, which exhibited reduced potency

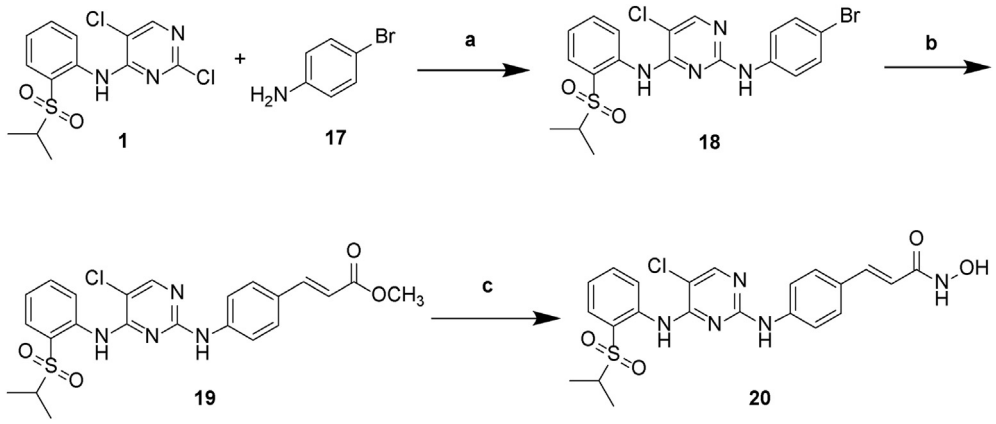

Scheme 4. *Reagents and conditions*: (a) HCl, *i*-PrOH, 90 °C, 6 h; (b) methyl acrylate, $Pd(OAc)_2$, tri(*o*-tolyl)phosphine, CH_3CN, DMF, 90 °C, 6 h; and (c) NH_2OH, KOH, CH_3OH, 0 °C, 2 h.

compared to compounds **6a-d** with the same carbon chain in enzyme assays. This SAR result suggested that the para-substituted side chain might be more accessible for occupation of the tunnel in HDAC proteins. Optimization was further conducted to identify the contributions of various linkers to the potency. Unfortunately, replacement of the alkyl with a cinnamic linkage as in Panobinostat led to compound **20**, which suffered an HDAC1 inhibition potency loss.

Next, we replaced 2-isopropylsulphonyl with different groups and continued to further investigate the SARs based on **10f**. As shown in Table 2, when 2-isopropylsulphonyl was substituted by CH_3, OCH_3, Cl, and Br at different positions, a dramatic loss of ALK potency was observed, which demonstrated that 2-isopropylsulphonyl group was important and showed a decisive effect on ALK inhibitory (Table 2, **16a-l**). On the other hand, the target compounds with different substituents such as F, OCH_3, and CH_3 groups at R5-position in pyrimidine ring were well tolerated in both ALK and HDAC1 as compound **10f** dose (Table 2, **16k-m**).

In view of the encouraging potencies that were demonstrated by compounds **6f** and **10f** on ALK^{wt} and HDAC1, the activity and selectivity profiles of these two compounds were further evaluated using two common ALK mutant enzymes and three HDAC kinase subtypes. Overall, as presented in Table 3, both selected compounds displayed almost equivalent inhibition toward HDAC1, HDAC2 and HDAC6, which is in line with the positive control SAHA. Moreover, compounds **6f** (IC_{50} = 2.4 nM) and **10f** (IC_{50} = 1.7 nM) showed satisfactory inhibitory activities against the ALK^{L1196M} mutant, which was regarded as being responsible for Crizotinib (IC_{50} = 16 nM) resistance. More strikingly, in the case of the ALK^{G1202R} mutant, to which the drug resistance of Ceritinib is attributed, compound **10f** (IC_{50} = 0.4 nM) showed almost 10-fold superior activity to Ceritinib (IC_{50} = 3.3 nM) and fourth-generation ALK inhibitor Repotrectinib (IC_{50} = 4.5 nM), thereby suggesting that compound **10f** might be a promising ALK inhibitor for overcoming the G1202R mutant.

2.2.2. *Anti-proliferative activities of compounds **6f** and **10f** against cancer cell lines*

A CCK-8 assay was conducted to evaluate the antiproliferative activities of compounds **6f** and **10f** on the HepG2 (liver cancer), MDA-MB-231 (breast cancer), A549, H2228 (NSCLC), SK-N-BE2, and SH-SY5Y (neuroblastoma) cancer cell lines. As shown in Table 4, both compounds **6f** and **10f** displayed similar activities to positive controls SAHA and Ceritinib, with approximately 1 μM IC_{50} values for the MDA-MB-231, A549 and HepG2 cell lines. Moreover, for the SK-N-BE2, SH-SY5Y (F1174L) and H2228 (EML4-ALK) ALK-addicted cancer cells, compounds **6f** and **10f** demonstrated almost 3- to 20-fold higher anticancer activities than the reference compounds Ceritinib and Crizotinib. Especially in H2228 cells, compounds **6f** and **10f** displayed potent activities with IC_{50} values of 0.18 and 0.13 μM, respectively. These results demonstrate that the dual inhibitors may exhibit enhanced antiproliferative capacities.

2.2.3. *Effect of compound **10f** on the proliferative ability of cancer cells*

Since compound **10f** showed desirable activity according to enzyme and cell viability assays, it was selected for further exploration. Colony formation was conducted to determine the effect of compound **10f** on the proliferative ability of cancer cells. In this assay, MDA-MB-231 and SH-SY5Y cells were selected and exposed to various concentrations of compound **10f** (0.1 μM, 0.2 μM, and 0.4 μM) for 72 h. Then, the cells were cultured in a fresh medium for another two weeks. The results in Fig. 3 demonstrate that the numbers of clones in the **10f** treatment group were significantly reduced compared with those in the control group. The results demonstrate that the proliferation activities of MDA-MB-231 and SH-SY5Y cells were remarkably decreased by compound **10f**, which is in accordance with the CCK-8 assay results.

2.2.4. *Effects of compound **10f** on cell migration and repair capability*

In addition, a cell scratch assay was conducted to examine the effects of compound **10f** on cell migration and repair capability. MDA-MB-231 and SH-SY5Y cells were cultured with compound **10f** at three concentrations (0.1 μM, 0.2 μM, and 0.4 μM) for 48 h. The migration of both tested cell lines was apparently suppressed by compound **10f** (Fig. 4). The wound of MDA-MB-231 in the control group showed 30.3% closure after 48 h, while the wound was decreased to 3.7% with **10f** treatment (0.4 μM). A similar result was observed in SH-SY5Y cells, as the wound was 2.8% in the **10f** treatment group versus 15.1% in the control group. These results demonstrate that compound **10f** can suppress cell migration and repair capability.

2.2.5. *Effects of compound **10f** on cell apoptosis and cell cycle*

To preliminarily investigate whether compound **10f** induces apoptosis of MDA-MB-231 cells, AO/EB and Hoechst 33258 staining were conducted after compound **10f** treatment for 24 h. According to the results of AO/EB staining, the orange-red fluorescence was emerged in the cells after treated with different concentrations of **10f** (1.0 μM, 2.0 μM, and 4.0 μM) or Ceritinib (4.0 μM) (Fig. 5A). Moreover, the results of Hoechst 33258 staining further supported

Table 1
Inhibitory activities of target compounds against the ALK^{wt} and HDAC1 kinases.

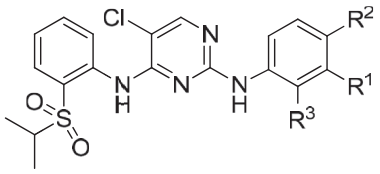

Cops.	R^1	R^2	R^3	HDAC1 inhibition[a] (%)		ALK^{wt} inhibition (%)	
				@10 nM	@100 nM	@10 nM	@100 nM
6a	H		H	0.1	ND[b]	81.1	ND
6b	H	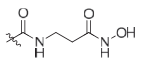	H	−1	3	86.7	97.3
6c	H	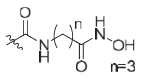	H	−2	4	91.2	97.9
6d	H	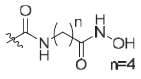	H	8	31	85.2	98.8
6e	H	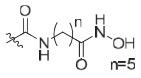	H	55	101	89.4	98.1
6f	H	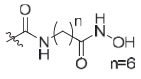	H	49	100	84.5	102.7
6g	CH_3	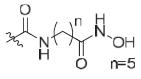	H	48	93	97.8	101.5
6h	CH_3	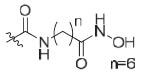	H	35	78	98.1	101.1
6i	Cl	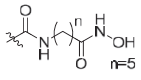	H	45	93	87.7	97.8
6j	Cl	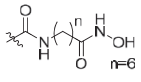	H	24	67	70.3	100.4

Table 1 (*continued*)

Cops.	R^1	R^2	R^3	HDAC1 inhibition[a] (%)		ALK^{wt} inhibition (%)	
				@10 nM	@100 nM	@10 nM	@100 nM
6k	OCH_3	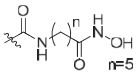	H	26	74	99.0	100.9
6l	H	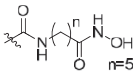	OCH_3	45	86	97.3	98.5
6m	H	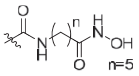	CH_3	58	96	93.1	97.3
6n		H	H	−3	ND	ND	ND
6o	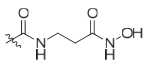	H	H	−1	4	81.0	99.1
6p	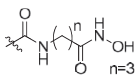	H	H	4	44	85.7	98.0
6q	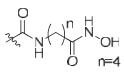	H	H	23	65	81.0	97.7
6r	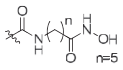	H	H	35	84	83.2	97.3
6s	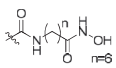	H	H	41	84	82.6	96.6
6t	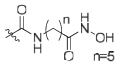	H	CH_3	7	49	86.8	98.5
10a	H	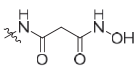	H	−10	−7	92.1	98.2
10b	H	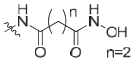	H	−2	ND	ND	ND

(*continued on next page*)

Table 1 (*continued*)

Cops.	R^1	R^2	R^3	HDAC1 inhibition[a] (%)		ALK^{wt} inhibition (%)	
				@10 nM	@100 nM	@10 nM	@100 nM
10c	H	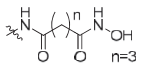	H	4	17	87.6	98.5
10d	H	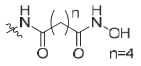	H	−8	20	84.7	99.0
10e	H	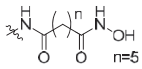	H	52	90	86.5	98.8
10f	H	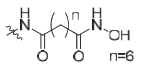	H	54	87	80.8	96.6
10g	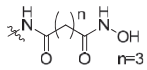	H	H	38	83	87.0	98.1
10h	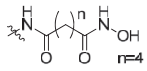	H	H	10	41	87.2	98.0
10i	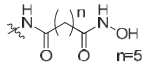	H	H	55	86	89.4	98.0
10j	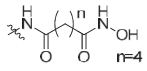	CH_3	H	8	39	76.9	98.5
20	H	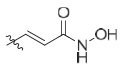	H	0	3	71.6	101.1
Crizotinib				2.6 nM			
SAHA						12 nM	

[a] The values indicate the kinase inhibition percentages at 10 nM and 100 nM, which are the average values from two independent experiments.
[b] Not determined.

the results of the AO/EB staining. As shown in Fig. 5B, the uneven blue fluorescence was gradually enhanced accompanied with the escalation of the compound concentration**,** and the apoptosis promoting effect of compound **10f** was stronger than that of Ceritinib at 4.0 μM.

Flow cytometry was conducted to further determine whether the anti-proliferation effect that was induced by compound **10f** was related to apoptosis in MDA-MB-231 and SH-SY5Y cells. Both cell lines were incubated with compound **10f** at three concentrations (1.0 μM, 2.0 μM, and 4.0 μM) and with positive control Ceritinib (1.0 μM) for 24 h. Annexin V-FITC and PI staining methods were used for apoptosis analysis, and the percentage of apoptotic cells was defined as the sum of the percentages for early and late apoptosis. As shown in Fig. 6A, both cell lines displayed an increasing dose-dependent apoptosis rate after 24 h of incubation with compound **10f**. In MDA-MB-231 cells, the apoptosis rate was increased from 5.92% (control) to 19.27% (**10f,** 4.0 μM). Likewise, the apoptosis rate in SH-SY5Y cells that were treated with compound **10f** was 22.26% at a concentration of 1.0 μM, which was comparable to that of Ceritinib at 1.0 μM (Fig. 6C).

Next, Annexin V-FITC/PI was conducted to determine compound **10f** induced cell cycle arrest in MDA-MB-231 and SH-SY5Y cells. Then, the DNA content was analyzed to identify the effect of compound **10f** on the cell cycle (Fig. 6B). In MDA-MB-231 cells, the percentage of cells in the G2 phase when treated with compound **10f** increased significantly from 13.23% to 48.70%, 75.94% and

Table 2
Inhibitory activities of target compounds **16a-m** against the ALK^{wt} and HDAC1 kinases.

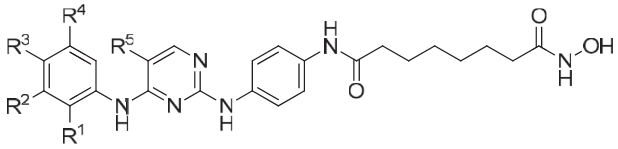

Cops.	R^1	R^2	R^3	R^4	R^5	HDAC1 inhibition[a] (%)		ALK^{wt} inhibition (%)	
						@10 nM	@100 nM	@10 nM	@100 nM
16a	H	H	H	H	Cl	84	99	4.9	36.9
16b	CH_3	H	H	H	Cl	91	99	1.2	27.8
16c	H	CH_3	H	H	Cl	ND [b]	ND	0.2	4.9
16d	H	H	CH_3	H	Cl	86	97	7.2	30.1
16e	Cl	H	H	H	Cl	67	90	3.1	21.2
16f	Br	H	H	H	Cl	67	88	0.2	25.0
16g	H	OCH_3	H	H	Cl	83	97	1.2	20.0
16h	CH_3	H	H	OCH_3	Cl	ND	ND	−0.7	4.9
16i	H	OCH_3	OCH_3	H	Cl	65	94	3.1	17.6
16j	H	OCH_3	H	H	CF_3	56	89	4.9	7.6
16k		H	H	H	F	70	94	66.3	96.0
16l		H	H	H	CH_3	63	93	83.5	97.9
16m		H	H	H	OCH_3	68	91	60.4	94.9

[a] The values indicate the kinase inhibition percentages at 10 nM and 100 nM, which are the average values from two independent experiments.
[b] Not determined.

Table 3
Inhibitory activities of compounds **6f** and **10f** against ALK and HDAC kinases[a].

Compd.	IC_{50} (nM)					
	HDAC1	HDAC2	HDAC6	ALK^{wt}	ALK^{L1196M}	ALK^{G1202R}
6f	12	15	6.7	4.3	2.4	1.0
10f	7.9	9.3	4.4	2.1	1.7	0.4
SAHA	12	12	10	ND[b]	ND	ND
Ceritinib	ND	ND	ND	<1.0	0.25	3.3
Crizotinib	ND	ND	ND	2.6	16	12
Repotrectinib	ND	ND	ND	ND	ND	4.5

[a] The reported data are the mean values from two independent experiments.
[b] Not determined.

88.07% in a dose-dependent manner. This trend was also observed in SH-SY5Y cells. Compared with the untreated group, the percentage of cells in the G2 phase increased from 23.89% to 50.99%, which was accompanied by a dramatic loss of G1-and S-phase populations (Fig. 6D). According to these results, compound **10f** could induce cell death via cell apoptosis and G2 phase arrest.

2.2.6. Cellular effects of compound *10f* on HDAC- and ALK-mediated signaling pathways

A Western blot analysis was conducted to further evaluate the intracellular effects of compound **10f** on the HDAC- and ALK-

Table 4
Anti-proliferative activities of compounds **6f** and **10f** against cancer cell lines [a].

Compd.	Cell lines/IC_{50} (μM)					
	HepG2	MDA-MB-231	A549	SK-N-BE2 (ALK wt)	SH-SY5Y(F1174L)	H2228 (EML4-ALK)
6f	0.91 ± 0.19	0.39 ± 0.02	3.42 ± 0.21	0.22 ± 0.01	0.34 ± 0.01	0.18 ± 0.11
10f	0.64 ± 0.07	0.46 ± 0.06	0.46 ± 0.08	0.05 ± 0.01	0.11 ± 0.02	0.13 ± 0.05
SAHA	1.43 ± 0.17	0.61 ± 0.09	0.59 ± 0.02	0.77 ± 0.11	0.73 ± 0.04	ND[b]
Ceritinib	4.08 ± 0.27	1.82 ± 0.63	2.16 ± 0.10	2.66 ± 0.20	0.37 ± 0.10	1.98 ± 0.13
Crizotinib	0.32 ± 0.06	0.79 ± 0.06	0.41 ± 0.12	0.78 ± 0.03	0.32 ± 0.01	2.62 ± 0.21

[a] The reported data are the mean values from three independent experiments.
[b] Not determined.

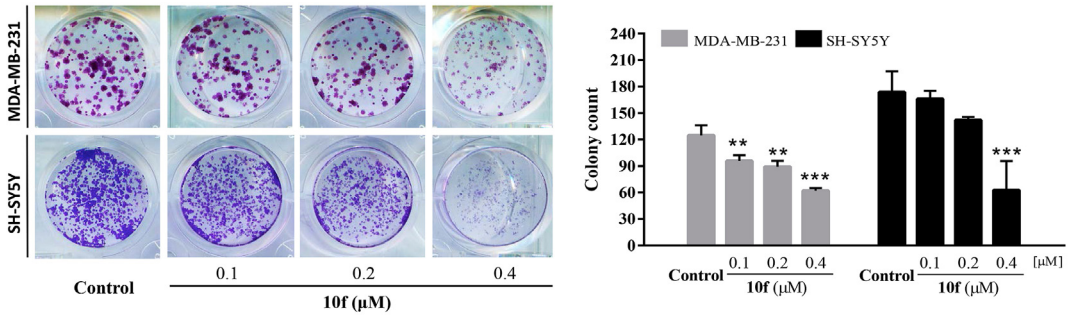

Fig. 3. Effects of compound **10f** on the antiproliferative activities of MDA-MB-231 and SH-SY5Y cells according to colony formation experiments. SH-SY5Y and MDA-MB-231 cells (400/well) were cultured with concentrations of compound **10f** of 0.1, 0.2 and 0.4 μM for 3 days. Then, the cells were imaged after an additional 12 days of drug-free medium incubation. A bar chart representation of the colonies that formed after treatment with compound **10f** is presented. The data are presented as the mean ± SD of three independent experiments. Colony counts are presented in the bar chart. The data are presented as the mean ± SD (n = 3), with **p < 0.01 and ***p < 0.001 compared with the control.

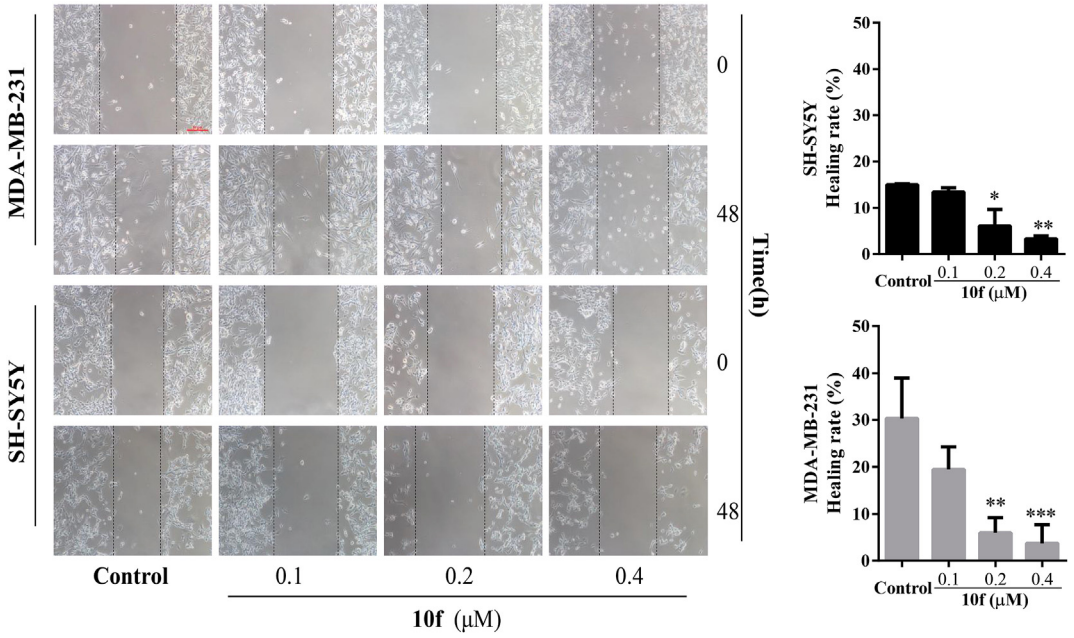

Fig. 4. Representative images and quantitative analysis of a cell scratch assay for the MDA-MB-231 and SH-SY5Y cell lines. The healing rates are presented as the mean ± SD (n = 3), where **p < 0.01 and ***p < 0.001, compared with the control.

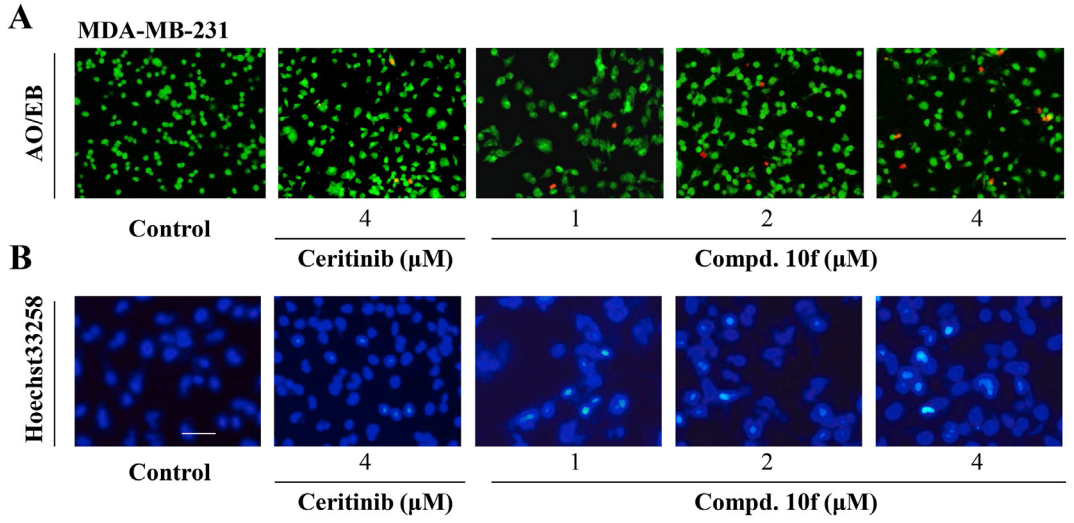

Fig. 5. MDA-MB-231 cells were treated with compound **10f** (1.0, 2.0, 4.0 μM) or Ceritinib (4.0 μM) for 24 h, then stained with AO/EB (A) or Hoechst 33258 (B) and photographed.

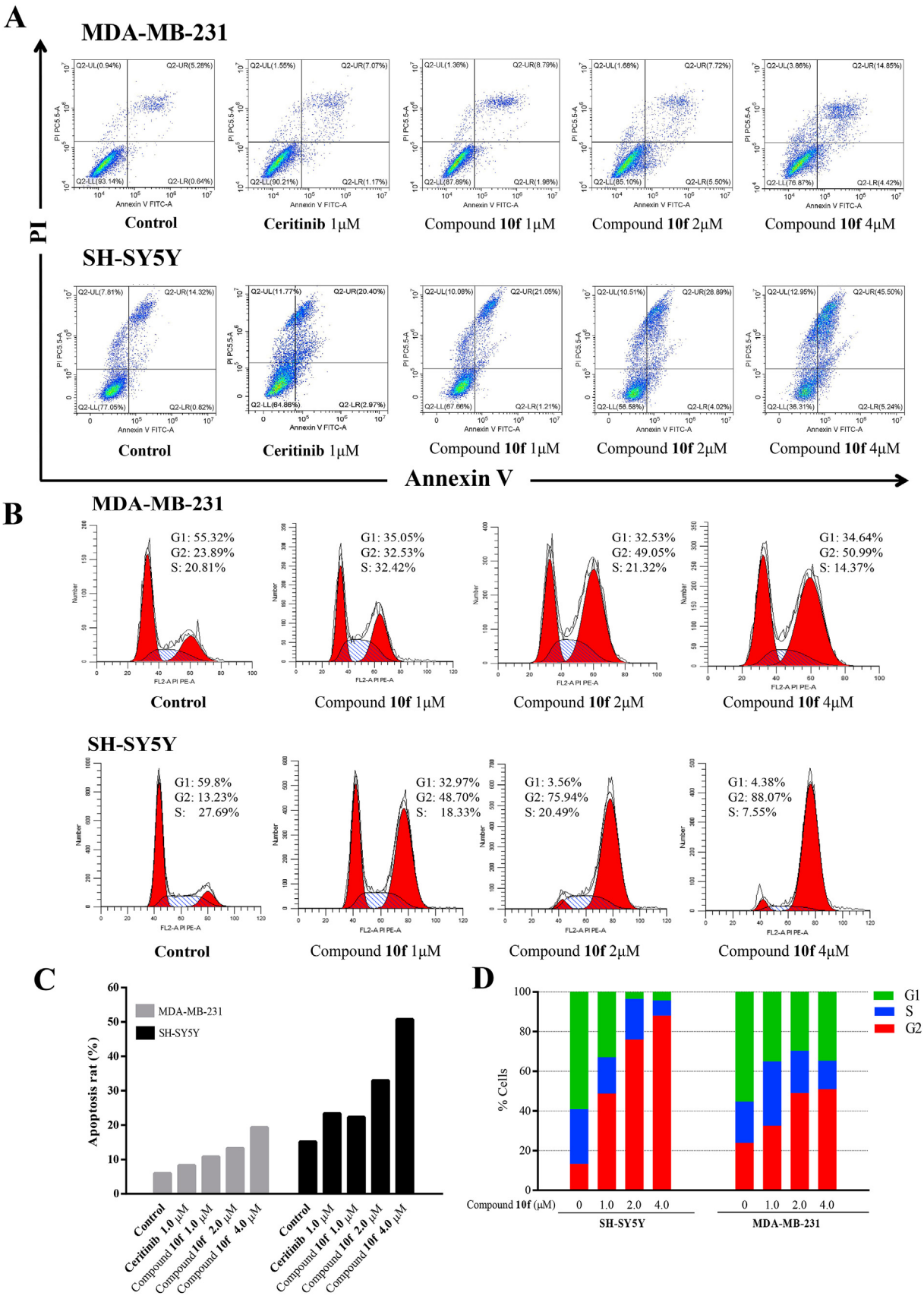

Fig. 6. (A) Flow cytometry was used to identify the impact of compound **10f** on cell apoptosis in the MDA-MB-231 and SH-SY5Y cell lines. Both cell lines were treated with compound **10f** and Ceritinib for 24 h and stained with an FITC Annexin V/PI kit. Cells in the upper-right quadrant correspond to PI-positive/Annexin V-positive, late apoptotic or necrotic cells, and cells in the lower-right quadrant correspond to early apoptotic cells. (B) Both cell lines were treated with compound **10f** at concentrations of 1.0, 2.0 and 4.0 μM

mediated signaling pathways. After exposure to compound **10f** (at 1.0 μM, 2.0 μM, and 4.0 μM) for 24 h, increasing levels of intracellular acetylated histone 3 (Ac-H3), which is regarded as a marker of HDAC 1/2/3 inhibition, were observed in the MDA-MB-231 and SH-SY5Y cell lines as expected, although the efficacy was inferior to that of SAHA (Fig. 7). Meanwhile, the selected compound was also found to suppress the ALK-mediated signaling pathway in a dose-dependent manner (Fig. 8). Accordingly, it was demonstrated that the levels of phosphorylation of ALK and its key downstream proteins, namely, *p*-AKT and *p*-ERK, were significantly blocked by compound **10f** at a 4.0 μM concentration in both tested cell lines with respect to the control group. Taken together, these findings show that compound **10f** acted as a dual inhibitor that could inhibit both the HDAC 1/2/3- and ALK-mediated signaling pathways.

*2.2.7. Protein kinase selectivity and pharmacokinetic (PK) profiles of compound **10f***

Since the isopropoxy moiety in Ceritinib was responsible for the kinase selectivity and metabolic liability [35], compound **10f** was further evaluated against a panel of 123 kinases to characterize its protein kinase selectivity profile at 1 μM (Fig. 9 and Table S1). Similar to Ceritinib, compound **10f** exhibited satisfactory inhibition of the ALK, IGF-1R, InsR and FLT kinases. However, compound **10f** also led to over 95% inhibition of the Aurora, CDK and FGFR kinases. The kinase profiling indicated a relatively low kinase selectivity of compound **10f** and demonstrated the necessity of the isopropoxy group.

Next, compound **10f** was selected to investigate in vivo pharmacokinetic characteristics. Compound **10f** was administered intravenously (iv) at 1 mg/kg or orally (po) at 10 mg/kg to Sprague-Dawley (SD) rats. As presented in Table 5, the clearance rate (CL) of compound **10f** was 88.6 mL/min/kg, hence, the compound was rapidly cleared with a short terminal half-life of 0.42 h. The oral bioavailability was also measurable, however, no results were detected, which was likely due to the low permeability or aqueous solubility of **10f** [36]. These results suggested that **10f** has poor PK properties, and further optimization of **10f** is necessary prior to in vivo studies.

2.3. Molecular docking studies

To better explain the interaction between compound **10f** and ALK or HDAC, molecular docking studies of compound **10f** in ALK^{wt} (PDB ID: 4MKC) and HDAC2 (PDB ID: 4LXZ) were conducted using Softwire Discovery Studio 2018. As shown in Fig. 10A, compound **10f** could occupy the ATP binding site of ALK similarly to Ceritinib. The 2-aminopyrimidine fragment could interact with M1199 via a hydrogen bond in the hinge region, which are critical for binding to ALK. In addition, the oxygen of the sulfonyl group was also found to form two hydrogen bonds with the amino group of the K1150 amino residue. Moreover, the "tail" of compound **10f**, which was oriented toward the solvent-exposed area, formed an additional carbon hydrogen bond with R1120, which might enhance the affinity of **10f** with ALK^{wt} (Fig. 10B).

In contrast to the ALK^{wt} model, detrimental bump interactions were induced between the piperidine ring of Ceritinib and the R1202 side chain in the G1202R mutant model, as illustrated in Fig. 10C. In comparison, the aliphatic chain of compound **10f** undergoes less steric collision with R1202, as we expected. Interestingly, the hydroxamic acid group were engaged in three additional hydrogen bonds with R1202 and G1121, which explains the increased G1202R mutant activity of compound **10f** over that of Ceritinib (Fig. 10D).

As depicted in Fig. 11A, the proposed binding mode of compound **10f** to HDAC2 was also similar to that of SAHA. For instance, two coordination bonds were formed between the oxygen atoms on the hydroxamic acid group and the zinc atom in the active site of HDAC2, which may be the key contributors to the comparable potency of compound **10f** against HDAC2 with that of SAHA. It was also found that the amide group in compound **10f** participated in a new hydrogen bond interaction with amino reside D104 (Fig. 11B).

3. Conclusion

In summary, a series of 2,4-pyrimidinediamine derivatives that target HDAC and ALK were designed and synthesized in this study. Enzyme assays demonstrated that most of these new compounds could simultaneously inhibit ALK and HDAC proteins, and representative compound **10f** exhibited potent inhibitory activity with IC_{50} values of 2.1 nM and 7.9 nM against ALK and HDAC1, respectively. Moreover, compound **10f** also showed impressive enzyme activity against the challenging Crizotinib-resistant ALK^{L1196M} (IC_{50} = 1.7 nM) and Ceritinib-resistant ALK^{G1202R} mutations (IC_{50} = 0.4 nM) and was approximately 10-fold more potent than Crizotinib and Ceritinib. The following cytotoxicity experiments showed that compound **10f** possessed comparable antiproliferative activity to Crizotinib and Ceritinib against ALK-addicted cell lines. Preliminary mechanistic studies showed that the levels of phosphorylated ALK and Ac-H3 were significantly inhibited or increased in both tested cell lines after treatment with compound **10f**, as was found for Ceritinib and SAHA. These results suggested that compound **10f** might be a promising lead compound for the treatment of NSCLC, especially Ceritinib- or Crizotinib-resistant NSCLC.

4. Experimental

4.1. Chemistry

All reagents were obtained from Adamas, tansoole and Macklin and were used without further purification unless otherwise noted. The melting point of the sample was determined by X-4 microscopic melting point instrument. Routine ^{1}H NMR and ^{13}C HNMR spectra were noted from solution in deuterated chloroform ($CDCl_3$) or dimethyl sulfoxide (DMSO-d_6) with tetramethylsilane (TMS) as internal standard using a Bruker-600 MHz spectrometer. Chemical shifts are reported in ppm and coupling constants (J) in Hz. HRMS spectra were acquired with an Aglient 6470/AB Sciex 4600 Triple Quad LC-MS apparatus. Column chromatography was performed on silica gel (200−300 mesh).

*4.1.1. General procedure for the synthesis of intermediates **3a-h***

2,5-Dichloro-*N*-(2-(isopropylsulfonyl)phenyl)pyrimidin-4-amine (1.02 g, 2.95 mmol, **1**) and methyl 4-aminobenzoate (0.48 g, 3.17 mmol, **2a**) was dissolved in 20 mL isopropanol and 0.1 mL HCl solution (37%) was added. The resulting mixture was then stirred at 90 °C for 6 h. After reaction completion, the reaction mixture was extracted with 100 mL EtOAc, then the organic layer was washed with saturated NaCl aqueous solution twice, dried overnight with anhydrous Na_2SO_4 and filtered. The resulting filtrate was concentrated under vacuum and can be directly used without further purification.

for 24 h. Then, the cells were fixed in ice-cold 70% ethanol at 4 °C and stained with propidium iodide dye, and the cell cycle was evaluated via flow cytometry. The bar graph shows the percentages of cells in apoptosis (C) or the G1, S and G2 phases (D).

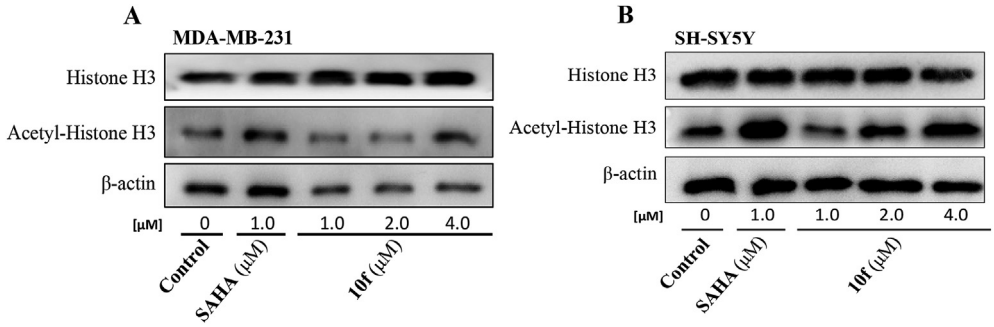

Fig. 7. Inhibitory effects of compound **10f** on Ac-H3 in the MDA-MB-231 (A) and SH-SY5Y (B) cell lines according to Western blot analysis.

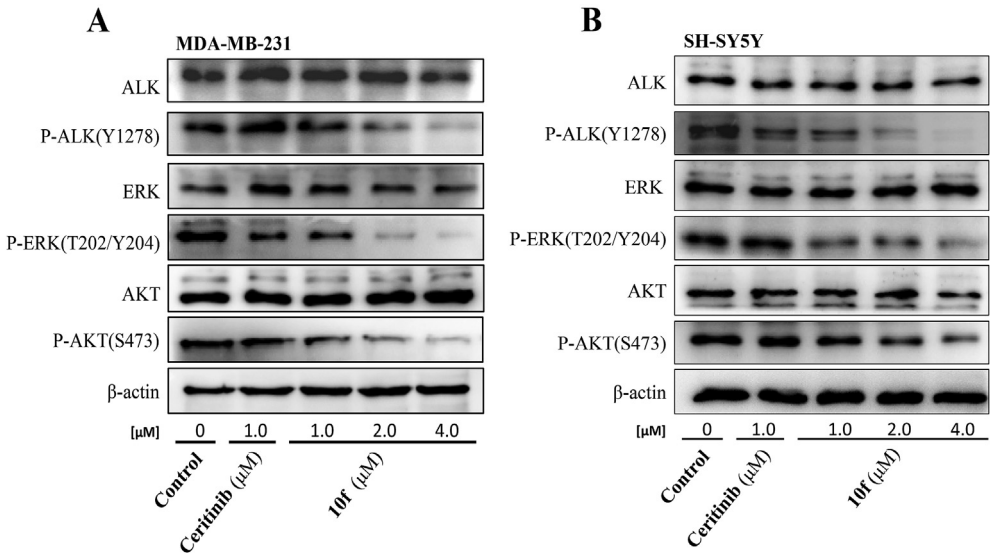

Fig. 8. Western blot analysis of ALK and its downstream pathway after treatment with compound **10f** in the MDA-MB-231 (A) and SH-SY5Y (B) cell lines.

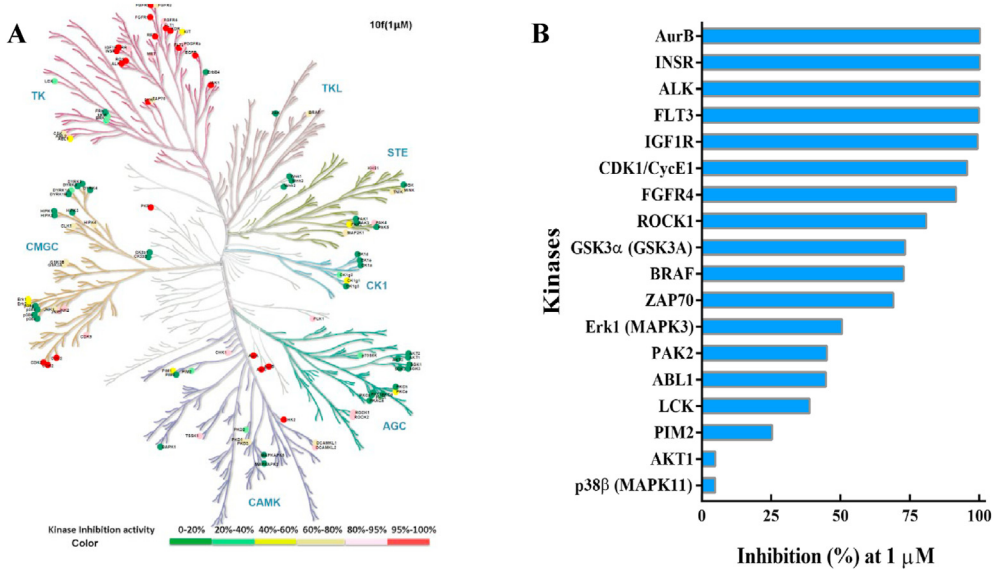

Fig. 9. (A). Distribution of kinases inhibited by compound **10f** within the human kinome. The color for inhibition is indicated. Enzymatic activities were determined in single-dose duplicates at concentrations of 1 μM. Staurosporine served as a positive control. The experiment was performed by ICE bioscience (Beijing, China). (B). Inhibition rate of compound **10f** against some representative kinases.

Table 5
PK properties of compound **10f** in SD rats (N = 3).

Comp.	Dose (mg/kg)	Route	$AUC_{0-\infty}$ (h·ng/mL)	C_{max} (ng/mL)	CL (mL/min/kg)	$MRT_{0-\infty}$ (h)	Vss (L/kg)	$t_{1/2}$ (h)
10f	1	iv.	205.1	1480.0	88.6	0.13	3.3	0.42

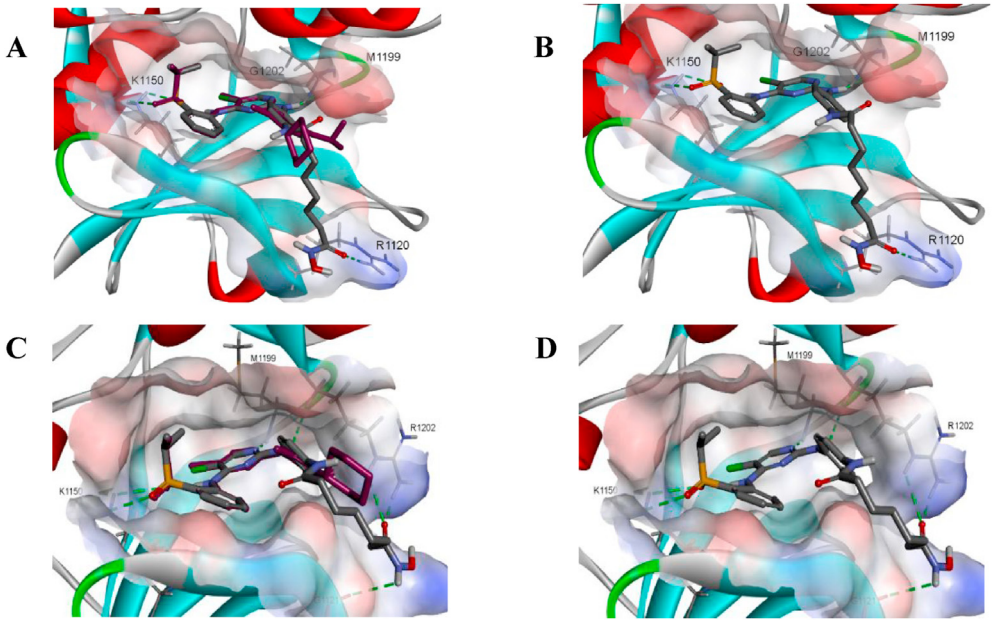

Fig. 10. (A). The overlap of the proposed binding modes of compound **10f** (Grey) and Ceritinib (Purple) in ALK^{wt} (PDB ID: 4MKC). (B). The predicted binding mode for compound **10f** in the binding site cavity of ALK^{wt} (C). The predicted binding modes of both Ceritinib and compound **10f** in the binding site cavity of ALK^{G1202R}. (D). The predicted binding modes of compound **10f** in the binding site cavity of ALK^{G1202R}. Green dashed lines indicate hydrogen bonds.

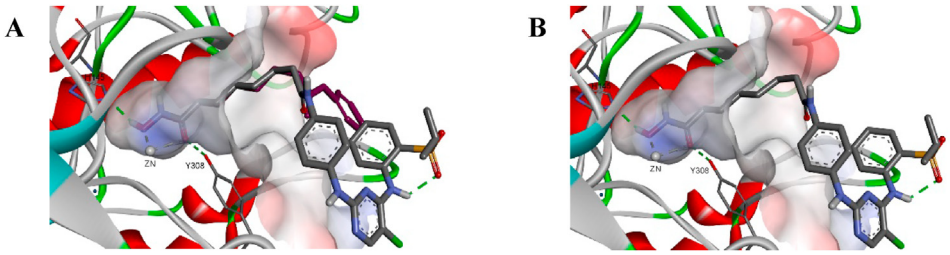

Fig. 11. (A). The overlap of the proposed binding modes of compound **10f** (Grey) and SAHA (Purple) in HDAC2 (PDB ID: 4LXZ). (B). The predicted binding mode of compound **10f** in the binding site cavity of HDAC2. Green dashed lines indicate hydrogen bonds, and grey dashed lines indicate metal interactions.

*4.1.2. General procedure for the synthesis of intermediates **4a-h***

*4.1.2.1. 4-((5-Chloro-4-((2-(isopropylsulfonyl)phenyl)amino)pyrimidin-2-yl)amino)benzoic acid (**4a**).* **3a** (1.80 g, 3.61 mmol) was added into 15 mL 35% NaOH aqueous solution and 5 mL EtOH. The mixture was then stirred at 50 °C for 3 h and the solution finally became clear. The pH of the reaction mixture was adjusted to 5–6 with 2 N HCl, the precipitate was collected by filtration, washed with water and dried under vacuum to afford 1.60 g of intermediate **4a** as a white solid. Yield: 91.6%. M.p. 272–274 °C. ^{1}H NMR (600 MHz, DMSO-d_6) δ 12.55 (s, 1H), 9.94 (s, 1H), 9.48 (s, 1H), 8.52 (d, J = 7.5 Hz, 1H), 8.37 (s, 1H), 7.89 (dd, J = 7.9, 1.4 Hz, 1H), 7.85–7.81 (m, 1H), 7.79 (d, J = 8.8 Hz, 2H), 7.74 (d, J = 8.7 Hz, 2H), 7.50–7.43 (m, 1H), 3.51–3.40 (m, 1H), 1.16 (d, J = 6.8 Hz, 6H). MS (ESI) m/z: $[M+H]^+$: 447.1.

*4.1.2.2. 3-((5-Chloro-4-((2-(isopropylsulfonyl)phenyl)amino)pyrimidin-2-yl)amino)benzoic acid (**4b**).* White solid. Yield: 62.5%. M.p. 235–237 °C. ^{1}H NMR (600 MHz, DMSO-d_6) δ 12.87 (s, 1H), 9.74 (s, 1H), 9.52 (s, 1H), 8.61 (s, 1H), 8.34 (s, 1H), 8.19 (s, 1H), 7.89 (dd, J = 4.8, 3.0 Hz, 1H), 7.85 (dd, J = 8.0, 1.5 Hz, 1H), 7.72 (t, J = 7.4 Hz, 1H), 7.54 (d, J = 7.7 Hz, 1H), 7.37 (q, J = 7.5 Hz, 2H), 3.47–3.43 (m, 1H), 1.17 (d, J = 6.7 Hz, 6H). MS (ESI) m/z: $[M+H]^+$: 447.1.

*4.1.2.3. 4-((5-Chloro-4-((2-(isopropylsulfonyl)phenyl)amino)pyrimidin-2-yl)amino)-2-methylbenzoic acid (**4c**).* White solid. Yield: 93.5%. M.p. > 250 °C. ^{1}H NMR (600 MHz, DMSO-d_6) δ 12.39 (s, 1H), 9.82 (s, 1H), 9.45 (s, 1H), 8.52 (d, J = 7.2 Hz, 1H), 8.35 (s, 1H), 7.88 (dd, J = 8.0, 1.4 Hz, 1H), 7.81–7.73 (m, 2H), 7.59–7.49 (m, 2H), 7.47–7.40 (m, 1H), 3.51–3.41 (m, 1H), 2.42 (s, 3H), 1.16 (d, J = 6.8 Hz, 6H). MS (ESI) m/z: $[M+H]^+$: 461.1.

*4.1.2.4. 2-Chloro-4-((5-chloro-4-((2-(isopropylsulfonyl)phenyl)amino)pyrimidin-2-yl)amino)benzoic acid (**4d**).* White solid. Yield: 97.7%. M.p. 98–100 °C. 1H NMR (600 MHz, DMSO-d_6) δ 12.89 (s, 1H),

10.03 (s, 1H), 9.47 (s, 1H), 8.47 (d, J = 7.5 Hz, 1H), 8.39 (s, 1H), 7.94 (d, J = 1.4 Hz, 1H), 7.88 (dd, J = 8.0, 1.5 Hz, 1H), 7.84–7.80 (m, 1H), 7.75 (d, J = 8.7 Hz, 1H), 7.57 (dd, J = 8.6, 1.5 Hz, 1H), 7.47–7.42 (m, 1H), 3.50–3.42 (m, 1H), 1.16 (d, J = 6.8 Hz, 6H). MS (ESI) m/z: $[M+H]^+$: 481.0.

*4.1.2.5. 4-((5-Chloro-4-((2-(isopropylsulfonyl)phenyl)amino)pyrimidin-2-yl)amino)-2-methoxybenzoic acid (**4e**).* White solid. Yield: 97.7%. M.p. 214–215 °C. ^{1}H NMR (600 MHz, DMSO-d_6) δ 12.11 (s, 1H), 9.86 (s, 1H), 9.48 (s, 1H), 8.54 (d, J = 7.3 Hz, 1H), 8.39 (s, 1H), 7.88 (dd, J = 8.0, 1.5 Hz, 1H), 7.82–7.76 (m, 1H), 7.62 (d, J = 8.6 Hz, 1H), 7.46–7.40 (m, 2H), 7.35 (d, J = 8.4 Hz, 1H), 3.63 (s, 3H), 3.52–3.45 (m, 1H), 1.17 (d, J = 6.8 Hz, 6H). MS (ESI) m/z: $[M+H]^+$: 477.1.

*4.1.2.6. 4-((5-Chloro-4-((2-(isopropylsulfonyl)phenyl)amino)pyrimidin-2-yl)amino)-3-methoxybenzoic acid (**4f**).* White solid. Yield: 95.3%. M.p. 88–90 °C. ^{1}H NMR (600 MHz, DMSO-d_6) δ 10.05 (s, 1H), 9.17 (s, 1H), 8.50 (s, 1H), 8.19 (d, J = 7.9 Hz, 1H), 7.93 (dd, J = 7.9, 1.4 Hz, 1H), 7.85–7.75 (m, 2H), 7.57 (t, J = 7.6 Hz, 1H), 7.49 (d, J = 1.7 Hz, 1H), 7.32 (dd, J = 8.4, 1.3 Hz, 1H), 3.88 (s, 3H), 3.52–3.39 (m, 1H), 1.12 (d, J = 6.8 Hz, 6H). MS (ESI) m/z: $[M+H]^+$: 477.1.

*4.1.2.7. 4-((5-Chloro-4-((2-(isopropylsulfonyl)phenyl)amino)pyrimidin-2-yl)amino)-3-methylbenzoic acid (**4g**).* White solid. Yield: 95.3%. M.p. 234–237 °C. ^{1}H NMR (600 MHz, DMSO-d_6) δ 12.70 (s, 1H), 9.59 (s, 1H), 9.02 (s, 1H), 8.53 (d, J = 8.4 Hz, 1H), 8.28 (s, 1H), 7.83–7.78 (m, 2H), 7.75 (dd, J = 8.3, 1.9 Hz, 1H), 7.68 (d, J = 8.4 Hz, 1H), 7.57–7.52 (m, 1H), 7.36–7.30 (m, 1H), 3.51–3.40 (m, 1H), 2.28 (s, 3H), 1.17 (d, J = 6.8 Hz, 6H). MS (ESI) m/z: $[M+H]^+$: 461.1.

*4.1.2.8. 3-((5-Chloro-4-((2-(isopropylsulfonyl)phenyl)amino)pyrimidin-2-yl)amino)-2-methylbenzoic acid (**4h**).* White solid. Yield: 95.3%. M.p. 230–233 °C. ^{1}H NMR (600 MHz, DMSO-d_6) δ 12.91 (s, 1H), 9.59 (s, 1H), 9.12 (s, 1H), 8.45 (s, 1H), 8.22 (s, 1H), 7.77 (d, J = 7.8 Hz, 1H), 7.62 (d, J = 7.6 Hz, 1H), 7.51 (d, J = 7.7 Hz, 1H), 7.46 (s, 1H), 7.30 (t, J = 7.7 Hz, 1H), 7.25 (t, J = 7.5 Hz, 1H), 3.47–3.40 (m, 1H), 2.34 (s, 3H), 1.16 (d, J = 6.7 Hz, 6H). MS (ESI) m/z: $[M+H]^+$: 461.1.

*4.1.3. General procedure for the synthesis of intermediates **5b-t***

*4.1.3.1. Methyl 3-(4-((5-chloro-4-((2-(isopropylsulfonyl)phenyl)amino)pyrimidin-2-yl)amino)benzamido)propanoate (**5b**).* To a 100 mL round bottle was charged with **4a** (0.80 g, 1.80 mmol), HOBT (0.27 g, 2.04 mmol), EDCI (0.40 g, 2.02 mmol), DIPEA (0.50 g, 3.83 mmol) and 20 mL DCM. The resulting solution was warmed to 30 °C, stirred at this temperature for 0.5 h, and methyl 3-aminopropionate hydrochloride (0.29 g, 2.07 mmol) was added and stirred for another 12 h. Then the reaction mixture was added into 40 mL water and extracted by DCM. The combined organic layer was successively washed with saturated NaCl twice, dried overnight with anhydrous Na_2SO_4, and filtered under reduced pressure. The resulting filtrate was concentrated under vacuum and purified by column chromatography on silica gel with DCM and methanol (30:1) to afford 0.60g of **5b** as a white crystal. Yield: 57.1%. M.p. 148–150 °C. ^{1}H NMR (600 MHz, $CDCl_3$) δ 9.63 (s, 1H), 8.50 (d, J = 8.3 Hz, 1H), 8.18 (s, 1H), 7.93 (d, J = 7.9 Hz, 1H), 7.72 (d, J = 8.2 Hz, 2H), 7.67 (t, J = 7.7 Hz, 1H), 7.61 (d, J = 8.1 Hz, 2H), 7.35–7.28 (m, 2H), 6.81 (s, 1H), 3.77–3.66 (m, 5H), 3.28–3.19 (m, 1H), 2.67 (t, J = 5.6 Hz, 2H), 1.32 (d, J = 6.8 Hz, 6H). MS (ESI) m/z: $[M+H]^+$: 532.1.

*4.1.3.2. Methyl 4-(4-((5-chloro-4-((2-(isopropylsulfonyl)phenyl)amino)pyrimidin-2-yl)amino)benzamido)butanoate (**5c**).* White solid. Yield: 71.2%. M.p. 190–192 °C. ^{1}H NMR (600 MHz, DMSO-d_6) δ 9.81 (s, 1H), 9.48 (s, 1H), 8.56 (d, J = 7.3 Hz, 1H), 8.35 (s, 1H), 8.30 (t, J = 5.6 Hz, 1H), 7.88 (dd, J = 7.9, 1.5 Hz, 1H), 7.84–7.78 (m, 1H), 7.72 (d, J = 8.8 Hz, 2H), 7.69 (d, J = 8.8 Hz, 2H), 7.44 (t, J = 7.6 Hz, 1H), 3.58 (s, 3H), 3.51–3.41 (m, 1H), 3.28–3.23 (m, 2H), 2.36 (t, J = 7.4 Hz, 2H), 1.77 (p, J = 7.2 Hz, 2H), 1.16 (d, J = 6.8 Hz, 6H). MS (ESI) m/z: $[M+H]^+$: 546.2.

*4.1.3.3. Methyl 5-(4-((5-chloro-4-((2-(isopropylsulfonyl)phenyl)amino)pyrimidin-2-yl)amino)benzamido)pentanoate (**5d**).* White solid. Yield: 68.4%. M.p. 161–164 °C. ^{1}H NMR (600 MHz, DMSO-d_6) δ 9.81 (s, 1H), 9.49 (s, 1H), 8.57 (d, J = 6.7 Hz, 1H), 8.35 (s, 1H), 8.28 (t, J = 5.6 Hz, 1H), 7.88 (dd, J = 7.9, 1.2 Hz, 1H), 7.85–7.79 (m, 1H), 7.73 (d, J = 8.8 Hz, 2H), 7.70 (d, J = 8.7 Hz, 2H), 7.44 (t, J = 7.6 Hz, 1H), 3.58 (s, 3H), 3.50–3.41 (m, 1H), 3.27–3.22 (m, 2H), 2.34 (t, J = 7.2 Hz, 2H), 1.60–1.48 (m, 4H), 1.17 (d, J = 6.8 Hz, 6H). MS (ESI) m/z: $[M+H]^+$: 560.2.

*4.1.3.4. Methyl 6-(4-((5-chloro-4-((2-(isopropylsulfonyl)phenyl)amino)pyrimidin-2-yl)amino)benzamido)hexanoate (**5e**).* White solid. Yield: 56.2%. M.p. 144–147 °C. ^{1}H NMR (600 MHz, DMSO-d_6) δ 9.71 (s, 1H), 9.57 (s, 1H), 8.66 (s, 1H), 8.42 (t, J = 5.6 Hz, 1H), 8.33 (s, 1H), 8.03 (s, 1H), 7.84 (dd, J = 7.9, 1.3 Hz, 1H), 7.76 (d, J = 6.7 Hz, 1H), 7.70–7.64 (m, 1H), 7.42 (d, J = 7.7 Hz, 1H), 7.39–7.29 (m, 2H), 3.58 (s, 3H), 3.50–3.41 (m, 1H), 3.27–3.21 (m, 2H), 2.36 (t, J = 7.4 Hz, 2H), 1.75 (q, J = 7.2 Hz, 2H), 1.38–1.30 (m, 2H), 1.28–1.23 (m, 2H), 1.17 (d, J = 6.8 Hz, 6H). MS (ESI) m/z: $[M+H]^+$: 574.2.

*4.1.3.5. Methyl 7-(4-((5-chloro-4-((2-(isopropylsulfonyl)phenyl)amino)pyrimidin-2-yl)amino)benzamido)heptanoate (**5f**).* White solid. Yield: 70.0%. M.p. 152–154 °C. ^{1}H NMR (600 MHz, $CDCl_3$) δ 9.66 (s, 1H), 8.51 (d, J = 8.3 Hz, 1H), 8.17 (d, J = 2.5 Hz, 1H), 7.93 (dd, J = 9.0, 4.0 Hz, 1H), 7.73–7.71 (m, 2H), 7.66 (t, J = 7.1 Hz, 1H), 7.62–7.60 (m, 2H), 7.5–7.45 (m, 1H), 7.30 (t, J = 7.6 Hz, 1H), 6.21–6.12 (m, 1H), 3.68 (s, 3H), 3.50–3.36 (m, 2H), 3.24–3.22 (m, 1H), 2.33–2.31 (m, 2H), 1.68–1.58 (m, 4H), 1.43–1.39 (m, 4H), 1.31 (d, J = 6.8 Hz, 6H). MS (ESI) m/z: $[M+H]^+$: 588.2.

*4.1.3.6. Methyl 6-(4-((5-chloro-4-((2-(isopropylsulfonyl)phenyl)amino)pyrimidin-2-yl)amino)-2-methylbenzamido)hexanoate (**5g**).* White solid. Yield: 64.9%. M.p. 130–132 °C. ^{1}H NMR (600 MHz, $CDCl_3$) δ 9.72 (s, 1H), 8.53 (d, J = 8.3 Hz, 1H), 8.15 (s, 1H), 7.94 (dd, J = 7.9, 1.3 Hz, 1H), 7.71–7.64 (m, 1H), 7.58 (s, 1H), 7.40–7.38 (m, 2H), 7.34–7.29 (m, 2H), 5.88 (s, 1H), 3.68 (s, 3H), 3.48–3.41 (m, 2H), 3.29–3.20 (m, 1H), 2.42 (s, 3H), 2.36 (t, J = 7.4 Hz, 2H), 1.70–1.62 (m, 4H), 1.49–1.40 (m, 2H), 1.33 (d, J = 6.8 Hz, 6H). MS (ESI) m/z: $[M+H]^+$: 588.2.

*4.1.3.7. Methyl 7-(4-((5-chloro-4-((2-(isopropylsulfonyl)phenyl)amino)pyrimidin-2-yl)amino)-2-methylbenzamide) heptanoate (**5h**).* White solid. Yield: 47.0%. M.p. 78–80 °C. ^{1}H NMR (600 MHz, $CDCl_3$) δ 9.68 (s, 1H), 8.51 (d, J = 8.2 Hz, 1H), 8.15 (s, 1H), 7.93 (dd, J = 8.0, 1.5 Hz, 1H), 7.69–7.61 (m, 1H), 7.39–7.37 (m, 3H), 7.33–7.27 (m, 2H), 5.76 (t, J = 5.6 Hz, 1H), 3.67 (s, 3H), 3.45–3.40 (m, 2H), 3.31–3.19 (m, 1H), 2.41 (s, 3H), 2.32 (t, J = 7.5 Hz, 2H), 1.69–1.58 (m, 4H), 1.44–1.36 (m, 4H), 1.32 (d, J = 6.9 Hz, 6H). MS (ESI) m/z: $[M+H]^+$: 602.2.

*4.1.3.8. Methyl 6-(2-chloro-4-((5-chloro-4-((2-(isopropylsulfonyl)phenyl)amino)pyrimidin-2-yl)amino)benzamido)hexanoate (**5i**).* White solid. Yield: 42.6%. M.p. 135–136 °C. ^{1}H NMR (600 MHz, $CDCl_3$) δ 9.68 (s, 1H), 8.45 (d, J = 8.2 Hz, 1H), 8.18 (s, 1H), 7.94 (dd, J = 8.0, 1.5 Hz, 1H), 7.84 (d, J = 2.1 Hz, 1H), 7.75–7.67 (m, 2H), 7.50 (s, 1H), 7.35–7.29 (m, 2H), 6.42 (t, J = 5.6 Hz, 1H), 3.67 (s, 3H), 3.49–3.45 (m, 2H), 3.27–3.19 (m, 1H), 2.34 (t, J = 7.4 Hz, 2H), 1.74–1.62 (m, 4H), 1.48–1.40 (m, 2H), 1.31 (d, J = 6.9 Hz, 6H). MS (ESI) m/z: $[M+H]^+$: 608.1.

*4.1.3.9. Methyl 7-(2-chloro-4-((5-chloro-4-((2-(isopropylsulfonyl) phenyl)amino)pyrimidin-2-yl)amino)benzamido)heptanoate (**5j**).* White solid. Yield: 37.9%. M.p. 130–132 °C. ^{1}H NMR (600 MHz, DMSO-d_6) δ 9.86 (s, 1H), 9.47 (s, 1H), 8.50 (s, 1H), 8.41–8.32 (m, 1H), 8.23 (t, J = 5.6 Hz, 1H), 7.88 (dd, J = 7.8, 1.4 Hz, 2H), 7.85–7.79 (m, 1H), 7.51 (d, J = 7.9 Hz, 1H), 7.44 (t, J = 7.6 Hz, 1H), 7.28 (d, J = 8.4 Hz, 1H), 3.58 (s, 3H), 3.50–3.42 (m, 1H), 3.21–3.14 (m, 2H), 2.31 (t, J = 7.4 Hz, 2H), 1.58–1.51 (m, 2H), 1.51–1.44 (m, 2H), 1.36–1.24 (m, 4H), 1.17 (t, J = 8.3 Hz, 6H). MS (ESI) m/z: $[M+H]^+$: 622.2.

*4.1.3.10. Methyl 6-(4-((5-chloro-4-((2-(isopropylsulfonyl)phenyl) amino)pyrimidin-2-yl)amino)-2-methoxybenzamido)hexanoate (**5k**).* White solid. Yield: 39.6%. M.p. 150–152.0 °C. ^{1}H NMR (600 MHz, $CDCl_3$) δ 9.67 (s, 1H), 8.51 (d, J = 8.3 Hz, 1H), 8.19 (d, J = 2.3 Hz, 1H), 8.13 (d, J = 8.6, 2.8 Hz, 1H), 7.93 (dd, J = 7.9, 1.4 Hz, 1H), 7.80 (t, J = 5.5 Hz, 1H), 7.69–7.63 (m, 1H), 7.49–7.40 (m, 1H), 7.37 (s, 1H), 7.32–7.27 (m, 1H), 7.18 (d, J = 8.6, 1.4 Hz, 1H), 3.85 (s, 3H), 3.67 (s, 3H), 3.51–3.42 (m, 2H), 3.29–3.22 (m, 1H), 2.39–2.28 (m, 2H), 1.74–1.59 (m, 4H), 1.50–1.42 (m, 2H), 1.31 (d, J = 6.8 Hz, 6H). MS (ESI) m/z: $[M+H]^+$: 604.2.

*4.1.3.11. Methyl 6-(4-((5-chloro-4-((2-(isopropylsulfonyl)phenyl) amino)pyrimidin-2-yl)amino)-3-methoxybenzamido)hexanoate (**5l**).* White solid. Yield: 38.6%. M.p. 118–120 °C. ^{1}H NMR (600 MHz, $CDCl_3$) δ 9.60 (s, 1H), 8.51 (t, J = 8.6 Hz, 1H), 8.38–8.30 (m, 1H), 8.18 (d, J = 7.0 Hz, 1H), 7.94 (dd, J = 8.1, 1.9 Hz, 1H), 7.89–7.78 (m, 1H), 7.73–7.66 (m, 1H), 7.44 (s, 1H), 7.36–7.27 (m, 1H), 7.21 (dd, J = 8.4, 1.7 Hz, 1H), 6.18 (s, 1H), 3.93 (s, 3H), 3.69 (s, 3H), 3.52–3.41 (m, 2H), 3.30–3.21 (m, 1H), 2.43–2.31 (m, 2H), 1.71–1.63 (m, 4H), 1.50–1.39 (m, 2H), 1.32 (d, J = 6.8 Hz, 6H). MS (ESI) m/z: $[M+H]^+$: 604.2.

*4.1.3.12. Methyl 6-(4-((5-chloro-4-((2-(isopropylsulfonyl)phenyl) amino)pyrimidin-2-yl)amino)-3-methylbenzamido)hexanoate (**5m**).* White solid. Yield: 45.2%. M.p. 99–102 °C. ^{1}H NMR (600 MHz, $CDCl_3$) δ 9.73 (s, 1H), 8.49 (d, J = 8.4 Hz, 1H), 8.15 (s, 1H), 8.06 (d, J = 8.4 Hz, 1H), 7.91 (d, J = 7.9 Hz, 1H), 7.64 (s, 1H), 7.63–7.42 (m, 2H), 7.28 (s, 1H), 7.07 (s, 1H), 6.19 (s, 1H), 3.67 (s, 3H), 3.53–3.41 (m, 2H), 3.29–3.19 (m, 1H), 2.44–2.30 (m, 5H), 1.74–1.61 (m, 4H), 1.43 (t, J = 7.7 Hz, 2H), 1.32 (d, J = 6.8 Hz, 6H). MS (ESI) m/z: $[M+H]^+$: 588.2.

*4.1.3.13. Methyl 3-(3-((5-chloro-4-((2-(isopropylsulfonyl)phenyl) amino)pyrimidin-2-yl)amino)benzamido)propanoate (**5o**).* White solid. Yield: 63.7%. M.p. 142–144 °C. ^{1}H NMR (600 MHz, $CDCl_3$) δ 9.75 (s, 1H), 8.54 (d, J = 8.3 Hz, 1H), 8.16 (s, 1H), 7.91 (dd, J = 8.0, 1.5 Hz, 2H), 7.77–7.71 (m, 1H), 7.63–7.58 (m, 1H), 7.42 (d, J = 7.7 Hz, 2H), 7.37 (t, J = 7.8 Hz, 1H), 7.28 (s, 1H), 6.82 (s, 1H), 3.71 (s, 3H), 3.27–3.20 (m, 1H), 2.65 (t, J = 5.9 Hz, 2H), 2.05–1.93 (m, 2H), 1.32 (d, J = 6.9 Hz, 6H). MS (ESI) m/z: $[M+H]^+$:532.1.

*4.1.3.14. Methyl 4-(3-((5-chloro-4-((2-(isopropylsulfonyl)phenyl) amino)pyrimidin-2-yl)amino)benzamido)butanoate (**5p**).* White solid. Yield: 59.0%. M.p. 138–140 °C. ^{1}H NMR (600 MHz, DMSO-d_6) δ 9.68 (s, 1H), 9.57 (s, 1H), 8.66 (d, J = 6.2 Hz, 1H), 8.39 (t, J = 5.6 Hz, 1H), 8.32 (s, 1H), 8.03 (s, 1H), 7.83 (dd, J = 7.9, 1.4 Hz, 1H), 7.76 (d, J = 7.4 Hz, 1H), 7.67 (t, J = 7.7 Hz, 1H), 7.43 (d, J = 7.7 Hz, 1H), 7.36–7.30 (m, 2H), 3.58 (s, 3H), 3.49–3.40 (m, 1H), 3.27–3.23 (m, 2H), 2.35 (t, J = 7.4 Hz, 2H), 1.76 (p, J = 7.2 Hz, 2H), 1.17 (d, J = 6.8 Hz, 6H). MS (ESI) m/z: $[M+H]^+$: 546.2.

*4.1.3.15. Methyl 5-(3-((5-chloro-4-((2-(isopropylsulfonyl)phenyl) amino)pyrimidin-2-yl)amino)benzamido)pentanoate (**5q**).* White solid. Yield: 63.4%. M.p. 58–60 °C. ^{1}H NMR (600 MHz, $CDCl_3$) δ 9.67 (s, 1H), 8.56 (d, J = 8.3 Hz, 1H), 8.17 (s, 1H), 7.91 (d, J = 9.3 Hz, 2H), 7.74 (d, J = 7.8 Hz, 1H), 7.60 (t, J = 7.7 Hz, 1H), 7.42 (d, J = 7.6 Hz, 1H), 7.36 (t, J = 7.8 Hz, 1H), 7.24 (d, J = 7.5 Hz, 1H), 7.19 (s, 1H), 6.31 (s, 1H), 3.68 (s, 3H), 3.44 (q, J = 6.4 Hz, 2H), 3.28–3.20 (m, 1H), 2.38 (t, J = 7.0 Hz, 2H), 1.71 (d, J = 6.1 Hz, 3H), 1.66–1.61 (m, 1H), 1.32 (d, J = 6.8 Hz, 6H). MS (ESI) m/z: $[M+H]^+$: 560.2.

*4.1.3.16. Methyl 6-(3-((5-chloro-4-((2-(isopropylsulfonyl)phenyl) amino)pyrimidin-2-yl)amino)benzamido)hexanoate (**5r**).* White solid. Yield: 52.2%. M.p. 108–110 °C. ^{1}H NMR (600 MHz, DMSO-d_6) δ 9.67 (s, 1H), 9.56 (s, 1H), 8.64 (s, 1H), 8.32 (d, J = 7.4 Hz, 2H), 8.01 (s, 1H), 7.83 (d, J = 7.6 Hz, 1H), 7.75 (d, J = 6.9 Hz, 1H), 7.67 (d, J = 7.9 Hz, 1H), 7.41 (d, J = 7.4 Hz, 1H), 7.36–7.29 (m, 2H), 3.57 (s, 3H), 3.44 (dd, J = 7.5, 5.0 Hz, 1H), 3.22–3.18 (m, 2H), 2.29 (t, J = 7.4 Hz, 2H), 1.59–1.42 (m, 4H), 1.34–1.23 (m, 2H), 1.16 (d, J = 6.8 Hz, 6H). MS (ESI) m/z: $[M+H]^+$: 574.2.

*4.1.3.17. Methyl 7-(3-((5-chloro-4-((2-(isopropylsulfonyl)phenyl) amino)pyrimidin-2-yl)amino)benzamido)heptanoate (**5s**).* White solid. Yield: 50.0%. M.p. 128–129 °C. ^{1}H NMR (600 MHz, DMSO-d_6) δ 9.70 (s, 1H), 9.56 (s, 1H), 8.65 (s, 1H), 8.39–8.29 (m, 2H), 8.01 (s, 1H), 7.83 (dd, J = 8.0, 1.3 Hz, 1H), 7.74 (d, J = 6.8 Hz, 1H), 7.67 (t, J = 7.5 Hz, 1H), 7.41 (d, J = 7.7 Hz, 1H), 7.36–7.30 (m, 2H), 3.57 (s, 3H), 3.48–3.41 (m, 1H), 3.22–3.17 (m, 2H), 2.28 (t, J = 7.4 Hz, 2H), 1.56–1.42 (m, 4H), 1.30–1.20 (m, 4H), 1.16 (d, J = 6.8 Hz, 6H). MS (ESI) m/z: $[M+H]^+$: 588.2.

*4.1.3.18. Methyl 6-(3-((5-chloro-4-((2-(isopropylsulfonyl)phenyl) amino)pyrimidin-2-yl)amino)-2-methylbenzamido)hexanoate (**5t**).* White solid. Yield: 45.2%. M.p. 123–125 °C. ^{1}H NMR (600 MHz, $CDCl_3$) δ 9.64 (s, 1H), 8.44 (d, J = 8.4 Hz, 1H), 8.05 (s, 1H), 7.80 (d, J = 7.9 Hz, 1H), 7.73 (d, J = 8.0 Hz, 1H), 7.45 (t, J = 7.8 Hz, 1H), 7.20–7.11 (m, 2H), 7.09 (d, J = 7.5 Hz, 1H), 6.73 (s, 1H), 5.76 (s, 1H), 3.59 (s, 3H), 3.45–3.32 (m, 2H), 3.20–3.12 (m, 1H), 2.32–2.23 (m, 5H), 1.63–1.53 (m, 4H), 1.38–1.33 (m, 2H), 1.24 (d, J = 6.7 Hz, 6H). MS (ESI) m/z: $[M+H]^+$: 588.2.

*4.1.4. General procedure for the synthesis of **6a-t***

*4.1.4.1. 4-((5-Chloro-4-((2-(isopropylsulfonyl)phenyl)amino)pyrimidin-2-yl)amino)-N-hydroxybenzamide (**6a**).* A solution of potassium hydroxide (5.6 g, 100 mmol) in methanol (14 mL) was added to a stirred solution of hydroxylamine hydrochloride (4.67 g, 67.2 mmol) in methanol (24 mL) at 0 °C. The reaction mixture was stirred at this temperature for 1 h. The precipitate was removed by filtration and the filtrate was collected to provide fresh hydroxylamine solution which was stored in a refrigerator before use. **3a** (0.20g, 0.43 mmol) was weighed into 20 mL freshly prepared hydroxylamine methanol solution and stirred at room temperature for 2 h. The pH value of reaction mixture was adjusted to 6–7 with saturated NH_4Cl solution. The white solid was precipitated, filtered and washed with water and 0.10 g of **6a** was obtained as white solid by recrystallization of methanol. Yield: 52.1%. M.p. 175–176 °C. ^{1}H NMR (600 MHz, DMSO-d_6) δ 9.84 (s, 1H), 8.94 (s, 1H), 8.54 (s, 1H), 8.36 (s, 1H), 7.96–7.78 (m, 2H), 7.69–7.65 (m, 4H), 7.45 (s, 1H), 3.47 (s, 1H), 1.16 (d, J = 5.6 Hz, 6H). ^{13}C NMR (151 MHz, DMSO-d_6) δ 164.47, 157.71, 155.60, 143.24, 138.31, 135.40, 131.46, 127.85, 125.86, 125.72, 125.15, 124.60, 118.61, 105.93, 55.25, 15.32. HRMS m/z calcd for $C_{20}H_{21}ClN_5O_4S$ $[M+H]^+$ 462.0997, found: 462.1001.

*4.1.4.2. 4-((5-Chloro-4-((2-(isopropylsulfonyl)phenyl)amino)pyrimidin-2-yl)amino)-N-(3-(hydroxyamino)-3-oxopropyl)benzamide (**6b**).* White solid. Yield: 40.4%. M.p. 156–158 °C. ^{1}H NMR (600 MHz, DMSO-d_6) δ 10.43 (s, 1H), 9.83 (s, 1H), 8.83 (s, 1H), 8.54 (s, 1H), 8.39 (s, 1H), 8.35 (s, 1H), 7.89 (d, J = 7.8 Hz, 1H), 7.82 (d, J = 7.3 Hz, 1H), 7.80–7.71 (m, 4H), 7.65 (d, J = 8.3 Hz, 1H), 7.45 (t, J = 7.2 Hz, 1H), 3.49 (s, 1H), 3.47–3.42 (m, 2H), 2.26 (t, J = 7.0 Hz, 2H), 1.16 (d, J = 6.6 Hz, 6H). ^{13}C NMR (151 MHz, DMSO-d_6) δ 167.81,

166.24, 157.72, 155.60, 143.28, 135.36, 131.42, 128.21, 127.84, 127.59, 125.67, 125.02, 124.49, 118.61, 118.40, 106.02, 55.23, 36.45, 33.04, 15.32. HRMS *m/z* calcd for $C_{23}H_{26}ClN_6O_5S$ $[M+H]^+$ 533.1368, found: 533.1368.

*4.1.4.3. 4-((5-Chloro-4-((2-(isopropylsulfonyl)phenyl)amino)pyrimidin-2-yl)amino)-N-(4-(hydroxyamino)-4-oxobutyl)benzamide (**6c**).* White solid. Yield: 40.0%. M.p. 177–178 °C. ^{1}H NMR (600 MHz, DMSO-d_6) δ 10.39 (s, 1H), 9.81 (s, 1H), 9.46 (s, 1H), 8.70 (s, 1H), 8.56 (d, *J* = 7.0 Hz, 1H), 8.36 (d, *J* = 6.7 Hz, 1H), 8.32 (t, *J* = 5.4 Hz, 1H), 7.88 (dd, *J* = 7.9, 1.3 Hz, 1H), 7.84–7.80 (m, 1H), 7.73 (d, *J* = 8.7 Hz, 2H), 7.69 (d, *J* = 8.7 Hz, 2H), 7.44 (t, *J* = 7.5 Hz, 1H), 3.50–3.42 (m, 1H), 3.27–3.18 (m, 2H), 2.01 (t, *J* = 7.5 Hz, 2H), 1.78–1.70 (m, 2H), 1.16 (d, *J* = 6.8 Hz, 6H). ^{13}C NMR (151 MHz, DMSO-d_6) δ 168.94, 165.75, 157.25, 155.20, 155.10, 142.72, 137.84, 134.94, 130.99, 130.09, 127.33, 125.12, 124.52, 124.10, 117.96, 105.47, 54.81, 38.86, 30.06, 25.42, 14.85. HRMS *m/z* calcd for $C_{24}H_{28}ClN_6O_5S$ $[M+H]^+$ 547.1530, found: 547.1539.

*4.1.4.4. 4-((5-Chloro-4-((2-(isopropylsulfonyl)phenyl)amino)pyrimidin-2-yl)amino)-N-(5-(hydroxyamino)-5-oxopentyl)benzamide (**6d**).* White solid. Yield: 60.6%. M.p. 135–137 °C. ^{1}H NMR (600 MHz, DMSO-d_6) δ 9.84 (s, 1H), 8.57 (s, 1H), 8.41–8.32 (m, 2H), 7.88 (d, *J* = 7.8 Hz, 1H), 7.84 (t, *J* = 7.3 Hz, 2H), 7.75 (d, *J* = 8.6 Hz, 2H), 7.73–7.55 (m, 4H), 7.45 (t, *J* = 7.4 Hz, 1H), 3.52–3.45 (m, 1H), 3.22 (d, *J* = 5.8 Hz, 2H), 1.99 (t, *J* = 6.5 Hz, 2H), 1.61–1.42 (m, 4H), 1.17 (d, *J* = 6.7 Hz, 6H). ^{13}C NMR (151 MHz, DMSO-d_6) δ169.47, 166.10, 157.72, 155.65, 155.53, 143.15, 138.30, 135.47, 131.43, 128.71, 128.21, 127.85, 124.55, 118.62, 118.42, 105.90, 55.36, 55.28, 32.49, 29.36, 23.27, 15.32. HRMS *m/z* calcd for $C_{25}H_{30}ClN_6O_5S$ $[M+H]^+$ 561.1681, found: 561.1680.

*4.1.4.5. 4-((5-Chloro-4-((2-(isopropylsulfonyl)phenyl)amino)pyrimidin-2-yl)amino)-N-(6-(hydroxyamino)-6-oxohexyl)benzamide (**6e**).* White solid. Yield: 65.3%. M.p. 167–169 °C. ^{1}H NMR (600 MHz, DMSO-d_6) δ 10.35 (s, 1H), 9.83 (s, 1H), 9.49 (s, 1H), 8.68 (s, 1H), 8.56 (s, 1H), 8.36 (s, 1H), 8.28 (t, *J* = 5.3 Hz, 1H), 7.89 (d, *J* = 7.9 Hz, 1H), 7.83 (t, *J* = 7.7 Hz, 1H), 7.72 (d, *J* = 8.6 Hz, 2H), 7.69 (d, *J* = 8.5 Hz, 2H), 7.45 (t, *J* = 7.6 Hz, 1H), 3.52–3.41 (m, 1H), 3.35–3.15 (m, 2H), 1.96 (t, *J* = 7.3 Hz, 2H), 1.55–1.47 (m, 4H), 1.33–1.24 (m, 2H), 1.17 (d, *J* = 6.8 Hz, 6H). ^{13}C NMR (151 MHz, DMSO-d_6) δ 169.54, 166.10, 157.72, 155.67, 155.56, 143.13, 138.31, 135.40, 131.46, 128.18, 127.91, 125.57, 124.96, 124.56, 118.43, 105.93, 55.27, 34.10, 32.72, 29.52, 26.63, 25.42, 15.32. HRMS *m/z* calcd for $C_{26}H_{32}ClN_6O_5S$ $[M+H]^+$ 575.1838, found: 575.1825.

*4.1.4.6. 4-((5-Chloro-4-((2-(isopropylsulfonyl)phenyl)amino)pyrimidin-2-yl)amino)-N-(7-(hydroxyamino)-7-oxoheptyl)benzamide (**6f**).* White solid. Yield: 49.2%. M.p. 184–186 °C. ^{1}H NMR (600 MHz, DMSO-d_6) δ 10.37 (s, 1H), 9.83 (s, 1H), 9.49 (d, *J* = 0.9 Hz, 1H), 8.71 (s, 1H), 8.57 (d, *J* = 5.4 Hz, 1H), 8.36 (s, 1H), 8.28 (t, *J* = 5.4 Hz, 1H), 7.89 (d, *J* = 7.9 Hz, 1H), 7.83 (t, *J* = 7.8 Hz, 1H), 7.73 (d, *J* = 8.7 Hz, 2H), 7.70 (d, *J* = 8.6 Hz, 2H), 7.45 (t, *J* = 7.6 Hz, 1H), 3.51–3.46 (m, 1H), 3.25–3.20 (m, 2H), 1.95 (t, *J* = 7.4 Hz, 2H), 1.51 (d, *J* = 6.0 Hz, 4H), 1.35–1.22 (m, 4H), 1.17 (d, *J* = 6.8 Hz, 6H). ^{13}C NMR (151 MHz, DMSO-d_6) δ 169.59, 166.10, 157.73, 155.67, 155.54, 143.12, 138.31, 135.45, 131.45, 128.20, 127.93, 125.53, 124.97, 124.54, 118.43, 105.91, 55.28, 32.70, 29.64, 28.84, 26.72, 25.58, 15.32. HRMS *m/z* calcd for $C_{27}H_{34}ClN_6O_5S$ $[M+H]^+$ 589.1994, found: 589.1998.

*4.1.4.7. 4-((5-Chloro-4-((2-(isopropylsulfonyl)phenyl)amino)pyrimidin-2-yl)amino)-N-(6-(hydroxyamino)-6-oxohexyl)-2-methylbenzamide (**6g**).* White solid. Yield: 50.5%. M.p. 161–162 °C. 1H NMR (600 MHz, DMSO-d_6) δ 10.35 (s, 1H), 9.64 (s, 1H), 9.46 (s, 1H), 8.66 (s, 1H), 8.56 (s, 1H), 8.33 (s, 1H), 8.06 (t, *J* = 5.6 Hz, 1H), 7.87 (dd, *J* = 7.9, 1.4 Hz, 1H), 7.82–7.75 (m, 1H), 7.50 (s, 1H), 7.47–7.38 (m, 2H), 7.21 (d, *J* = 8.3 Hz, 1H), 3.49–3.41 (m, 1H), 3.22–3.15 (m, 2H), 2.25 (s, 3H), 1.96 (t, *J* = 7.4 Hz, 2H), 1.60–1.44 (m, 4H), 1.32–1.26 (m, 2H), 1.17 (d, *J* = 6.8 Hz, 6H). ^{13}C NMR (151 MHz, DMSO-d_6) δ 169.52, 169.15, 157.89, 155.71, 155.45, 141.29, 138.38, 136.44, 135.49, 131.44, 130.98, 128.13, 125.36, 124.67, 124.41, 120.97, 116.32, 105.56, 55.28, 39.22, 32.73, 29.39, 26.59, 25.38, 20.52, 15.33. HRMS *m/z* calcd for $C_{27}H_{34}ClN_6O_5S$ $[M+H]^+$ 589.1994, found: 589.1991.

*4.1.4.8. 4-((5-Chloro-4-((2-(isopropylsulfonyl)phenyl)amino)pyrimidin-2-yl)amino)-N-(7-(hydroxyamino)-7-oxoheptyl)-2-methylbenzamide (**6h**).* White solid. Yield: 66.6%. M.p. 146–147 °C. ^{1}H NMR (600 MHz, DMSO-d_6) δ 10.36 (s, 1H), 9.66 (s, 1H), 9.47 (s, 1H), 8.68 (s, 1H), 8.56 (s, 1H), 8.33 (s, 1H), 8.08 (t, *J* = 5.5 Hz, 1H), 7.88 (dd, *J* = 7.9, 1.2 Hz, 1H), 7.81–7.77 (m, 1H), 7.50 (s, 1H), 7.47–7.39 (m, 2H), 7.21 (d, *J* = 8.3 Hz, 1H), 3.52–3.44 (m, 1H), 3.21–3.15 (m, 2H), 2.25 (s, 3H), 1.95 (t, *J* = 7.4 Hz, 2H), 1.59–1.43 (m, 4H), 1.36–1.24 (m, 4H), 1.17 (d, *J* = 6.8 Hz, 6H). ^{13}C NMR (151 MHz, DMSO-d_6) δ 169.59, 169.16, 157.89, 155.71, 155.45, 141.28, 138.38, 136.39, 135.48, 131.44, 131.02, 128.11, 125.37, 124.68, 124.40, 120.98, 116.34, 105.56, 55.29, 39.27, 32.73, 29.52, 28.82, 26.69, 25.62, 20.49, 15.33. HRMS *m/z* calcd for $C_{28}H_{36}ClN_6O_5S$ $[M+H]^+$ 603.2156, found: 603.2169.

*4.1.4.9. 2-Chloro-4-((5-chloro-4-((2-(isopropylsulfonyl)phenyl)amino)pyrimidin-2-yl)amino)-N-(6-(hydroxyamino)-6-oxohexyl)benzamide (**6i**).* White solid. Yield: 31.5%. M.p. 168–169 °C. ^{1}H NMR (600 MHz, DMSO-d_6) δ 10.36 (s, 1H), 9.88 (s, 1H), 9.47 (s, 1H), 8.68 (s, 1H), 8.50 (s, 1H), 8.38 (s, 1H), 8.25 (t, *J* = 5.6 Hz, 1H), 7.97–7.86 (m, 2H), 7.86–7.78 (m, 1H), 7.51 (d, *J* = 8.1 Hz, 1H), 7.44 (t, *J* = 7.6 Hz, 1H), 7.28 (d, *J* = 8.4 Hz, 1H), 3.52–3.44 (m, 1H), 3.20–3.15 (m, 2H), 1.95 (t, *J* = 7.4 Hz, 2H), 1.45–1.55 (m, 4H), 1.32–1.20 (m, 2H), 1.16 (d, *J* = 6.8 Hz, 6H). ^{13}C NMR (151 MHz, DMSO-d_6) δ 169.53, 166.50, 157.56, 155.63, 142.41, 138.48, 138.19, 135.69, 131.48, 130.63, 130.23, 129.56, 125.71, 124.84, 124.69, 119.18, 117.35, 106.27, 55.24, 39.35, 32.72, 29.18, 26.52, 25.34, 15.32. HRMS *m/z* calcd for $C_{26}H_{31}Cl_2N_6O_5S$ $[M+H]^+$ 609.1454, found: 609.1463.

*4.1.4.10. 2-Chloro-4-((5-chloro-4-((2-(isopropylsulfonyl)phenyl)amino)pyrimidin-2-yl)amino)-N-(7-(hydroxyamino)-7-oxoheptyl)benzamide (**6j**).* White solid. Yield: 61.5%. M.p. 194–196 °C. ^{1}H NMR (600 MHz, DMSO-d_6) δ 10.34 (s, 1H), 9.87 (s, 1H), 9.47 (s, 1H), 8.66 (s, 1H), 8.50 (s, 1H), 8.37 (s, 1H), 8.23 (t, *J* = 5.5 Hz, 1H), 7.93–7.86 (m, 2H), 7.83 (t, *J* = 7.8 Hz, 1H), 7.52 (d, *J* = 8.1 Hz, 1H), 7.44 (t, *J* = 7.6 Hz, 1H), 7.28 (d, *J* = 8.4 Hz, 1H), 3.52–3.44 (m, 1H), 3.23–3.10 (m, 2H), 1.95 (t, *J* = 7.4 Hz, 2H), 1.55–1.43 (m, 4H), 1.37–1.21 (m, 4H), 1.17 (d, *J* = 6.8 Hz, 6H). ^{13}C NMR (151 MHz, DMSO-d_6) δ 169.59, 166.51, 157.56, 155.63, 142.41, 138.19, 135.68, 131.48, 130.61, 130.26, 129.55, 125.71, 124.85, 124.68, 119.19, 117.37, 106.26, 95.46, 55.24, 39.40, 32.74, 29.32, 28.79, 26.60, 25.61, 15.33. HRMS *m/z* calcd for $C_{27}H_{33}Cl_2N_6O_5S$ $[M+H]^+$ 623.1610, found: 623.1618.

*4.1.4.11. 4-((5-Chloro-4-((2-(isopropylsulfonyl)phenyl)amino)pyrimidin-2-yl)amino)-N-(6-(hydroxyamino)-6-oxohexyl)-2-methoxybenzamide (**6k**).* White solid. Yield: 55.2%. M.p. 167–169 °C. ^{1}H NMR (600 MHz, DMSO-d_6) δ 10.35 (s, 1H), 9.81 (s, 1H), 9.47 (s, 1H), 8.68 (s, 1H), 8.54 (s, 1H), 8.37 (s, 1H), 7.99 (t, *J* = 5.3 Hz, 1H), 7.87 (d, *J* = 7.7 Hz, 1H), 7.78 (t, *J* = 7.7 Hz, 1H), 7.70 (d, *J* = 8.5 Hz, 1H), 7.49–7.40 (m, 2H), 7.38 (d, *J* = 8.2 Hz, 1H), 3.72 (s, 3H), 3.52–3.44 (m, 1H), 3.27–3.22 (m, 2H), 1.95 (t, *J* = 7.2 Hz, 2H), 1.55–1.48 (m, 4H), 1.34–1.25 (m, 2H), 1.17 (d, *J* = 6.7 Hz, 6H). ^{13}C NMR (151 MHz, DMSO-d_6) δ 169.53, 164.74, 158.03, 157.68, 155.63, 155.44, 144.48, 138.31, 135.44, 131.70, 131.47, 125.37, 124.63, 124.46, 115.91, 111.17, 106.25, 102.42, 56.05, 55.27, 39.34, 32.71, 29.47, 26.60, 25.37, 15.32. HRMS *m/z* calcd for $C_{27}H_{34}ClN_6O_6S$ $[M+H]^+$ 605.1949, found: 605.1963.

*4.1.4.12. 4-((5-Chloro-4-((2-(isopropylsulfonyl)phenyl)amino)pyrimidin-2-yl)amino)-N-(6-(hydroxyamino)-6-oxohexyl)-3-methoxybenzamide (**6l**).* White solid. Yield: 61.5%. M.p. 93–95 °C. ^{1}H NMR (600 MHz, DMSO-d_6) δ 10.35 (s, 1H), 9.51 (s, 1H), 8.66 (s, 1H), 8.50 (s, 1H), 8.44–8.21 (m, 3H), 7.96 (s, 1H), 7.85 (d, J = 7.7 Hz, 1H), 7.72 (s, 1H), 7.50 (s, 1H), 7.40 (d, J = 7.7 Hz, 2H), 3.89 (s, 3H), 3.46 (s, 1H), 3.25 (d, J = 5.9 Hz, 2H), 1.96 (t, J = 7.1 Hz, 2H), 1.53 (s, 4H), 1.29 (d, J = 6.8 Hz, 2H), 1.16 (d, J = 6.7 Hz, 6H). ^{13}C NMR (151 MHz, DMSO-d_6) δ 169.54, 165.96, 157.76, 156.18, 155.57, 149.37, 138.25, 135.37, 131.43, 131.23, 129.64, 125.33, 124.68, 124.44, 120.36, 119.97, 110.12, 105.95, 56.36, 55.30, 32.72, 29.72, 29.51, 26.64, 25.42, 15.31. HRMS m/z calcd for $C_{27}H_{34}ClN_6O_6S$ $[M+H]^+$ 605.1944, found: 605.1944.

*4.1.4.13. 4-((5-Chloro-4-((2-(isopropylsulfonyl)phenyl)amino)pyrimidin-2-yl)amino)-N-(6-(hydroxyamino)-6-oxohexyl)-3-methylbenzamide (**6m**).* White solid. Yield: 20.6%. M.p. 178–180 °C. ^{1}H NMR (600 MHz, DMSO-d_6) δ 10.35 (s, 1H), 9.60 (s, 1H), 9.00 (s, 1H), 8.67 (s, 1H), 8.54 (d, J = 7.1 Hz, 1H), 8.35 (s, 1H), 8.25 (s, 1H), 7.80 (d, J = 7.5 Hz, 1H), 7.73 (s, 1H), 7.68 (d, J = 7.7 Hz, 1H), 7.59–7.52 (m, 2H), 7.31 (t, J = 7.1 Hz, 1H), 3.51–3.40 (m, 1H), 3.26 (t, J = 5.1 Hz, 2H), 2.26 (s, 3H), 1.96 (d, J = 6.4 Hz, 2H), 1.53 (s, 4H), 1.30 (s, 2H), 1.17 (d, J = 6.3 Hz, 6H). ^{13}C NMR (151 MHz, DMSO-d_6) δ 169.53, 166.20, 159.03, 155.92, 155.24, 140.81, 138.60, 135.21, 132.00, 131.41, 130.93, 129.79, 125.37, 124.99, 123.98, 123.63, 123.25, 105.19, 55.38, 40.53, 32.73, 29.45, 26.61, 25.42, 18.60, 15.32. HRMS m/z calcd for $C_{27}H_{34}ClN_6O_5S$ $[M+H]^+$ 589.2000, found: 589.2007.

*4.1.4.14. 3-((5-Chloro-4-((2-(isopropylsulfonyl)phenyl)amino)pyrimidin-2-yl)amino)-N-hydroxybenzamide (**6n**).* White solid. Yield: 36.8%. M.p. 95–96 °C. ^{1}H NMR (600 MHz, DMSO-d_6) δ 9.69 (s, 1H), 8.66 (d, J = 6.0 Hz, 3H), 8.33 (s, 1H), 7.96 (s, 1H), 7.88–7.67 (m, 4H), 7.37 (t, J = 7.6 Hz, 1H), 7.34–7.29 (m, 2H), 3.48–3.42 (m, 1H), 1.17 (d, J = 6.8 Hz, 6H). ^{13}C NMR (151 MHz, DMSO-d_6) δ 164.79, 158.05, 155.65, 155.36, 140.62, 138.43, 135.53, 133.99, 131.39, 128.85, 124.68, 124.17, 124.08, 122.58, 120.49, 119.17, 105.70, 55.34, 15.33. HRMS m/z calcd for $C_{20}H_{21}ClN_5O_4S$ $[M+H]^+$ 462.0997, found: 462.1003.

*4.1.4.15. 3-((5-Chloro-4-((2-(isopropylsulfonyl)phenyl)amino)pyrimidin-2-yl)amino)-N-(3-(hydroxyamino)-3-oxopropyl)benzamide (**6o**).* White solid. Yield: 52.6%. M.p. 119–121 °C. ^{1}H NMR (600 MHz, DMSO-d_6) δ 9.68 (s, 1H), 8.65 (s, 2H), 8.43 (s, 1H), 8.32 (s, 1H), 8.03 (s, 1H), 7.84 (d, J = 7.6 Hz, 1H), 7.77 (d, J = 6.9 Hz, 1H), 7.69 (t, J = 7.2 Hz, 1H), 7.42 (d, J = 7.4 Hz, 1H), 7.38–7.29 (m, 2H), 3.51–3.40 (m, 3H), 2.25 (t, J = 7.1 Hz, 2H), 1.17 (d, J = 6.7 Hz, 6H). ^{13}C NMR (151 MHz, DMSO-d_6) δ 167.74, 166.81, 158.08, 155.70, 155.30, 140.54, 138.41, 135.53, 135.43, 131.39, 128.76, 124.59, 124.09, 124.02, 122.79, 120.88, 119.58, 105.63, 55.36, 36.56, 32.86, 15.34. HRMS m/z calcd for $C_{23}H_{26}ClN_6O_5S$ $[M+H]^+$ 533.1368, found: 533.1378.

*4.1.4.16. 3-((5-Chloro-4-((2-(isopropylsulfonyl)phenyl)amino)pyrimidin-2-yl)amino)-N-(4-(hydroxyamino)-4-oxobutyl)benzamide (**6p**).* White solid. Yield: 46.3%. M.p. 176–178 °C. ^{1}H NMR (600 MHz, DMSO-d_6) δ 10.40 (s, 1H), 9.70 (s, 1H), 9.57 (s, 1H), 8.73 (s, 1H), 8.66 (s, 1H), 8.42 (t, J = 5.5 Hz, 1H), 8.33 (s, 1H), 8.04 (s, 1H), 7.84 (d, J = 7.9, 1.1 Hz, 1H), 7.77 (d, J = 7.2 Hz, 1H), 7.68 (t, J = 7.6 Hz, 1H), 7.44 (d, J = 7.7 Hz, 1H), 7.39–7.30 (m, 2H), 3.52–3.44 (m, 1H), 3.29–3.17 (m, 2H), 2.01 (t, J = 7.5 Hz, 2H), 1.78–1.67 (m, 2H), 1.17 (d, J = 6.8 Hz, 6H). ^{13}C NMR (151 MHz, DMSO-d_6) δ 169.33, 166.85, 158.09, 155.73, 155.29, 140.51, 138.41, 135.75, 135.41, 133.07, 131.40, 128.75, 124.57, 124.00, 122.73, 120.92, 119.64, 105.61, 55.36, 40.89, 30.50, 25.76, 15.33. HRMS m/z calcd for $C_{24}H_{28}ClN_6O_5S$ $[M+H]^+$ 547.1525, found: 547.1523.

*4.1.4.17. 3-((5-Chloro-4-((2-(isopropylsulfonyl)phenyl)amino)pyrimidin-2-yl)amino)-N-(5-(hydroxyamino)-5-oxopentyl)benzamide (**6q**).* White solid. Yield: 46.3%. M.p. 196–198 °C. ^{1}H NMR (600 MHz, DMSO-d_6) δ 10.36 (s, 1H), 9.68 (s, 1H), 9.56 (s, 1H), 8.67 (s, 2H), 8.37 (t, J = 5.1 Hz, 1H), 8.33 (s, 1H), 8.02 (s, 1H), 7.84 (d, J = 7.8 Hz, 1H), 7.77 (d, J = 7.0 Hz, 1H), 7.68 (t, J = 7.5 Hz, 1H), 7.42 (d, J = 7.6 Hz, 1H), 7.39–7.28 (m, 2H), 3.53–3.41 (m, 1H), 3.30–3.22 (m, 2H), 1.98 (t, J = 7.0 Hz, 2H), 1.57–1.49 (m, 4H), 1.17 (d, J = 6.8 Hz, 6H). ^{13}C NMR (151 MHz, DMSO-d_6) δ 169.41, 166.77, 159.51, 158.10, 155.71, 155.30, 140.50, 138.43, 135.84, 135.41, 131.40, 128.73, 124.56, 124.03, 122.69, 120.90, 119.63, 105.60, 55.35, 39.42, 32.46, 29.22, 23.21, 15.33. HRMS m/z calcd for $C_{25}H_{30}ClN_6O_5S$ $[M+H]^+$ 561.1681, found: 561.1683.

*4.1.4.18. 3-((5-Chloro-4-((2-(isopropylsulfonyl)phenyl)amino)pyrimidin-2-yl)amino)-N-(6-(hydroxyamino)-6-oxohexyl)benzamide (**6r**).* White solid. Yield: 44.8%. M.p. 90–92 °C. ^{1}H NMR (600 MHz, DMSO-d_6) δ 10.36 (s, 1H), 9.70 (s, 1H), 9.57 (s, 1H), 8.68 (s, 2H), 8.37 (s, 1H), 8.33 (s, 1H), 8.03 (s, 1H), 7.84 (d, J = 7.7 Hz, 1H), 7.77 (d, J = 5.9 Hz, 1H), 7.68 (d, J = 6.8 Hz, 1H), 7.43 (d, J = 7.5 Hz, 1H), 7.39–7.24 (m, 2H), 3.52–3.44 (m, 1H), 3.22 (t, J = 5.9 Hz, 2H), 2.03–1.95 (m, 2H), 1.59–1.45 (m, 4H), 1.36–1.22 (m, 2H), 1.17 (d, J = 6.7 Hz, 6H). ^{13}C NMR (151 MHz, DMSO-d_6) δ 169.52, 166.75, 158.10, 155.72, 155.29, 148.65, 140.48, 138.43, 135.86, 135.41, 131.40, 128.74, 124.53, 123.97, 122.70, 120.93, 119.65, 105.60, 55.36, 32.71, 29.35, 26.60, 25.40, 15.33, 14.56. HRMS m/z calcd for $C_{26}H_{32}ClN_6O_5S$ $[M+H]^+$ 575.1838, found: 575.1840.

*4.1.4.19. 3-((5-Chloro-4-((2-(isopropylsulfonyl)phenyl)amino)pyrimidin-2-yl)amino)-N-(7-(hydroxyamino)-7-oxoheptyl)benzamide (**6s**).* White solid. Yield: 49.2%. M.p. 182–184 °C. ^{1}H NMR (600 MHz, DMSO-d_6) δ 10.35 (s, 1H), 9.70 (s, 1H), 9.57 (s, 1H), 8.68 (s, 2H), 8.36 (s, 1H), 8.33 (s, 1H), 8.03 (s, 1H), 7.84 (d, J = 7.8 Hz, 1H), 7.77 (d, J = 6.2 Hz, 1H), 7.68 (t, J = 7.0 Hz, 1H), 7.43 (d, J = 7.5 Hz, 1H), 7.39–7.28 (m, 2H), 3.50–3.42 (m, 1H), 3.22 (d, J = 6.0 Hz, 2H), 1.94 (t, J = 7.1 Hz, 2H), 1.49 (s, 4H), 1.27 (s, 4H), 1.17 (d, J = 6.5 Hz, 6H). ^{13}C NMR (151 MHz, DMSO-d_6) δ 169.56, 166.77, 158.10, 155.72, 155.28, 140.47, 138.43, 135.89, 135.40, 131.41, 128.74, 124.52, 124.00, 123.95, 122.69, 120.94, 119.66, 105.60, 55.36, 32.71, 31.30, 29.48, 28.83, 26.72, 25.57, 15.33. HRMS m/z calcd for $C_{27}H_{34}ClN_6O_5S$ $[M+H]^+$ 589.1994, found: 589.1997.

*4.1.4.20. 3-((5-Chloro-4-((2-(isopropylsulfonyl)phenyl)amino)pyrimidin-2-yl)amino)-N-(6-(hydroxyamino)-6-oxohexyl)-2-methylbenzamide (**6t**).* White solid. Yield: 33.8%. M.p. 56–58 °C. ^{1}H NMR (600 MHz, DMSO-d_6) δ 10.34 (s, 1H), 9.56 (s, 1H), 9.05 (s, 1H), 8.68 (s, 1H), 8.55 (s, 1H), 8.28 (s, 1H), 8.21 (s, 1H), 7.78 (d, J = 7.7 Hz, 1H), 7.61 (t, J = 7.5 Hz, 1H), 7.44 (d, J = 7.8 Hz, 1H), 7.32–7.19 (m, 2H), 7.12 (d, J = 7.4 Hz, 1H), 3.50–3.41 (m, 1H), 3.20 (t, J = 6.1 Hz, 2H), 2.19 (s, 3H), 2.01–1.94 (m, 2H), 1.55–1.46 (m, 4H), 1.32–1.26 (m, 2H),1.16 (d, J = 6.7 Hz, 6H). ^{13}C NMR (151 MHz, DMSO-d_6) δ 169.55, 159.57, 155.96, 155.17, 139.57, 138.66, 135.53, 131.35, 130.95, 127.65, 125.85, 124.81, 124.08, 123.58, 123.38, 122.96, 104.70, 55.36, 49.07, 39.20, 32.71, 29.29, 26.55, 25.35, 15.33, 15.24. HRMS m/z calcd for $C_{27}H_{34}ClN_6O_5S$ $[M+H]^+$ 589.1994, found: 589.1993.

*4.1.5. General procedure for the synthesis of intermediates **8a-c***

*4.1.5.1. N^2-(4-aminophenyl)-5-chloro-N^4-(2-(isopropylsulfonyl)phenyl)pyrimidine-2,4-diamine (**8a**).* Synthesized using the preparation method of **3a** using 5.00 g (14.50 mmol) of **1** and 1.94 g (18.00 mmol) of *p*-phenylenediamine (**7a**) in 20 mL IPA and 0.3 mL HCl solution (37%) was added, and 3.20 g of **8a** was obtained as white solid; yield: 52.9%. M.p. 218–219 °C. ^{1}H NMR (600 MHz, DMSO-d_6) δ 9.47 (s, 1H), 9.08 (s, 1H), 8.65 (s, 1H), 8.19 (s, 1H), 7.84–7.81 (m, 1H), 7.67 (s, 1H), 7.42–7.26 (m, 1H), 7.18 (d, J = 7.4 Hz,

2H), 6.52 (d, J = 8.7 Hz, 2H), 4.83 (s, 2H), 3.51–3.36 (m, 1H), 1.26–1.01 (m, 6H). MS (ESI) m/z: $[M+H]^+$: 418.1.

*4.1.5.2. N^2-(3-aminophenyl)-5-chloro-N^4-(2-(isopropylsulfonyl) phenyl)pyrimidine-2,4-diamine (**8b**).* White solid. Yield: 59.9%. M.p. 141–144 °C. ^{1}H NMR (600 MHz, DMSO-d_6) δ 9.52 (s, 1H), 9.26 (s, 1H), 8.74 (d, J = 8.3 Hz, 1H), 8.26 (d, J = 8.4 Hz, 1H), 7.83 (dd, J = 7.9, 1.5 Hz, 1H), 7.77–7.33 (m, 1H), 7.39–7.33 (m, 1H), 6.89 (t, J = 7.9 Hz, 1H), 6.83 (s, 1H), 6.77 (d, J = 7.9 Hz, 1H), 6.23 (dd, J = 7.9, 1.3 Hz, 1H), 4.94 (s, 2H), 3.48–3.41 (m, 1H), 1.17 (d, J = 6.8 Hz, 6H). MS (ESI) m/z: $[M+H]^+$: 418.1.

*4.1.5.3. N^2-(3-amino-4-methylphenyl)-5-chloro-N^4-(2-(iso-propylsulfonyl)phenyl)pyrimidine-2,4-diamine (**8c**).* White solid. Yield: 42.6%. M.p. 232–233 °C. ^{1}H NMR (600 MHz, DMSO-d_6) δ 9.52 (s, 1H), 9.21 (s, 1H), 8.75 (d, J = 7.8 Hz, 1H), 8.23 (s, 1H), 7.83 (dd, J = 7.9, 1.5 Hz, 1H), 7.79–7.71 (m, 1H), 7.37–7.32 (m, 1H), 6.84 (s, 1H), 6.80 (d, J = 8.1 Hz, 1H), 6.73 (dd, J = 8.0, 1.7 Hz, 1H), 4.72 (s, 2H), 3.48–3.40 (m, 1H), 2.01 (s, 3H), 1.18 (t, J = 6.3 Hz, 6H). MS (ESI) m/z: $[M+H]^+$: 432.0.

*4.1.6. General procedure for the synthesis of intermediates **9a-j***

*4.1.6.1. Methyl 3-((4-((5-chloro-4-((2-(isopropylsulfonyl)phenyl) amino)pyrimidin-2-yl)amino)phenyl)amino)-3-oxopropanoate (**9a**).* Synthesized using the preparation method of **5b** using **8a** (0.80 g, 1.91 mmol), HOBT (0.27 g, 2.04 mmol), EDCI (0.40 g, 2.02 mmol), DIPEA (0.50 g, 3.83 mmol) and monomethyl malonate hydrochloride (0.27 g, 2.02 mmol) in 20 mL DCM, and 0.57 g of **9a** was obtained as white solid. Yield: 56.1%. M.p. 180–181 °C. ^{1}H NMR (600 MHz, $CDCl_3$) δ 9.61 (s, 1H), 9.17 (s, 1H), 8.55 (d, J = 8.4 Hz, 1H), 8.14 (s, 1H), 7.94–7.88 (m, 1H), 7.63 (s, 1H), 7.49 (s, 4H), 7.27 (s, 1H), 7.15 (s, 1H), 3.82 (s, 3H), 3.51 (s, 2H), 3.29–3.18 (m, 1H), 1.31 (d, J = 6.9 Hz, 6H). MS (ESI) m/z: $[M+H]^+$: 518.1.

*4.1.6.2. Methyl 4-((4-((5-chloro-4-((2-(isopropylsulfonyl)phenyl) amino)pyrimidin-2-yl)amino)phenyl)amino)-4-oxobutanoate (**9b**).* White solid. Yield: 61.4%. M.p. 206–209 °C. ^{1}H NMR (600 MHz, $CDCl_3$) δ 9.61 (s, 1H), 8.55 (d, J = 8.4 Hz, 1H), 8.13 (s, 1H), 7.90 (d, J = 7.9 Hz, 1H), 7.65–7.57 (m, 2H), 7.52–7.44 (m, 4H), 7.25 (d, J = 7.6 Hz, 1H), 7.09 (s, 1H), 3.72 (s, 3H), 3.24 (s, 1H), 2.78 (t, J = 6.5 Hz, 2H), 2.68 (t, J = 6.5 Hz, 2H), 1.31 (d, J = 6.9 Hz, 6H). MS (ESI) m/z: $[M+H]^+$: 532.1.

*4.1.6.3. Methyl 5-((4-((5-chloro-4-((2-(isopropylsulfonyl)phenyl) amino)pyrimidin-2-yl)amino)phenyl)amino)-5-oxopentanoate (**9c**).* White solid. Yield: 65.4%. M.p. 180–183 °C. ^{1}H NMR (600 MHz, $CDCl_3$) δ 9.61 (s, 1H), 8.55 (d, J = 8.4 Hz, 1H), 8.13 (s, 1H), 7.90 (d, J = 7.9 Hz, 1H), 7.63 (t, J = 7.8 Hz, 1H), 7.46 (s, 5H), 7.25 (d, J = 7.6 Hz, 1H), 7.16 (s, 1H), 3.70 (s, 3H), 3.27–3.19 (m, 1H), 2.50–2.39 (m, 4H), 2.10–2.01 (m, 2H), 1.31 (d, J = 6.8 Hz, 6H). MS (ESI) m/z: $[M+H]^+$: 546.1.

*4.1.6.4. Methyl 6-((4-((5-chloro-4-((2-(isopropylsulfonyl)phenyl) amino)pyrimidin-2-yl)amino)phenyl)amino)-6-oxohexanoate (**9d**).* White solid. Yield: 55.6%. M.p. 180–181 °C. ^{1}H NMR (600 MHz, $CDCl_3$) δ 9.62 (s, 1H), 8.56 (d, J = 8.4 Hz, 1H), 8.13 (s, 1H), 7.90 (d, J = 7.9 Hz, 1H), 7.63 (t, J = 7.8 Hz, 1H), 7.52–7.45 (m, 4H), 7.41 (s, 1H), 7.25 (d, J = 7.6 Hz, 1H), 7.10 (s, 1H), 3.69 (s, 3H), 3.28–3.18 (m, 1H), 2.40 (t, J = 6.4 Hz, 4H), 1.78–1.71 (m, 4H), 1.31 (d, J = 6.8 Hz, 6H). MS (ESI) m/z: $[M+H]^+$: 560.2.

*4.1.6.5. Methyl 7-((4-((5-chloro-4-((2-(isopropylsulfonyl)phenyl) amino)pyrimidin-2-yl)amino)phenyl)amino)-7-oxoheptanoate (**9e**).* White solid. Yield: 55.7%. M.p. 175–176 °C. ^{1}H NMR (600 MHz, $CDCl_3$) δ 9.62 (s, 1H), 8.56 (d, J = 8.4 Hz, 1H), 8.13 (s, 1H), 7.90 (d, J = 7.9 Hz, 1H), 7.63 (t, J = 7.8 Hz, 1H), 7.47 (s, 4H), 7.28 (s, 1H), 7.25 (d, J = 7.7 Hz, 1H), 7.13 (s, 1H), 4.13 (q, J = 7.1 Hz, 2H), 3.26–3.21 (m, 1H), 2.37 (t, J = 7.5 Hz, 2H), 2.33 (t, J = 7.4 Hz, 2H), 1.83–1.71 (m, 4H), 1.71–1.63 (m, 3H), 1.32 (t, J = 5.6 Hz, 6H). MS (ESI) m/z: $[M+H]^+$: 574.2.

*4.1.6.6. Methyl 8-((4-((5-chloro-4-((2-(isopropylsulfonyl)phenyl) amino)pyrimidin-2-yl)amino)phenyl)amino)-8- oxooctanoate (**9f**).* White solid. Yield: 55.7%. M.p. 174–176 °C. ^{1}H NMR (600 MHz, $CDCl_3$) δ 9.62 (s, 1H), 8.55 (d, J = 7.9 Hz, 1H), 8.12 (s, 1H), 7.90 (dd, J = 7.9, 1.5 Hz, 1H), 7.65–7.58 (m, 1H), 7.46 (s, 4H), 7.25 (d, J = 5.0 Hz, 2H), 7.18 (s, 1H), 3.67 (s, 3H), 3.26–3.18 (m, 1H), 2.38–2.66 (m, 4H), 1.77–1.71 (m, 2H), 1.69–1.57 (m, 2H), 1.47–1.35 (m, 4H), 1.31 (d, J = 6.9 Hz, 6H). MS (ESI) m/z: $[M+H]^+$: 588.2.

*4.1.6.7. Methyl 5-((3-((5-chloro-4-((2-(isopropylsulfonyl)phenyl) amino)pyrimidin-2-yl)amino)phenyl)amino)-5-oxopentanoate (**9g**).* White solid. Yield: 62.6%. M.p. > 250 °C. ^{1}H NMR (600 MHz, DMSO-d_6) δ 9.84 (s, 1H), 9.56 (s, 2H), 8.71 (d, J = 6.4 Hz, 1H), 8.28 (s, 1H), 7.93–7.78 (m, 2H), 7.68 (t, J = 7.6 Hz, 1H), 7.35 (t, J = 7.5 Hz, 2H), 7.24–7.09 (m, 2H), 3.59 (s, 3H), 3.48–3.40 (m, 1H), 2.39–2.30 (m, 4H), 1.86–1.77 (m, 2H), 1.18 (d, J = 6.8 Hz, 6H). MS (ESI) m/z: $[M+H]^+$: 546.2.

*4.1.6.8. Methyl 6-((3-((5-chloro-4-((2-(isopropylsulfonyl)phenyl) amino)pyrimidin-2-yl)amino)phenyl)amino)-6-oxohexanoate (**9h**).* White solid. Yield: 64.7%. M.p. 110–112 °C. ^{1}H NMR (600 MHz, DMSO-d_6) δ 9.81 (s, 1H), 9.55 (s, 2H), 8.70 (d, J = 7.4 Hz, 1H), 8.29 (s, 1H), 7.90–7.79 (m, 2H), 7.71–7.65 (m, 1H), 7.37–7.31 (m, 2H), 7.20–7.13 (m, 2H), 3.58 (d, J = 4.0 Hz, 3H), 3.47–3.41 (m, 1H), 2.36–2.24 (m, 5H), 1.60–1.48 (m, 3H), 1.17 (d, J = 6.8 Hz, 6H). MS (ESI) m/z: $[M+H]^+$:560.0.

*4.1.6.9. Ethyl 7-((3-((5-chloro-4-((2-(isopropylsulfonyl)phenyl) amino)pyrimidin-2-yl)amino)phenyl)amino)-7-oxoheptanoate (**9i**).* White solid. Yield: 55.7%. M.p. > 250 °C. ^{1}H NMR (600 MHz, DMSO-d_6) δ 9.80 (s, 1H), 9.55 (d, J = 7.1 Hz, 2H), 8.71 (d, J = 6.2 Hz, 1H), 8.28 (s, 1H), 7.88–7.80 (m, 2H), 7.68 (t, J = 7.5 Hz, 1H), 7.38–7.29 (m, 2H), 7.22–7.12 (m, 2H), 4.03 (q, J = 7.0 Hz, 2H), 3.47–3.41 (m, 1H), 2.28 (t, J = 5.8 Hz, 5H), 1.47–1.62 (m, 5H), 1.34–1.25 (m, 3H), 1.17 (d, J = 6.6 Hz, 6H). MS (ESI) m/z: $[M+H]^+$: 574.2.

*4.1.6.10. Methyl 6-((5-((5-chloro-4-((2-(isopropylsulfonyl)phenyl) amino)pyrimidin-2-yl)amino)-2-methylphenyl)amino)-6-oxohexanoate (**9j**).* White solid. Yield: 31.5%. M.p. 134–137 °C. ^{1}H NMR (600 MHz, $CDCl_3$) δ 9.59 (s, 1H), 8.57 (d, J = 8.3 Hz, 1H), 8.14 (d, J = 9.1 Hz, 1H), 7.94 (s, 1H), 7.90 (d, J = 7.0 Hz, 1H), 7.60 (t, J = 7.6 Hz, 1H), 7.48–7.41 (m, 1H), 7.24 (t, J = 7.7 Hz, 1H), 7.16–7.07 (m, 2H), 7.05 (s, 1H), 3.68 (s, 3H), 3.29–3.20 (m, 1H), 2.45–2.34 (m, 4H), 2.24 (s, 3H), 1.78–1.70 (m, 4H), 1.31 (d, J = 6.8 Hz, 6H). MS (ESI) m/z: $[M+H]^+$: 574.2.

*4.1.7. General procedure for the synthesis of **10a-j***

*4.1.7.1. N^1-(4-((5-chloro-4-((2-(isopropylsulfonyl)phenyl)amino)pyr-imidin-2-yl)amino)phenyl)-N^3-hydroxymalonamide (**10a**).* Synthesized using the preparation method of **6a** using **9a** (0.20 g, 0.38 mmol) in 20 mL hydroxylamine methanol solution, and 0.12 g of **10a** was obtained as white solid. Yield: 60.3%. M.p. 148–149 °C. ^{1}H NMR (600 MHz, DMSO-d_6) δ 10.62 (s, 1H), 10.04 (s, 1H), 9.52 (s, 1H), 9.47 (s, 1H), 8.99 (s, 1H), 8.60 (s, 1H), 8.28 (s, 1H), 7.86 (d, J = 7.9 Hz, 1H), 7.74 (t, J = 7.6 Hz, 1H), 7.52 (d, J = 7.0 Hz, 2H), 7.45 (d, J = 8.2 Hz, 2H), 7.40 (t, J = 7.5 Hz, 1H), 3.52–3.42 (m, 1H), 3.10 (s, 2H), 1.17 (d, J = 6.6 Hz, 6H). ^{13}C NMR (151 MHz, DMSO-d_6) δ 165.30, 164.04, 158.14, 155.73, 155.35, 138.50, 136.05, 135.25, 133.88, 131.41,

125.08, 124.63, 124.15, 120.53, 119.86, 104.94, 60.23, 55.32, 42.42, 15.33, 14.56. HRMS *m/z* calcd for $C_{22}H_{24}ClN_6O_5S$ $[M+H]^+$: 519.1212, found: 519.1210.

*4.1.7.2. N^1-(4-((5-chloro-4-((2-(isopropylsulfonyl)phenyl)amino)pyrimidin-2-yl)amino)phenyl)-N^4-hydroxysuccinamide (**10b**).* White solid. Yield: 40.0%. M.p. 151–153 °C. ^{1}H NMR (600 MHz, DMSO-d_6) δ 10.44 (s, 1H), 9.88 (s, 1H), 9.50–9.44 (m, 2H), 8.73 (s, 1H), 8.60 (s, 1H), 8.27 (s, 1H), 7.86 (d, *J* = 7.9 Hz, 1H), 7.74 (t, *J* = 7.6 Hz, 1H), 7.50 (d, *J* = 7.4 Hz, 2H), 7.45 (d, *J* = 8.3 Hz, 2H), 7.40 (t, *J* = 7.5 Hz, 1H), 3.48–3.42 (m, 1H), 2.54 (t, *J* = 7.1 Hz, 2H), 2.28 (t, *J* = 7.1 Hz, 2H),1.16 (d, *J* = 6.6 Hz, 6H). ^{13}C NMR (151 MHz, DMSO-d_6) δ 170.22, 168.87, 158.17, 155.74, 155.34, 138.51, 135.66, 135.25, 134.30, 131.41, 125.05, 124.56, 124.15, 120.52, 119.68, 104.86, 55.32, 31.87, 27.98, 15.32. HRMS *m/z* calcd for $C_{23}H_{26}ClN_6O_5S$ $[M+H]^+$: 533.1368, found: 533.1368.

*4.1.7.3. N^1-(4-((5-chloro-4-((2-(isopropylsulfonyl)phenyl)amino)pyrimidin-2-yl)amino)phenyl)-N^5-hydroxyglutaramide (**10c**).* White solid. Yield: 66.3%. M.p. 159–160 °C. ^{1}H NMR (600 MHz, DMSO-d_6) δ 10.42 (s, 1H), 9.83 (s, 1H), 9.54–9.41 (m, 2H), 8.72 (s, 1H), 8.61 (s, 1H), 8.28 (s, 1H), 7.86 (d, *J* = 7.8 Hz, 1H), 7.74 (t, *J* = 7.5 Hz, 1H), 7.53–7.46 (m, 4H), 7.40 (t, *J* = 7.5 Hz, 1H), 3.49–3.41 (m, 1H), 2.35–2.27 (m, 2H), 2.02 (t, *J* = 7.1 Hz, 2H), 1.86–1.71 (m, 2H), 1.17 (d, *J* = 6.5 Hz, 6H). ^{13}C NMR (151 MHz, DMSO-d_6) δ 170.83, 169.23, 158.17, 155.72, 155.31, 138.51, 135.66, 135.29, 134.35, 131.39, 124.93, 124.61, 124.11, 120.50, 119.84, 104.81, 55.33, 36.01, 32.15, 21.74, 15.32. HRMS *m/z* calcd for $C_{24}H_{28}ClN_6O_5S$ $[M+H]^+$: 547.1525, found: 547.1530.

*4.1.7.4. N^1-(4-((5-chloro-4-((2-(isopropylsulfonyl)phenyl)amino)pyrimidin-2-yl)amino)phenyl)-N^6-hydroxyadipamide (**10d**).* White solid. Yield: 68.4%. M.p. 199–200 °C. ^{1}H NMR (600 MHz, DMSO-d_6) δ 10.37 (s, 1H), 9.77 (s, 1H), 9.47 (s, 2H), 8.68 (s, 1H), 8.60 (s, 1H), 8.27 (s, 1H), 7.85 (d, *J* = 7.8 Hz, 1H), 7.74 (t, *J* = 7.3 Hz, 1H), 7.54–7.48 (m, 4H), 7.40 (t, *J* = 7.4 Hz, 1H), 3.50–3.39 (m, 1H), 2.28 (d, *J* = 5.8 Hz, 2H), 1.99 (d, *J* = 6.4 Hz, 2H), 1.54 (s, 4H), 1.17 (d, *J* = 6.5 Hz, 6H). ^{13}C NMR (151 MHz, DMSO-d_6) δ 171.10, 169.42, 158.18, 155.74, 155.33, 138.51, 135.69, 135.25, 134.31, 131.40, 125.14, 124.69, 124.12, 120.54, 119.82, 104.86, 55.32, 36.59, 32.66, 25.38, 25.36, 15.33. HRMS *m/z* calcd for $C_{25}H_{30}ClN_6O_5S$ $[M+H]^+$: 561.1681, found: 561.1686.

*4.1.7.5. N^1-(4-((5-chloro-4-((2-(isopropylsulfonyl)phenyl)amino)pyrimidin-2-yl)amino)phenyl)-N^7-hydroxyheptanediamide (**10e**).* White solid. Yield: 51.0%. M.p. 195–196 °C. ^{1}H NMR (600 MHz, DMSO-d_6) δ 10.35 (s, 1H), 9.77 (s, 1H), 9.52–9.42 (m, 2H), 8.68 (s, 1H), 8.60 (s, 1H), 8.27 (s, 1H), 7.86 (d, *J* = 6.1 Hz, 1H), 7.74 (s, 1H), 7.54–7.46 (m, 4H), 7.40 (s, 1H), 3.45 (s, 1H), 2.27 (s, 2H), 1.95 (s, 2H), 1.59–1.52 (m, 4H), 1.27 (s, 2H), 1.17 (s, 6H). ^{13}C NMR (151 MHz, DMSO-d_6) δ 171.20, 169.52, 158.17, 155.76, 155.34, 138.51, 135.67, 135.26, 134.34, 131.41, 125.08, 124.59, 124.13, 120.52, 119.81, 104.87, 55.32, 36.64, 32.64, 28.75, 25.42, 25.38, 15.33. HRMS *m/z* calcd for $C_{26}H_{32}ClN_6O_5S$ $[M+H]^+$: 575.1838, found: 575.1834.

*4.1.7.6. N^1-(4-((5-chloro-4-((2-(isopropylsulfonyl)phenyl)amino)pyrimidin-2-yl)amino)phenyl)-N^8-hydroxyoctanediamide (**10f**).* White solid. Yield: 81.2%. M.p. 172–174 °C. ^{1}H NMR (600 MHz, DMSO-d_6) δ 10.33 (s, 1H), 9.75 (s, 1H), 9.46 (s, 2H), 8.65 (s, 1H), 8.60 (s, 1H), 8.26 (s, 1H), 7.85 (dd, *J* = 7.9, 1.3 Hz, 1H), 7.73 (t, *J* = 7.6 Hz, 1H), 7.49 (d, *J* = 8.3 Hz, 2H), 7.45 (d, *J* = 8.9 Hz, 2H), 7.39 (t, *J* = 7.6 Hz, 1H), 3.53–3.40 (m, 1H), 2.26 (t, *J* = 7.4 Hz, 2H), 1.94 (t, *J* = 7.4 Hz, 2H), 1.65–1.52 (m, 2H), 1.53–1.44 (m, 2H), 1.27 (s, 4H), 1.16 (d, *J* = 6.8 Hz, 6H). ^{13}C NMR (151 MHz, DMSO-d_6) δ 171.26, 169.57, 158.18, 155.73, 155.33, 138.51, 135.66, 135.24, 134.35, 131.41, 124.99, 124.58, 124.11, 120.54, 119.83, 104.87, 55.33, 36.75, 32.72, 28.92, 28.89, 25.56, 25.52, 15.33. HRMS *m/z* calcd for $C_{27}H_{34}ClN_6O_5S$ $[M+H]^+$: 589.1998, found: 589.1998.

*4.1.7.7. N^1-(3-((5-chloro-4-((2-(isopropylsulfonyl)phenyl)amino)pyrimidin-2-yl)amino)phenyl)-N^5-hydroxyglutaramide (**10g**).* White solid. Yield: 81.2%. M.p. 217–218 °C. ^{1}H NMR (600 MHz, DMSO-d_6) δ 10.41 (s, 1H), 9.86 (s, 1H), 9.57 (d, *J* = 8.6 Hz, 2H), 8.72 (s, 2H), 8.30 (s, 1H), 7.88–7.82 (m, 2H), 7.70 (t, *J* = 7.7 Hz, 1H), 7.38–7.32 (m, 2H), 7.23–7.16 (m, 2H), 3.52–3.48 (m, 1H), 2.31 (t, *J* = 7.4 Hz, 2H), 2.01 (t, *J* = 7.4 Hz, 2H), 1.81–1.76 (m, 2H), 1.18 (d, *J* = 6.8 Hz, 6H). ^{13}C NMR (151 MHz, DMSO-d_6) δ 171.08, 169.19, 158.17, 155.61, 155.19, 140.65, 139.87, 138.49, 135.35, 131.38, 128.89, 124.39, 124.02, 123.89, 115.51, 113.84, 111.65, 105.36, 55.40, 36.07, 32.13, 21.64, 15.34. HRMS *m/z* calcd for $C_{24}H_{28}ClN_6O_5S$ $[M+H]^+$: 547.1525, found: 547.1532.

*4.1.7.8. N^1-(3-((5-chloro-4-((2-(isopropylsulfonyl)phenyl)amino)pyrimidin-2-yl)amino)phenyl)-N^6-hydroxyadipamide (**10h**).* White solid. Yield: 71.0%. M.p. 215–216 °C. ^{1}H NMR (600 MHz, DMSO-d_6) δ 10.41 (s, 1H), 9.89 (s, 1H), 9.57 (d, *J* = 6.6 Hz, 2H), 8.71 (s, 2H), 8.30 (s, 1H), 7.90–7.80 (m, 2H), 7.69 (t, *J* = 7.7 Hz, 1H), 7.37–7.33 (m, 2H), 7.21 (d, *J* = 8.1 Hz, 1H), 7.16 (t, *J* = 8.0 Hz, 1H), 3.49–3.43 (m, 1H), 2.29 (d, *J* = 6.8 Hz, 2H), 1.98 (t, *J* = 6.7 Hz, 2H), 1.54 (d, *J* = 3.0 Hz, 4H), 1.18 (d, *J* = 6.8 Hz, 6H). ^{13}C NMR (151 MHz, DMSO-d_6) δ 171.43, 169.43, 158.17, 155.60, 155.19, 140.63, 139.89, 138.49, 135.37, 131.37, 128.89, 124.34, 124.00, 123.87, 115.52, 113.87, 111.68, 105.34, 55.40, 36.61, 32.63, 25.35, 25.31, 15.34. HRMS *m/z* calcd for $C_{25}H_{30}ClN_6O_5S$ $[M+H]^+$: 561.1681, found: 561.1680.

*4.1.7.9. N^1-(3-((5-chloro-4-((2-(isopropylsulfonyl)phenyl)amino)pyrimidin-2-yl)amino)phenyl)-N^7-hydroxyheptanediamide (**10i**).* White solid. Yield: 65.3%. M.p. 202–203 °C. ^{1}H NMR (600 MHz, DMSO-d_6) δ 10.35 (s, 1H), 9.83 (s, 1H), 9.57 (d, *J* = 3.3 Hz, 2H), 8.75–8.68 (m, 2H), 8.30 (s, 1H), 7.89–7.80 (m, 2H), 7.70 (t, *J* = 7.7 Hz, 1H), 7.40–7.34 (m, 2H), 7.21–7.14 (m, 2H), 3.52–3.45 (m, 1H), 2.28 (t, *J* = 7.3 Hz, 2H), 1.95 (t, *J* = 7.4 Hz, 2H), 1.59–1.48 (m, 4H), 1.31–1.25 (m, 2H), 1.18 (d, *J* = 6.8 Hz, 6H). ^{13}C NMR (151 MHz, DMSO-d_6) δ 171.51, 169.51, 158.17, 155.60, 155.19, 140.64, 139.91, 138.50, 135.36, 131.38, 128.90, 124.36, 123.99, 123.86, 115.49, 113.83, 111.64, 105.36, 55.39, 36.68, 32.64, 28.75, 25.43, 25.33, 15.34. HRMS *m/z* calcd for $C_{26}H_{32}ClN_6O_5S$ $[M+H]^+$: 575.1838, found: 575.1850.

*4.1.7.10. N^1-(5-((5-chloro-4-((2-(isopropylsulfonyl)phenyl)amino)pyrimidin-2-yl)amino)-2-methylphenyl)-N^6-hydroxyadipamide (**10j**).* White solid. Yield: 65.3%. M.p. 194–196 °C. ^{1}H NMR (600 MHz, DMSO-d_6) δ 10.36 (s, 1H), 9.55–9.44 (m, 2H), 9.21 (s, 1H), 8.67 (s, 2H), 8.28 (s, 1H), 7.89–7.78 (m, 1H), 7.73 (t, *J* = 7.5 Hz, 1H), 7.61 (s, 1H), 7.42–7.31 (m, 2H), 7.07 (d, *J* = 8.3 Hz, 1H), 3.48–3.42 (m, 1H), 2.29 (s, 2H), 2.12 (s, 3H), 1.98 (s, 2H), 1.54 (s, 4H), 1.17 (d, *J* = 6.8 Hz, 6H). ^{13}C NMR (151 MHz, DMSO-d_6) δ 171.25, 169.43, 158.12, 155.69, 155.18, 138.50, 138.32, 136.79, 135.43, 131.38, 130.31, 126.04, 124.45, 123.95, 123.88, 117.29, 105.08, 55.38, 36.04, 32.64, 25.49, 25.36, 17.79, 15.34. HRMS *m/z* calcd for $C_{26}H_{32}ClN_6O_5S$ $[M+H]^+$: 575.1838, found: 575.1837.

*4.1.8. General procedure for the synthesis of intermediates **13a-m***

Aniline (1.02 g, 10.96 mmol, **11a**) and 2,4,5-trichloropyrimidine (2.04 g, 11.22 mmol, **12a**) was dissolved in 20 mL isopropanol and DIPEA (1.46 g, 11.32 mmol) was added. The resulting mixture was then stirred at 90 °C for 6 h. After reaction completion, the reaction mixture was extracted with 100 mL EtOAc, then the organic layer was washed with saturated NaCl aqueous solution twice, dried overnight with anhydrous Na_2SO_4 and filtered. The resulting filtrate (**13a**) was concentrated under vacuum and can be directly used without further purification. **13b-j** was synthesized using the

analog method that used to synthesize **13a**.

To a solution of 2-(isopropylsulfonyl)aniline (2.04 g, 21.92 mmol, **11j**) in DMF (20 mL) was added sodium hydride (1.04 g, 24.96 mmol, 60% in mineral oil) at 0 °C. After stirring for 0.5 h, 2,4-dichloro-5-fluoropyrimidine (3.66 g, 22.05 mmol, **12b**) was added to the reaction mixture followed by warming the mixture to room temperature. After stirring for 2 h, the reaction mixture was quenched with ice and diluted with excess water. The precipitate was filtered and the solid was dried to obtain **13k** as a brown solid which can be directly used without further purification. **13l-m** was synthesized using the analog method that used to synthesize **13k**.

*4.1.9. General procedure for the synthesis of intermediates **14a-m***

Synthesized using the preparation method of **3a** using 1.00 g (4.18 mmol) of **13a** and 0.45 g (4.17 mmol) of *p*-phenylenediamine (**7a**) in 20 mL IPA and 0.80g (4.17 mmol) TsOH was added, and 0.6 g of **14a** was obtained as purple solid which can be directly used without further purification. **14b-m** was synthesized using the analog method that used to synthesize **14a**.

*4.1.10. General procedure for the synthesis of intermediates **15a-m***

*4.1.10.1. Methyl 8-((4-((5-chloro-4-(phenylamino)pyrimidin-2-yl) amino)phenyl)amino)-8-oxooctanoate (**15a**).* Synthesized using the preparation method of **5b** using **14a** (0.60 g, 1.93 mmol), HOBT (0.52 g, 3.86 mmol), EDCI (0.74 g, 3.86 mmol), DIPEA (1.00 g, 7.75 mmol) and monomethyl suberate hydrochloride (0.44g, 1.96 mmol) in 20 mL DMF, and 0.40 g of **15a** was obtained as brown solid. Yield: 66.6%. M.p. 198–200 °C. ^{1}H NMR (600 MHz, DMSO-d_6) δ 9.70 (s, 1H), 9.24 (s, 1H), 8.80 (s, 1H), 8.12 (s, 1H), 7.66 (d, J = 7.6 Hz, 2H), 7.50 (d, J = 8.4 Hz, 2H), 7.42–7.33 (m, 4H), 7.14 (t, J = 7.3 Hz, 1H), 3.58 (s, 3H), 2.29 (t, J = 7.3 Hz, 2H), 2.25 (t, J = 7.3 Hz, 2H), 1.56 (d, J = 6.9 Hz, 2H), 1.53 (d, J = 7.0 Hz, 2H), 1.29 (s, 4H).

*4.1.10.2. Methyl 8-((4-((5-chloro-4-(o-tolylamino)pyrimidin-2-yl) amino)phenyl)amino)-8-oxooctanoate (**15b**).* White solid. Yield: 70.2%. M.p. 168–170 °C. ^{1}H NMR (600 MHz, DMSO-d_6) δ 9.61 (s, 1H), 9.13 (s, 1H), 8.67 (s, 1H), 8.05 (s, 1H), 7.37–7.28 (m, 4H), 7.28–7.23 (m, 2H), 7.21 (d, J = 8.8 Hz, 2H), 3.58 (s, 3H), 2.29 (t, J = 7.4 Hz, 2H), 2.22 (t, J = 7.4 Hz, 2H), 2.17 (s, 3H), 1.59–1.49 (m, 4H), 1.30–1.26 (m, 4H).

*4.1.10.3. Methyl 8-((4-((5-chloro-4-(m-tolylamino)pyrimidin-2-yl) amino)phenyl)amino)-8-oxooctanoate (**15c**).* White solid. Yield: 50.4%. M.p. 178–180 °C. ^{1}H NMR (600 MHz, DMSO-d_6) δ 9.69 (s, 1H), 9.24 (s, 1H), 8.72 (s, 1H), 8.10 (s, 1H), 7.53–7.47 (m, 3H), 7.39 (d, J = 8.6 Hz, 3H), 7.24–7.21 (m, 1H), 6.96 (d, J = 7.4 Hz, 1H), 3.58 (s, 3H), 2.30 (d, J = 10.8 Hz, 4H), 2.25 (t, J = 7.3 Hz, 2H), 1.59–1.46 (m, 5H), 1.29 (s, 4H).

*4.1.10.4. Methyl 8-((4-((5-chloro-4-(p-tolylamino)pyrimidin-2-yl) amino)phenyl)amino)-8-oxooctanoate (**15d**).* White solid. Yield: 69.8%. M.p. 200–201 °C. ^{1}H NMR (600 MHz, DMSO-d_6) δ 9.68 (s, 1H), 9.19 (s, 1H), 8.73 (s, 1H), 8.08 (s, 1H), 7.55–7.48 (m, 4H), 7.37 (d, J = 8.2 Hz, 2H), 7.16 (d, J = 7.7 Hz, 2H), 3.58 (s, 3H), 2.33 (s, 2H), 2.29 (d, J = 5.9 Hz, 3H), 2.25 (d, J = 6.9 Hz, 2H), 1.60–1.51 (m, 4H), 1.29 (s, 4H).

*4.1.10.5. Methyl 8-((4-((5-chloro-4-((2-chlorophenyl)amino)pyrimidin-2-yl)amino)phenyl)amino)-8-oxooctanoate (**15e**).* White solid. Yield: 72.1%. M.p. 201–202 °C. ^{1}H NMR (600 MHz, DMSO-d_6) δ 9.64 (s, 1H), 9.24 (s, 1H), 8.78 (s, 1H), 8.12 (s, 1H), 7.69 (s, 1H), 7.60 (d, J = 7.6 Hz, 1H), 7.41 (d, J = 7.6 Hz, 1H), 7.38–7.29 (m, 3H), 7.26 (d, J = 7.0 Hz, 2H), 3.58 (s, 3H), 2.29 (d, J = 6.5 Hz, 2H), 2.23 (s, 2H), 1.53 (d, J = 6.2 Hz, 4H), 1.28 (s, 4H).

*4.1.10.6. Methyl 8-((4-((4-((2-bromophenyl)amino)-5-chloropyrimidin-2-yl)amino)phenyl)amino)-8-oxooctanoate (**15f**).* White solid. Yield: 62.4%. M.p. 205–207 °C. ^{1}H NMR (600 MHz, DMSO-d_6) δ 9.63 (s, 1H), 9.23 (s, 1H), 8.76 (s, 1H), 8.12 (s, 1H), 7.75 (d, J = 8.0 Hz, 1H), 7.70 (d, J = 6.9 Hz, 1H), 7.45 (t, J = 7.6 Hz, 1H), 7.31 (d, J = 7.8 Hz, 2H), 7.26 (t, J = 7.1 Hz, 3H), 3.58 (s, 3H), 2.29 (t, J = 7.2 Hz, 2H), 2.23 (t, J = 7.4 Hz, 2H), 1.58–1.51 (m, 4H), 1.28 (s, 4H).

*4.1.10.7. Methyl 8-((4-((5-chloro-4-((3-methoxyphenyl)amino)pyrimidin-2-yl)amino)phenyl)amino)-8-oxooctanoate (**15g**).* White solid. Yield: 70.3%. M.p. 128–130 °C. ^{1}H NMR (600 MHz, DMSO-d_6) δ 9.69 (s, 1H), 9.26 (s, 1H), 8.75 (s, 1H), 8.12 (s, 1H), 7.51 (d, J = 8.9 Hz, 2H), 7.38 (d, J = 8.9 Hz, 2H), 7.29 (d, J = 7.8 Hz, 1H), 7.26–7.21 (m, 2H), 6.71 (dd, J = 8.1, 1.9 Hz, 1H), 3.73 (s, 3H), 3.57 (s, 3H), 2.29 (t, J = 7.4 Hz, 2H), 2.25 (t, J = 7.4 Hz, 2H), 1.61–1.54 (m, 2H), 1.54–1.49 (m, 2H), 1.29 (dd, J = 8.0, 4.7 Hz, 4H).

*4.1.10.8. Methyl 8-((4-((5-chloro-4-((5-methoxy-2-methylphenyl) amino)pyrimidin-2-yl)amino)phenyl)amino)-8-oxooctanoate (**15h**).* Brown solid. Yield: 75.2%. M.p. 149–152 °C. ^{1}H NMR (600 MHz, DMSO-d_6) δ 9.62 (s, 1H), 9.16 (s, 1H), 8.62 (s, 1H), 8.06 (s, 1H), 7.35 (d, J = 8.4 Hz, 2H), 7.24 (d, J = 8.6 Hz, 2H), 7.21 (d, J = 8.4 Hz, 1H), 6.94 (d, J = 1.9 Hz, 1H), 6.83 (dd, J = 8.4, 2.1 Hz, 1H), 3.74 (s, 3H), 3.58 (s, 3H), 2.29 (t, J = 7.3 Hz, 2H), 2.23 (t, J = 7.4 Hz, 2H), 2.09 (s, 3H), 1.56–1.51 (m, 4H), 1.30–1.27 (m, 4H).

*4.1.10.9. Methyl 8-((4-((5-chloro-4-((3,4-dimethoxyphenyl)amino) pyrimidin-2-yl)amino)phenyl)amino)-8-oxooctanoate (**15i**).* Pink solid. Yield: 77.2%. M.p. 144–146 °C. ^{1}H NMR (600 MHz, DMSO-d_6) δ 9.69 (s, 1H), 9.19 (s, 1H), 8.70 (s, 1H), 8.07 (s, 1H), 7.50 (d, J = 8.7 Hz, 2H), 7.35 (d, J = 8.7 Hz, 2H), 7.18 (s, 1H), 7.14 (d, J = 8.1 Hz, 1H), 6.92 (d, J = 8.6 Hz, 1H), 3.78 (s, 3H), 3.69 (s, 3H), 3.58 (s, 3H), 2.29 (t, J = 7.2 Hz, 2H), 2.24 (t, J = 7.4 Hz, 2H), 1.57–1.51 (m, 4H), 1.29 (d, J = 6.9 Hz, 4H).

*4.1.10.10. Methyl 8-((4-((4-((3-methoxyphenyl)amino)-5-(trifluoromethyl)pyrimidin-2-yl)amino)phenyl)amino)-8-oxooctanoate (**15j**).* Grey solid. Yield: 67.6%. M.p. 143–146 °C. ^{1}H NMR (600 MHz, DMSO-d_6) δ 9.90 (s, 1H), 9.58 (s, 1H), 8.63 (s, 1H), 8.34 (s, 1H), 7.60 (d, J = 8.5 Hz, 2H), 7.37 (s, 2H), 7.17 (d, J = 5.6 Hz, 2H), 7.00 (s, 1H), 6.48 (d, J = 7.9 Hz, 1H), 3.58 (s, 6H), 2.33–2.29 (m, 4H), 1.63–1.59 (m, 2H), 1.56–1.53 (m, 2H), 1.32 (s, 4H).

*4.1.10.11. Methyl 8-((4-((5-fluoro-4-((2-(isopropylsulfonyl)phenyl) amino)pyrimidin-2-yl)amino)phenyl)amino)-8-oxooctanoate (**15k**).* Brown solid. Yield: 43.2%. M.p. 178–179 °C. ^{1}H NMR (600 MHz, DMSO-d_6) δ 9.72 (s, 1H), 9.45 (d, J = 2.1 Hz, 1H), 9.32 (s, 1H), 8.64 (d, J = 8.1 Hz, 1H), 8.23 (d, J = 3.0 Hz, 1H), 7.85 (dd, J = 8.0, 1.4 Hz, 1H), 7.76–7.73 (m, 1H), 7.51 (d, J = 8.8 Hz, 2H), 7.44 (d, J = 8.9 Hz, 2H), 7.38 (t, J = 7.6 Hz, 1H), 3.58 (s, 3H), 3.49 (m, 1H), 2.28 (m, 4H), 1.60–1.55 (m, 2H), 1.58–1.50 (m, 2H), 1.32–1.28 (m, 4H), 1.16 (d, J = 6.8 Hz, 6H).

*4.1.10.12. Methyl 8-((4-((4-((2-(isopropylsulfonyl)phenyl)amino)-5-methylpyrimidin-2-yl)amino)phenyl)amino)-8-oxooctanoate (**15l**).* Brown solid. Yield: 30.5%. M.p. 195–196 °C. ^{1}H NMR (600 MHz, DMSO-d_6) δ 9.70 (s, 1H), 9.13 (s, 1H), 9.01 (s, 1H), 8.71 (d, J = 7.8 Hz, 1H), 8.03 (s, 1H), 7.85–7.81 (m, 1H), 7.71 (t, J = 7.4 Hz, 1H), 7.54 (d, J = 8.7 Hz, 2H), 7.43 (d, J = 8.8 Hz, 2H), 7.32 (t, J = 7.6 Hz, 1H), 3.58–3.57 (m, 3H), 3.47–3.41 (m, 1H), 2.31–2.29 (m, 2H), 2.26 (t, J = 7.4 Hz, 2H), 2.11 (s, 3H), 1.59–1.56 (m, 2H), 1.55–1.52 (m, 2H), 1.30 (s, 4H), 1.16 (d, J = 6.8 Hz, 6H).

4.1.10.13. Methyl 8-((4-((4-((2-(isopropylsulfonyl)phenyl)amino)-5-methoxypyrimidin-2-yl)amino)phenyl)amino)-8-oxooctanoate

(***15 m***). Brown solid. Yield: 39.2%. M.p. 100–101 °C. ^{1}H NMR (600 MHz, DMSO-d_6) δ 9.70 (s, 1H), 9.55 (s, 1H), 9.05 (s, 1H), 8.85 (d, J = 8.4 Hz, 1H), 7.99 (s, 1H), 7.81 (dd, J = 6.4, 5.4 Hz, 1H), 7.71 (t, J = 7.4 Hz, 1H), 7.57 (d, J = 8.8 Hz, 2H), 7.45 (d, J = 8.8 Hz, 2H), 7.30 (t, J = 7.7 Hz, 1H), 3.89 (s, 3H), 3.58 (s, 3H), 3.44–3.40 (m, 1H), 2.30 (t, J = 7.3 Hz, 2H), 2.26 (t, J = 7.4 Hz, 2H), 1.61–1.55 (m, 2H), 1.55–1.51 (m, 2H), 1.30 (s, 4H), 1.17 (d, J = 6.7 Hz, 6H).

4.1.11. General procedure for the synthesis of ***16a-m***

*4.1.11.1. N^1-(4-((5-chloro-4-(phenylamino)pyrimidin-2-yl)amino) phenyl)-N^8-hydroxyoctanediamide (**16a**).* Synthesized using the preparation method of **6a** using **15a** (0.40 g, 0.83 mmol) in 20 mL hydroxylamine methanol solution, and 0.28 g of **16a** was obtained as Brown solid. Yield: 70.3%. M.p. 223–225 °C. ^{1}H NMR (600 MHz, DMSO-d_6) δ 10.33 (s, 1H), 9.72 (s, 1H), 9.24 (s, 1H), 8.80 (s, 1H), 8.64 (s, 1H), 8.12 (s, 1H), 7.66 (d, J = 7.6 Hz, 2H), 7.50 (d, J = 8.6 Hz, 2H), 7.41–7.30 (m, 4H), 7.14 (t, J = 7.3 Hz, 1H), 2.25 (t, J = 7.3 Hz, 2H), 1.94 (t, J = 7.3 Hz, 2H), 1.61–1.53 (m, 2H), 1.53–1.45 (m, 2H), 1.32–1.26 (m, 4H). ^{13}C NMR (151 MHz, DMSO-d_6) δ 171.17, 169.53, 158.19, 156.36, 155.11, 139.16, 136.11, 133.82, 128.75, 124.29, 123.71, 119.83, 119.73, 103.98, 36.73, 32.71, 28.92, 28.89, 25.57, 25.53. HRMS m/z calcd for $C_{24}H_{28}ClN_6O_3$ $[M+H]^+$ 483.1911, found: 483.1902.

*4.1.11.2. N^1-(4-((5-chloro-4-(o-tolylamino)pyrimidin-2-yl)amino) phenyl)-N^8-hydroxyoctanediamide (**16b**).* White solid. Yield: 85.3%. M.p. 193–195 °C. ^{1}H NMR (600 MHz, DMSO-d_6) δ 10.33 (s, 1H), 9.61 (s, 1H), 9.13 (s, 1H), 8.66 (d, J = 9.5 Hz, 2H), 8.06 (s, 1H), 7.36–7.29 (m, 4H), 7.26 (dt, J = 7.4, 6.1 Hz, 2H), 7.22 (d, J = 8.8 Hz, 2H), 2.22 (t, J = 7.4 Hz, 2H), 2.18 (s, 3H), 2.02–1.80 (m, 2H), 1.58–1.52 (m, 2H), 1.51–1.46 (m, 2H), 1.29–1.23 (m, 4H). ^{13}C NMR (151 MHz, DMSO-d_6) δ 171.04, 169.55, 158.20, 157.47, 154.65, 137.66, 136.47, 135.36, 133.25, 130.73, 128.40, 126.67, 126.61, 119.63, 118.77, 103.38, 36.69, 32.72, 28.92, 28.88, 25.55, 25.52, 18.43. HRMS m/z calcd for $C_{25}H_{30}ClN_6O_3$ $[M+H]^+$ 497.2068, found: 497.2059.

*4.1.11.3. N^1-(4-((5-chloro-4-(m-tolylamino)pyrimidin-2-yl)amino) phenyl)-N^8-hydroxyoctanediamide (**16c**).* Brown solid. Yield: 80.2%. M.p. 208–210 °C. ^{1}H NMR (600 MHz, DMSO-d_6) δ 10.20 (s, 1H), 9.73 (s, 1H), 9.24 (s, 1H), 8.72 (s, 1H), 8.10 (s, 1H), 7.61–7.44 (m, 4H), 7.40 (d, J = 8.7 Hz, 3H), 7.23 (t, J = 7.7 Hz, 1H), 6.97 (d, J = 7.4 Hz, 1H), 2.32 (s, 3H), 2.25 (t, J = 7.3 Hz, 2H), 2.02–1.86 (m, 2H), 1.59–1.54 (m, 2H), 1.51–1.46 (m, 2H), 1.27 (d, J = 10.9 Hz, 4H). ^{13}C NMR (151 MHz, DMSO-d_6) δ 171.17, 169.51, 158.20, 156.37, 155.11, 138.99, 138.05, 136.09, 133.83, 128.62, 125.05, 124.27, 120.82, 119.74, 119.68, 103.88, 36.75, 32.70, 28.91, 28.88, 25.57, 25.54, 21.64. HRMS m/z calcd for $C_{25}H_{30}ClN_6O_3$ $[M+H]^+$ 497.2068, found: 497.2065.

*4.1.11.4. N^1-(4-((5-chloro-4-(p-tolylamino)pyrimidin-2-yl)amino) phenyl)-N^8-hydroxyoctanediamide (**16d**).* White solid. Yield: 88.7%. M.p. 233–235 °C. ^{1}H NMR (600 MHz, DMSO-d_6) δ 10.19 (s, 1H), 9.76 (s, 1H), 9.20 (s, 1H), 8.73 (s, 1H), 8.08 (s, 1H), 7.55–7.44 (m, 5H), 7.39 (d, J = 8.7 Hz, 2H), 7.16 (d, J = 8.1 Hz, 2H), 2.33 (s, 3H), 2.26 (t, J = 7.3 Hz, 2H), 1.95 (t, J = 7.1 Hz, 2H), 1.59–1.54 (m, 2H), 1.49 (s, 2H), 1.27 (d, J = 11.8 Hz, 4H). ^{13}C NMR (151 MHz, DMSO-d_6) δ 171.17, 158.20, 156.49, 154.88, 136.54, 136.17, 133.77, 133.45, 129.23, 123.91, 119.73, 119.71, 103.90, 36.75, 31.62, 30.30, 28.93, 28.89, 25.59, 21.06. HRMS m/z calcd for $C_{25}H_{30}ClN_6O_3$ $[M+H]^+$ 497.2068, found: 497.2063.

*4.1.11.5. N^1-(4-((5-chloro-4-((2-chlorophenyl)amino)pyrimidin-2-yl) amino)phenyl)-N^8-hydroxyoctanediamide (**16e**).* White solid. Yield: 80.1%. M.p. 231–233 °C. ^{1}H NMR (600 MHz, DMSO-d_6) δ 10.32 (s, 1H), 9.65 (s, 1H), 9.23 (s, 1H), 8.78 (s, 1H), 8.65 (s, 1H), 8.12 (s, 1H), 7.69 (d, J = 6.8 Hz, 1H), 7.59 (d, J = 8.0 Hz, 1H), 7.41 (t, J = 7.1 Hz, 1H), 7.32 (m, 3H), 7.26 (d, J = 8.6 Hz, 2H), 2.23 (t, J = 7.4 Hz, 2H), 1.94 (t, J = 7.4 Hz, 2H), 1.61–1.52 (m, 2H), 1.52–1.43 (m, 2H), 1.32–1.23 (m, 4H). ^{13}C NMR (151 MHz, DMSO-d_6) δ 173.89, 171.10, 158.12, 157.62, 157.05, 155.09, 136.33, 136.22, 136.19, 133.57, 133.53, 129.98, 128.06, 127.69, 119.64, 119.17, 36.70, 32.70, 32.66, 28.92, 28.87, 25.54. HRMS m/z calcd for $C_{24}H_{27}Cl_2N_6O_3$ $[M+H]^+$ 517.1522, found: 517.1522.

*4.1.11.6. N^1-(4-((4-((2-bromophenyl)amino)-5-chloropyrimidin-2-yl) amino)phenyl)-N^8-hydroxyoctanediamide (**16f**).* Brown solid. Yield: 85.0%. M.p. 250–252 °C. ^{1}H NMR (600 MHz, DMSO-d_6) δ 10.22 (s, 1H), 9.66 (d, J = 9.1 Hz, 1H), 9.24 (s, 1H), 8.69 (s, 1H), 8.12 (s, 1H), 7.75 (d, J = 7.7 Hz, 1H), 7.68 (s, 1H), 7.45 (t, J = 7.3 Hz, 1H), 7.31 (s, 2H), 7.26 (s, 4H), 2.23 (t, J = 6.9 Hz, 2H), 1.94 (s, 2H), 1.55 (s, 2H), 1.48 (s, 2H), 1.25 (d, J = 14.9 Hz, 4H). ^{13}C NMR (151 MHz, DMSO-d_6) δ 171.11, 171.10, 158.10, 157.03, 155.07, 155.03, 137.85, 136.22, 133.51, 133.11, 128.67, 127.95, 121.67, 119.63, 119.16, 96.47, 51.65, 36.69, 33.70, 28.92, 25.53, 24.79. HRMS m/z calcd for $C_{24}H_{27}BrClN_6O_3$ $[M+H]^+$ 561.1017, found: 561.1020.

*4.1.11.7. N^1-(4-((5-chloro-4-((3-methoxyphenyl)amino)pyrimidin-2-yl)amino)phenyl)-N^8-hydroxyoctanediamide (**16g**).* White solid. Yield: 89.3%. M.p. 200–201 °C. ^{1}H NMR (600 MHz, DMSO-d_6) δ 9.80 (s, 1H), 9.26 (s, 1H), 8.76 (s, 1H), 8.12 (s, 1H), 7.52 (d, J = 8.8 Hz, 2H), 7.41 (d, J = 8.7 Hz, 2H), 7.30 (d, J = 7.5 Hz, 1H), 7.28–7.14 (m, 3H), 6.71 (d, J = 7.2 Hz, 1H), 3.74 (s, 3H), 2.26 (t, J = 7.4 Hz, 2H), 1.95 (t, J = 7.1 Hz, 2H), 1.59–1.55 (m, 2H), 1.49 (s, 2H), 1.27 (s, 4H). ^{13}C NMR (151 MHz, DMSO-d_6) δ 171.19, 159.83, 158.18, 156.30, 155.16, 140.29, 136.06, 133.89, 129.44, 119.80, 119.74, 115.75, 109.92, 109.23, 104.06, 100.00, 55.47, 36.73, 32.59, 28.92, 28.89, 25.58. HRMS m/z calcd for $C_{25}H_{30}ClN_6O_4$ $[M+H]^+$ 513.2017, found: 513.2013.

*4.1.11.8. N^1-(4-((5-chloro-4-((5-methoxy-2-methylphenyl)amino) pyrimidin-2-yl)amino)phenyl)-N^8-hydroxyoctanediamide (**16h**).* Brown solid. Yield: 87.6%. M.p. 219–221 °C. ^{1}H NMR (600 MHz, DMSO-d_6) δ 10.31 (s, 1H), 9.64 (s, 1H), 9.15 (s, 1H), 8.62 (s, 1H), 8.04 (d, J = 12.6 Hz, 1H), 7.35 (d, J = 8.3 Hz, 2H), 7.25 (d, J = 8.4 Hz, 2H), 7.21 (d, J = 8.2 Hz, 1H), 6.94 (s, 1H), 6.82 (d, J = 7.4 Hz, 1H), 3.70 (s, 3H), 2.23 (t, J = 7.2 Hz, 2H), 2.08 (s, 3H), 1.94 (t, J = 6.8 Hz, 2H), 1.55 (s, 2H), 1.48 (s, 2H), 1.29–1.20 (m, 4H). ^{13}C NMR (151 MHz, DMSO-d_6) δ 194.95, 182.88, 171.06, 158.20, 158.14, 157.36, 154.68, 138.33, 136.45, 133.32, 131.18, 126.86, 119.64, 118.81, 113.65, 112.35, 55.63, 36.76, 36.70, 28.93, 28.90, 25.62, 25.57, 17.58. HRMS m/z calcd for $C_{26}H_{32}ClN_6O_4$ $[M+H]^+$ 527.2174, found: 527.2170.

*4.1.11.9. N^1-(4-((5-chloro-4-((3,4-dimethoxyphenyl)amino)pyrimidin-2-yl)amino)phenyl)-N^8-hydroxyoctanediamide (**16i**).* White solid. Yield: 80.3%. M.p. 162–164 °C. ^{1}H NMR (600 MHz, DMSO-d_6) δ 10.37 (s, 1H), 9.77 (s, 1H), 9.23 (s, 1H), 8.74 (s, 1H), 8.08 (s, 1H), 7.49 (d, J = 8.5 Hz, 2H), 7.38 (s, 2H), 7.22 (s, 1H), 7.19 (s, 1H), 7.15 (d, J = 8.0 Hz, 1H), 6.93 (d, J = 8.6 Hz, 1H), 3.79 (s, 3H), 3.70 (s, 3H), 2.26 (t, J = 7.3 Hz, 2H), 1.95 (t, J = 7.3 Hz, 2H), 1.59–1.53 (m, 2H), 1.52–1.46 (m, 2H), 1.26 (d, J = 6.6 Hz, 4H). ^{13}C NMR (151 MHz, DMSO-d_6) δ 171.17, 169.58, 158.05, 156.66, 154.48, 148.89, 146.20, 136.12, 133.79, 132.16, 119.72, 119.66, 116.43, 112.02, 109.28, 103.74, 56.26, 55.85, 36.72, 32.72, 28.92, 28.89, 25.59, 25.52. HRMS m/z calcd for $C_{26}H_{31}ClN_6O_5Na$ $[M+Na]^+$ 565.1942, found: 565.1941.

*4.1.11.10. N^1-hydroxy-N^8-(4-((4-((3-methoxyphenyl)amino)-5-(trifluoromethyl)pyrimidin-2-yl)amino)phenyl)octanediamide (**16j**).* Brown solid. Yield: 82.7%. M.p. 180–182 °C. ^{1}H NMR (600 MHz, DMSO-d_6) δ 10.35 (s, 1H), 9.93 (s, 1H), 9.58 (s, 1H), 8.65 (d, J = 15.6 Hz, 2H), 8.34 (s, 1H), 7.60 (d, J = 8.4 Hz, 2H), 7.36 (d, J = 5.6 Hz, 2H), 7.17 (s, 2H), 7.00 (s, 1H), 6.48 (d, J = 7.7 Hz, 1H), 3.58 (s, 3H), 2.32 (t, J = 7.2 Hz, 2H), 1.95 (t, J = 7.2 Hz, 2H), 1.64–1.57 (m, 2H), 1.53–1.47 (m, 2H), 1.30 (s, 4H). ^{13}C NMR (151 MHz, DMSO-d_6) δ 171.57, 169.56, 161.07, 159.85, 155.92, 141.33, 137.07, 133.40, 129.41,

126.43, 124.34, 123.23, 119.49, 112.45, 107.67, 105.90, 55.21, 36.85, 32.73, 31.91, 30.47, 28.91, 25.59, 25.54. HRMS *m/z* calcd for $C_{26}H_{30}F_3N_6O_4$ $[M+H]^+$ 547.2281, found: 547.2277.

*4.1.11.11. N^1-(4-((5-fluoro-4-((2-(isopropylsulfonyl)phenyl)amino) pyrimidin-2-yl)amino)phenyl)-N^8-hydroxyoctanediamide (**16k**).* White solid. Yield: 78.5%. M.p. 188–190 °C. ^{1}H NMR (600 MHz, DMSO-d_6) δ 10.33 (s, 1H), 9.73 (s, 1H), 9.45 (s, 1H), 9.32 (s, 1H), 8.64 (d, J = 7.4 Hz, 2H), 8.23 (d, J = 2.4 Hz, 1H), 7.85 (d, J = 7.7 Hz, 1H), 7.74 (t, J = 7.6 Hz, 1H), 7.51 (d, J = 8.4 Hz, 2H), 7.45 (d, J = 8.7 Hz, 2H), 7.39 (t, J = 7.5 Hz, 1H), 3.53–3.47 (m, 1H), 2.26 (t, J = 7.2 Hz, 2H), 1.94 (t, J = 7.2 Hz, 2H), 1.60–1.54 (m, 2H), 1.53–1.47 (m, 2H), 1.28 (s, 4H), 1.17 (d, J = 6.7 Hz, 6H). ^{13}C NMR (151 MHz, DMSO-d_6) δ 171.20, 169.57, 155.95, 149.34, 149.28, 141.97, 140.34, 138.59, 136.21, 135.46, 133.94, 131.55, 123.98, 119.91, 119.86, 100.00, 55.45, 36.74, 32.73, 28.92, 28.89, 25.57, 25.52, 15.30. HRMS *m/z* calcd for $C_{27}H_{34}FN_6O_5S$ $[M+H]^+$ 573.2295, found: 573.2294.

*4.1.11.12. N^1-hydroxy-N^8-(4-((4-((2-(isopropylsulfonyl)phenyl) amino)-5-methylpyrimidin-2-yl)amino)phenyl)octanediamide (**16l**).* White solid. Yield: 69.5%. M.p. 209–211 °C. ^{1}H NMR (600 MHz, DMSO-d_6) δ 10.33 (s, 1H), 9.71 (s, 1H), 9.12 (s, 1H), 9.00 (s, 1H), 8.72 (d, J = 7.9 Hz, 1H), 8.65 (s, 1H), 8.03 (s, 1H), 7.82 (d, J = 7.9 Hz, 1H), 7.71 (t, J = 7.7 Hz, 1H), 7.54 (d, J = 8.5 Hz, 2H), 7.43 (d, J = 8.6 Hz, 2H), 7.32 (t, J = 7.6 Hz, 1H), 3.44 (dt, J = 13.4, 6.7 Hz, 1H), 2.26 (t, J = 7.1 Hz, 2H), 2.10 (s, 3H), 1.94 (t, J = 6.9 Hz, 2H), 1.59–1.55 (m, 2H), 1.51–1.47 (m, 2H), 1.27 (s, 4H), 1.16 (d, J = 6.7 Hz, 6H). ^{13}C NMR (151 MHz, DMSO-d_6) δ 171.16, 169.57, 158.68, 158.57, 157.07, 139.74, 136.58, 135.26, 133.56, 131.36, 124.00, 123.07, 119.89, 119.86, 119.78, 99.99, 55.31, 36.74, 32.72, 28.93, 28.89,25.58, 25.52, 15.32, 13.14. HRMS *m/z* calcd for $C_{28}H_{37}N_6O_5S$ $[M+H]^+$ 569.2546, found: 569.2541.

*4.1.11.13. N^1-hydroxy-N^8-(4-((4-((2-(isopropylsulfonyl)phenyl) amino)-5-methoxypyrimidin-2-yl)amino)phenyl)octanediamide (**16 m**).* White solid. Yield: 68.5%. M.p. 167–169 °C. ^{1}H NMR (600 MHz, DMSO-d_6) δ 10.33 (s, 1H), 9.70 (s, 1H), 9.55 (s, 1H), 9.05 (s, 1H), 8.84 (s, 1H), 8.65 (s, 1H), 7.99 (s, 1H), 7.81 (dd, J = 8.0, 1.4 Hz, 1H), 7.71 (s, 1H), 7.57 (d, J = 8.9 Hz, 2H), 7.45 (d, J = 8.9 Hz, 2H), 7.30 (s, 1H), 3.89 (s, 3H), 3.41 (d, J = 6.7 Hz, 1H), 2.26 (t, J = 7.4 Hz, 2H), 1.94 (t, J = 7.4 Hz, 2H), 1.57 (s, 2H), 1.49 (s, 2H), 1.30–1.26 (m, 4H), 1.17 (d, J = 6.8 Hz, 6H). ^{13}C NMR (151 MHz, DMSO-d_6) δ 171.13, 169.57, 154.10, 153.29, 151.06, 139.26, 136.94, 135.38, 135.25, 133.31, 131.43, 123.42, 122.83, 122.73, 119.97, 119.27, 58.04, 55.37, 36.74, 32.73, 28.93, 28.89, 25.59, 25.52, 15.36. HRMS *m/z* calcd for $C_{28}H_{37}N_6O_6S$ $[M+H]^+$ 585.2495, found: 585.2493.

*4.1.12. General procedure for the synthesis of **20***

To a solution of **1** in 20 mL isopropanol and 0.1 mL HCl solution (37%) was added **1** (1.02 g, 2.95 mmol) and 4-bromoaniline (0.54 g, 3.17 mmol, **2a**). The resulting mixture was then stirred at 90 °C for 6 h. After reaction completion, the reaction mixture was extracted with 100 mL EtOAc, then the organic layer was washed with saturated NaCl aqueous solution twice, dried overnight with anhydrous Na_2SO_4 and filtered. The resulting filtrate was concentrated under vacuum afford **18** as white solid. To a 50 mL three-necked round bottle was charged with **18** (2.4g, 5 mmol), methyl acrylate (0.86 g, 10 mmol), $Pd(OAc)_2$ (0.12 g), Tri(*o*-tolyl)phosphine (0.31 g, 1 mmol), 5 mL CH_3CN and 10 mL DMF. The resulting solution was warmed to 90 °C and stirred at this temperature for 6 h under N_2 atmosphere. When the reaction was completed, 100 mL water was added and the resulting mixture was extracted with ethyl acetate twice. The combined organic layer was successively washed with H_2O and then brine, then dried over anhydrous Na_2SO_4, filtered and concentrated under reduced pressure to give the product **19**. **19** (0.19 g, 0.4 mmol) was weighed into 20 mL freshly prepared hydroxylamine methanol solution and stirred at room temperature for 2 h. The pH value of reaction mixture was adjusted to 6–7 with saturated NH_4Cl solution. The white solid was precipitated, filtered and washed with water and 0.08 g of **20** was obtained. Yield: 42.2%. M.p. 162–164 °C. ^{1}H NMR (600 MHz, DMSO-d_6) δ 10.67 (s, 1H), 9.79 (s, 1H), 9.49 (s, 1H), 8.97 (s, 1H), 8.57 (s, 1H), 8.34 (s, 1H), 7.88 (d, J = 7.7 Hz, 1H), 7.82 (t, J = 7.5 Hz, 1H), 7.67 (d, J = 7.6 Hz, 2H), 7.51–7.34 (m, 4H), 6.39–6.28 (m, 1H), 3.49–3.42 (m, 1H), 1.16 (d, J = 6.6 Hz, 6H). ^{13}C NMR (151 MHz, DMSO-d_6) δ 163.71, 157.74, 155.66, 155.54, 141.83, 138.69, 138.35, 135.42, 131.46, 128.58, 128.46, 125.52, 124.93, 124.50, 119.58, 116.95, 105.79, 55.28, 15.32. HRMS *m/z* calcd for $C_{22}H_{23}ClN_5O_4S$ $[M+H]^+$ 488.1154, found: 488.1158.

4.2 . . Cell viability assay

All cancer cell lines (A549, HepG-2, MDA-MB-231, SH-SY5Y, H2228 and SK-N-BE2) were purchased from Cell Bank of China Science Academy (Shanghai, China). Cells were maintained in DMEM/F12 medium (Gibco, US) supplemented with 10% fetal bovine serum (Gibco, US) at 37 °C with 5% CO_2. Cell viability was determined with cell counting kit-8 (CCK-8) assay. Briefly, six cancer cell lines were seeded into 96-well plates at a density of 5×10^3 cells/well. After 24 h, the cells were treated with different concentrations of compounds (0.06, 0.125, 0.25, 0.5, 1, 2, 4, 8 μM). After 72 h, the drug containing medium in each well was replaced by 100 μL fresh medium and 10 μL CCK-8 (Yeasen, China) and incubated for extra 90 min. The OD_{450nm} value was measured using a microplate reader (BioTek, US). The data were calculated as the percent inhibition compared with control. The IC_{50} was the concentration at 50% inhibition ratio after fitting the curve in SPSS 17.0 software.

4.3 . . In Vitro ALK/HDAC1 inhibition assay

HDAC1 Enzyme Assay. The assays were carried out by Sundia MediTech Company, Ltd. Briefly, different concentrations of compounds were incubated with recombinant HDAC1 (BPS Biosciences, San Diego, CA, USA) at room temperature for 15 min, which was followed by adding mixture of Ac-peptide-AMC substrate and trypsin to initiate the coupled reaction in Tris-based assay buffer. Fluorescent AMC released from substrate was kinetically measured at RT in Synergy2 (BioTek, US) using filter sets as excitation = 355 nm and emission = 460 nm. IC_{50} values were calculated by GraphPad Prism software (California, US).

ALK Enzyme Assay. The assays were carried out by Sundia MediTech Company, Ltd. To make 100x solution from 10 μM with 3-fold serial dilution for total of 8 concentrations in DMSO. Transfer 250 nL samples to 384-well plate. Add 10 μL enzyme mix to assay plate with final concentration of 1.25 nM ALK. 10 μL 1x Kinase buffer was used as the negative control. Pre-incubate enzyme and samples at RT for 10 min. Add 15 μL substrate mix containing final concentration of 30 μM ATP and 3 μM kinase substrate to assay plate and incubate at RT for 25 min. 30 μL stop buffer containing EDTA will be added to stop the reaction. Read conversion rate with Caliper EZ Reader. The dose-response curve is fitted with GraphPad Prism 5 and IC_{50} calculated by log(inhibitor) vs. response -Variable slope.

4.4 . . Cloning formation assay

MDA-MB-231 or SH-SY5Y cells were seeded into 24-well plates at a density of 200 cells/well, and exposed in different concentrations of compound **10f** (0.1, 0.2, 0.4 μM) for three days. After that,

the drug containing medium was replaced by fresh drug-free medium and cells were cultured for two weeks until the colonies emerged. Then, cells were coped by crystal violet formalin solution for 30 min. Finally, the plates were washed and dried for images recording. ImageJ was used for colonies counting.

4.5. Cell scratch assay

MDA-MB-231 or SH-SY5Y cells were seeded into 6-well plates at a density of 5×10^5 cells/well. 24 h later, a straight line was scratched at the bottom of each well by a pipette. After washing with PBS for three times, cells were treated with different concentrations of **10f** (0.1, 0.2, 0.4 μM) for 48 h. Inverted microscope (× 200, Nikon, Japan) was used for images recording and width (W) of wounds were quantified by ImageJ software.

$$\text{Healing rate } (\%) = \frac{W_{0h} - W_{48h}}{W_{0h}} \times 100\%$$

4.6. AO/EB and Hoechst 33258 staining analysis

Apoptosis were detected by AO/EB or Hoechst 33258 staining in MDA-MB-231 cells. Briefly, cells were seeded into 6-well plates, then treated with compound **10f** (1.0, 2.0, 4.0 μM) or Ceritinib (40 nM) for 24 h. In terms of AO/EB staining method, cells were collected and washed with phosphate-buffered saline (PBS). The cells resuspended with an appropriate amount of PBS were counted and adjusted to a density of $(0.2-5) \times 10^6$/mL. Next, the suspension was stained with AO/EB mixed solution (AO: EB: dilution buffer = 1 : 1: 8) for 15 min and evaluated with a fluorescence microscope. In Hoechst 33258 staining, the cells were fixed with 0.5 mL fixative for 10 min. Then cells were washed with PBS for twice and stained with Hoechst 33258. After washing with PBS, anti-fluorescence quenching was added and each well was detected with a fluorescence microscope (Olympus, Tokyo, Japan).

4.7. Flow cytometric analysis

Apoptosis and cell cycle were detected by flow cytometric. MDA-MB-231 or SH-SY5Y cells were seeded into 6-well plates. After the plates were incubated overnight, cells in each well were treated with different concentrations of **10f** (1.0, 2.0, 4.0 μM) or Ceritinib (1.0 μM) for 24 h. In terms of apoptosis analysis, cells were gathered and washed with phosphate-buffered saline (PBS). Cells were then resuspended in cold PBS and incubated with 5 μL Annexin V-FITC and 5 μL propidium iodine (PI) for 30 min at room temperature. Finally, the samples were analyzed using flow cytometer. In terms of cell cycle analysis, cells were resuspended in cold ethanol (70%). Subsequently, cells were treated with RNase A and PI. Finally, the samples were detected with a flow cytometer (CytoFLEX, Beckman Coulter, US).

4.8. Western blot analysis

The MDA-MB-231 or SH-SY5Y cells were seeded into 6-well plates and treated with different concentrations of **10f** (1.0, 2.0, 4.0 μM) or Ceritinib (1.0 μM) or SAHA (1.0 μM). After 24 h, cells in each well were gathered and decomposed with lysis buffer. Subsequently, the lysates were mixed with loading buffer and boiled for 15 min. The samples were separated with SDS-PAGE and then transferred to polyvinylidene fluoride (PVDF) membranes, followed by incubated with 5% (w/v) bovine serum albumin (BSA) for 90 min. The membranes were incubated with 1/1000 primary antibody at 4 °C overnight and afterward, 1/3000 horseradish peroxidase (HRP) labeled secondary antibody at room temperature for 30 min. Finally, the bands were detected by a chemiluminescence imaging system (CLiNX, Shanghai, China) after incubation in ECL reagent. Antibody against β-actin, as well as secondary antibody was purchased from Beyotime institute of biotechnology (Shanghai, China). ALK was purchased from Proteintech (Wuhan, China). Phosphor-ALK (Y1278), AKT, phosphor-AKT (Ser473), ERK, phosphor-ERK (Thr202/Tyr204), Histone H3, acetyl- Histone H3 (Lys9/14/18/23/27) and ECL were purchased from Affinity Biosciences (Changzhou, China). All other kits were purchased from Beyotime institute of biotechnology (Shanghai, China).

4.9. Pharmacokinetic study

The pharmacokinetics analysis of **10f** was conducted in male Sprague−Dawley rats (Beijing Vital River Laboratory Animal Technology Co., Ltd). Compound **10f** was dissolved in a mixture of 20% DMSO +40% PEG +20% 5% glucose solution and administrated via the oral route at 10 mg/kg or administrated via the intravenous route at 1 mg/kg. Blood samples were collected from each animal via posterior orbital vein at the specific time points (2min、5min、15min、30min、1 h、2 h、4 h、6 h、8 h、12 h) and plasma was separated from the blood by centrifugation and stored in a freezer at −80 °C. The sample analysis was performed on a LC−MS/MS system. (mass spectrometer API 4000, using an Hedera ODS-2 column (100 × 2.1 mm, 5 μm), Shimadzu Corporation).

4.10. Molecular docking

The cocrystal structure of wild-type ALK complexed with Ceritinib (PDB ID: 4MKC), and HDAC2 complexed with SAHA (PDB ID: 4LXZ) were obtained from the Protein Data Bank (http://www.rcsb.org). The G1202R mutant ALK model was built using 4MKC as a template. The Prepare Protein protocol in Discovery Studio 2017R2 (DS) (www.3dsbiovia.com) was used for preparing the protein structures. The ligands were optimized using the Gaussian 09 (www.gaussian.com) by the density functional theory method at the B3LYP/6-311G** level. The binding models were visualized using CDOCKER protocol in DS. To verify the reliability of the docking results, Ceritinib and SAHA were re-docked to the active sites, respectively. The docking results with a root mean square deviation (RMSD) of heavy atoms less than 2.0 Å indicates that the docking method is feasible and the docking results are credible [37].

Declaration of competing interest

The authors declare that they have no known competing financial interests or personal relationships that could have appeared to influence the work reported in this paper.

Acknowledgments

We appreciate the financial support from National Natural Science Foundation of China (No. 21907013, and No. 81172097) and the Scientific and Technological Research Program of Chongqing Municipal Education Commission (KJQN201900431).

Appendix A. Supplementary data

Supplementary data to this article can be found online at https://doi.org/10.1016/j.ejmech.2021.113672.

References

[1] R. Chiarle, C. Voena, C. Ambrogio, R. Piva, G. Inghirami, The anaplastic lymphoma kinase in the pathogenesis of cancer, Nat. Rev. Canc. 8 (2008) 11–23.

[2] R.D. Gascoyne, L. Lamant, J.I. Martin-Subero, V.S. Lestou, N.L. Harris, H.K. Muller-Hermelink, J.F. Seymour, L.J. Campbell, D.E. Horsman, I. Auvigne, E. Espinos, R. Siebert, G. Delsol, ALK-positive diffuse large B-cell lymphoma is associated with Clathrin-ALK rearrangements: report of 6 cases, Blood 102 (2003) 2568–2573.

[3] C.M. Lovly, A. Gupta, D. Lipson, G. Otto, T. Brennan, C.T. Chung, S.C. Borinstein, J.S. Ross, P.J. Stephens, V.A. Miller, C.M. Coffin, Inflammatory myofibroblastic tumors harbor multiple potentially actionable kinase fusions, Canc. Discov. 4 (2014) 889–895.

[4] T. Sasaki, S.J. Rodig, L.R. Chirieac, P.A. Janne, The biology and treatment of EML4-ALK non-small cell lung cancer, Eur. J. Canc. 46 (2010) 1773–1780.

[5] M. Soda, Y.L. Choi, M. Enomoto, S. Takada, Y. Yamashita, S. Ishikawa, S.I. Fujiwara, H. Watanabe, K. Kurashina, H. Hatanaka, M. Bando, S. Ohno, Y. Ishikawa, H. Aburatani, T. Niki, Y. Sohara, Y. Sugiyama, H. Mano, Identification of the transforming EML4-ALK fusion gene in non-small-cell lung cancer, Nature 448 (2007) 561–U563.

[6] B. Golding, A. Luu, R. Jones, A.M. Viloria-Petit, The function and therapeutic targeting of anaplastic lymphoma kinase (ALK) in non-small cell lung cancer (NSCLC), Mol. Canc. 17 (2018).

[7] R. Roskoski, Anaplastic lymphoma kinase (ALK) inhibitors in the treatment of ALK-driven lung cancers, Pharmacol. Res. 117 (2017) 343–356.

[8] X.T. Kong, P.C. Pan, H.Y. Sun, H.G. Xia, X.W. Wang, Y.Y. Li, T.J. Hou, Drug discovery targeting anaplastic lymphoma kinase (ALK), J. Med. Chem. 62 (2019) 10927–10954.

[9] E.L. Kwak, Anaplastic lymphoma kinase inhibition in non-small-cell lung cancer (vol 363, pg 1693, 2010), N. Engl. J. Med. 364 (2011), 588-588.

[10] F. Casaluce, A. Sgambato, P.C. Sacco, G. Palazzolo, P. Maione, A. Rossi, F. Ciardiello, C. Gridelli, Resistance to crizotinib in advanced non-small cell lung cancer (NSCLC) with ALK rearrangement: mechanisms, treatment strategies and new targeted therapies, Curr. Clin. Pharmacol. 11 (2016) 77–87.

[11] I. Dagogo-Jack, A.T. Shaw, Crizotinib resistance: implications for therapeutic strategies, Ann. Oncol. 27 (2016) 42–50.

[12] L. Friboulet, N.X. Li, R. Katayama, C.C. Lee, J.F. Gainor, A.S. Crystal, P.Y. Michellys, M.M. Awad, N. Yanagitani, S. Kim, A.C. Pferdekamper, J. Li, S. Kasibhatla, F. Sun, X.Y. Sun, S. Hua, P. McNamara, S. Mahmood, E.L. Lockerman, N. Fujita, M. Nishio, J.L. Harris, A.T. Shaw, J.A. Engelman, The ALK inhibitor ceritinib overcomes crizotinib resistance in non-small cell lung cancer, Canc. Discov. 4 (2014) 662–673.

[13] T. Kodama, T. Tsukaguchi, M. Yoshida, O. Kondoh, H. Sakamoto, Selective ALK inhibitor alectinib with potent antitumor activity in models of crizotinib resistance, Canc. Lett. 351 (2014) 215–221.

[14] A. Markham, Brigatinib: first global approval, Drugs 77 (2017) 1131–1135.

[15] S. Basit, Z. Ashraf, K. Lee, M. Latif, First macrocyclic 3rd-generation ALK inhibitor for treatment of ALK/ROS1 cancer: clinical and designing strategy update of lorlatinib, Eur. J. Med. Chem. 134 (2017) 348–356.

[16] J.F. Gainor, L. Dardaei, S. Yoda, L. Friboulet, I. Leshchiner, R. Katayama, I. Dagogo-Jack, S. Gadgeel, K. Schultz, M. Singh, E. Chin, M. Parks, D. Lee, R.H. DiCecca, E. Lockerman, T. Huynh, J. Logan, L.L. Ritterhouse, L.P. Le, A. Muniappan, S. Digumarthy, C. Channick, C. Keyes, G. Getz, D. Dias-Santagata, R.S. Heist, J. Lennerz, L.V. Sequist, C.H. Benes, A.J. Iafrate, M. Mino-Kenudson, J.A. Engelman, A.T. Shaw, Molecular mechanisms of resistance to first- and second-generation ALK inhibitors in ALK-rearranged lung cancer, Canc. Discov. 6 (2016) 1118–1133.

[17] H.Y. Zou, L. Friboulet, D.P. Kodack, L.D. Engstrom, Q. Li, M. West, R.W. Tang, H. Wang, K. Tsaparikos, J. Wang, S. Timofeevski, R. Katayama, D.M. Dinh, H. Lam, J.L. Lam, S. Yamazaki, W. Hu, B. Patel, D. Bezwada, R.L. Frias, E. Lifshits, S. Mahmood, J.F. Gainor, T. Affolter, P.B. Lappin, H. Gukasyan, N. Lee, S. Deng, R.K. Jain, T.W. Johnson, A.T. Shaw, V.R. Fantin, T. Smeal, PF-06463922, an ALK/ROS1 inhibitor, overcomes resistance to first and second generation ALK inhibitors in preclinical models, Canc. Cell 28 (2015) 70–81.

[18] J.J. Lin, G.J. Riely, A.T. Shaw, Targeting ALK: precision medicine takes on drug resistance, Canc. Discov. 7 (2017) 137–155.

[19] A.T. Shaw, L. Friboulet, I. Leshchiner, J.F. Gainor, S. Bergqvist, A. Brooun, B.J. Burke, Y.L. Deng, W. Liu, L. Dardaei, R.L. Frias, K.R. Schultz, J. Logan, L.P. James, T. Smeal, S. Timofeevski, R. Katayama, A.J. Iafrate, L. Le, M. McTigue, G. Getz, T.W. Johnson, J.A. Engelman, Resensitization to crizotinib by the lorlatinib ALK resistance mutation L1198F, N. Engl. J. Med. 374 (2016) 54–61.

[20] J.J. Lin, A.T. Shaw, Resisting resistance: targeted therapies in lung cancer, Trends in Cancer 2 (2016) 350–364.

[21] R.C. Doebele, A.B. Pilling, D.L. Aisner, T.G. Kutateladze, A.T. Le, A.J. Weickhardt, K.L. Kondo, D.J. Linderman, L.E. Heasley, W.A. Franklin, M. Varella-Garcia, D.R. Camidge, Mechanisms of resistance to crizotinib in patients with ALK gene rearranged non-small cell lung cancer, Clin. Canc. Res. 18 (2012) 1472–1482.

[22] X.Y. Dong, E. Fernandez-Salas, E.X. Li, S.M. Wang, Elucidation of resistance mechanisms to second-generation ALK inhibitors alectinib and ceritinib in non-small cell lung cancer cells, Neoplasia 18 (2016) 162–171.

[23] R. Katayama, A.T. Shaw, T.M. Khan, M. Mino-Kenudson, B.J. Solomon, B. Halmos, N.A. Jessop, J.C. Wain, A.T. Yeo, C. Benes, L. Drew, J.C. Saeh, K. Crosby, L.V. Sequist, A.J. Iafrate, J.A. Engelman, Mechanisms of acquired crizotinib resistance in ALK-rearranged lung cancers, Sci. Transl. Med. 4 (2012).

[24] Y. Wang, S. Chen, G. Hu, J. Wang, W. Gou, D. Zuo, Y. Gu, P. Gong, X. Zhai, Discovery of novel 2,4-diarylaminopyrimidine analogues as ALK and ROS1 dual inhibitors to overcome crizotinib-resistant mutants including G1202R, Eur. J. Med. Chem. 143 (2018) 123–136.

[25] W. Chen, X. Guo, C. Zhang, D. Ke, G. Zhang, Y. Yu, Discovery of 2-aminopyridines bearing a pyridone moiety as potent ALK inhibitors to overcome the crizotinib-resistant mutants, Eur. J. Med. Chem. 183 (2019).

[26] K.J. Geng, Z.J. Xia, Y.C. Ji, R.S. Zhang, D.Q. Sun, J. Ai, Z.L. Song, M.Y. Geng, A. Zhang, Discovery of 2,4-diarylaminopyrimidines bearing a resorcinol motif as novel ALK inhibitors to overcome the G1202R resistant mutation, Eur. J. Med. Chem. 144 (2018) 386–397.

[27] G.R. Mathi, C.H. Kang, H.K. Lee, R. Achary, H.Y. Lee, J.Y. Lee, J. Du Ha, S. Ahn, C.H. Park, C.O. Lee, J.Y. Hwang, C.S. Yun, H.J. Jung, S.Y. Cho, H.R. Kim, P. Kim, Replacing the terminal piperidine in ceritinib with aliphatic amines confers activities against crizotinib-resistant mutants including G1202R, Eur. J. Med. Chem. 126 (2017) 536–549.

[28] D. Mottet, V. Castronovo, Histone deacetylases: target enzymes for cancer therapy, Clin. Exp. Metastasis 25 (2008) 183–189.

[29] J. Shen, S. Najafi, S. Stable, J. Fabian, E. Koeneke, F.R. Kolbinger, J.K. Wrobel, B. Meder, M. Distel, T. Heimburg, W. Sippl, M. Jung, H. Peterziel, D. Kranz, M. Boutros, F. Westermann, O. Witt, I. Oehme, A kinome-wide RNAi screen identifies ALK as a target to sensitize neuroblastoma cells for HDAC8-inhibitor treatment, Cell Death Differ. 25 (2018) 2053–2070.

[30] M.R. Yun, S.M. Lim, S.K. Kim, H.M. Choi, K.H. Pyo, S.K. Kim, J.M. Lee, Y.W. Lee, J.W. Choi, H.R. Kim, M.H. Hong, K. Haam, N. Huh, J.H. Kim, Y.S. Kim, H.S. Shim, R.A. Soo, J.Y. Shih, J.C.H. Yang, M. Kim, B.C. Cho, Enhancer remodeling and microRNA alterations are associated with acquired resistance to ALK inhibitors, Canc. Res. 78 (2018) 3350–3362.

[31] K. Fukuda, S. Takeuchi, R. Katayama, S. Nanjo, T. Yamada, T. Suzuki, K. Takeuchi, M. Nishio, S. Yano, HDAC inhibition overcomes crizotinib-resistance by mesenchymal-epithelial transition (MET) in EML4-ALK lung cancer cells, J. Thorac. Oncol. 12 (2017) S382–S383.

[32] T.A. Miller, D.J. Witter, S. Belvedere, Histone deacetylase inhibitors, J. Med. Chem. 46 (2003) 5097–5116.

[33] Y. Wang, G. Zhang, G. Hu, Y. Bu, H. Lei, D. Zuo, M. Han, X. Zhai, P. Gong, Design, synthesis and biological evaluation of novel 4-arylaminopyrimidine derivatives possessing a hydrazone moiety as dual inhibitors of L1196M ALK and ROS1, Eur. J. Med. Chem. 123 (2016) 80e89.

[34] Y.T. Lim, X.H. Luo, Q.X. Guo, Y.W. Nie, T.Q. Wang, C. Zhang, Z. Hui, X. Wang, Y.H. Liu, Y.N. Chen, J.Y. Zheng, S.Y. Shen, Y. Fan, R. Xiang, Discovery of N1-(4-((7-Cyclopentyl-6-(dimethylcarbamoyl)-7H-pyrrolo[2,3-d]pyrimidin-2-yl) amino)phenyl)-N8-hydroxyoctanediamide as a novel inhibitor targeting cyclin-dependent kinase 4/9 (CDK4/9) and histone Deacetlyase1 (HDAC1) against malignant cancer, J. Med. Chem. 61 (2018) 3166–3192.

[35] T.H. Marsilje, W. Pei, B. Chen, W.S. Lu, T.S. Uno, Y.H. Jin, T. Jiang, S.J. Kim, N.X. Li, M. Warmuth, Y. Sarkisova, F. Sun, A. Steffffy, A. Pferdekamper, A.G. Li, S.B. Joseph, Y. Kim, B. Liu, T. Tuntland, X.M. Cui, N.S. Gray, R. Steensma, Y.Q. Wan, J.Q. Jiang, G. Chopiuk, J. Li, W.P. Gordon, W. Richmond, K. Johnson, J. Chang, T. Groessl, Y.Q. He, A. Phimister, A. Aycinena, C. Lee, B. Bursulaya, D. Karanewsky, H.M. Seidel, J. Harris, P.Y. Michellys, Structure–Activity relationships, and in vivo efficacy of the novel potent and selective anaplastic lymphoma kinase (ALK) inhibitor 5-Chloro-N2-(2-isopropoxy-5-methyl-4-(piperidin-4-yl)phenyl)-N4-(2-(isopropylsulfonyl) phenyl)pyrimidine-2,4-diamine (LDK378) currently in Phase 1 and Phase 2 clinical trials, J. Med. Chem. 56 (2013) 5675–5690.

[36] L.B. Yao, N. Mustafa, E.C. Tan, A. Poulsen, P. Singh, M. Duong-Thi, J.X.T. Lee, P.M. Ramanujulu, W.J. Chng, J.J.Y. Yen, S. Ohlson, B.W. Dymock, Design and synthesis of ligand efficient dual inhibitors of Janus kinase (JAK) and histone deacetylase (HDAC) based on Ruxolitinib and Vorinostat, J. Med. Chem. 60 (2017) 8336–8357.

[37] J.H. Jiang, P. Deng, Discovery of new inhibitors of transforming growth factor-Beta type 1 receptor by utilizing docking and structure-activity relationship analysis, Int. J. Mol. Sci. 20 (2019) 4090–5001.